

IDENTIFICATION, CLASSIFICATION AND MITIGATION OF POWER
QUALITY ISSUES IN DISTRIBUTION NETWORK USING STOCKWELL
TRANSFORM AND DISTRIBUTION STATIC COMPENSATOR

(A CASE STUDY OF YIRGALEM SUBSTATION)

A THESIS SUBMITTED
IN PARTIAL FULFILLMENT OF THE REQUIREMENTS
FOR THE DEGREE OF
MASTER OF SCIENCE

in

POWER SYSTEM AND ENERGY ENGINEERING

By

EPAPHROS MENGISTU



HAWASSA UNIVERSITY
INSTITUTE OF TECHNOLOGY
SCHOOL OF ELECTRICAL AND COMPUTER ENGINEERING

HAWASSA (ETHIOPIA)

May 2022

IDENTIFICATION, CLASSIFICATION AND MITIGATION OF POWER
QUALITY ISSUES IN DISTRIBUTION NETWORK USING STOCKWELL
TRANSFORM AND DISTRIBUTION STATIC COMPENSATOR
(A CASE STUDY OF YIRGALEM SUBSTATION)

By

Epaphros Mengistu

A thesis submitted to Hawassa University, institute of technology, school of graduate studies, for the partial fulfillment of the requirement for the degree of masters of Science in power system and energy engineering.

Advisor: Mr. Tewodros Tesfaye

Co- Advisor: Mr. Mulualem Tesfaye

Hawassa, Ethiopia

May 2022

Declaration

I, the undersigned, declare that the thesis comprises my own work. In compliance with internationally accepted practices, I have acknowledged and refereed all materials used in this work. I know that non-adherence to the principles of academic honesty and integrity, misrepresentation/fabrication of any idea/data/fact/source will constitute sufficient ground for disciplinary action by the University and can evoke penal action from the sources, which have not properly cited or acknowledged.

Epaphros Mengistu

Student Name

Signature

Place: Hawassa institute of technology, Hawassa University, Hawassa, Ethiopia

Date of submission: _____

This thesis have submitted for examination with my approval as a university advisor

Mr. Tewodros Tesfaye_

Advisor Name

Signature

Mr. Mulualem Tesfaye

Co-Advisor

Signature

HAWASSA UNIVERSITY
INSTITUTE OF TECHNOLOGY
SCHOOL OF RESEARCH AND POSTGRADUATE STUDIES
FACULTY OF ELECTRICAL AND COMPUTER ENGINEERING
ADVISOR'S APPROVAL SHEET ONE

This is to certify that the thesis entitled “IDENTIFICATION, CLASSIFICATION AND MITIGATION OF POWER QUALITY ISSUES IN DISTRIBUTION NETWORK USING STOCKWELL TRANSFORM AND DISTRIBUTION STATIC COMPENSATOR (A CASE STUDY OF YIRGALEM SUBSTATION)” submitted in partial fulfillment of the requirements for the degree of Masters of Science in Electrical Engineering with specialization in “POWER SYSTEM AND ENERGY ENGINEERING”, The Graduate Program of the Department of Electrical and Computer Engineering, and has been carried out by Epaphros Mengistu ID No-PGPoSER/0011/12, under my supervision. Therefore, I recommend that the student has fulfilled the requirements and hence hereby can submit the thesis to the department.

Mr. Tewodros Tesfaye _____ Major Advisor

Signature

Date


Mr. Muluaem Tesfaye _____ Co-Advisor

Signature

Date

HAWASSA UNIVERSITY
SCHOOL OF RESEARCH AND POSTGRADUATE STUDIES
EXAMINER'S APPROVAL SHEET TWO

We the under signed Board of examiners of the final open defense by Epaphros Mengistu have read and evaluated his thesis entitled “IDENTIFICATION, CLASSIFICATION AND MITIGATION OF POWER QUALITY ISSUES IN DISTRIBUTION NETWORK USING STOCKWELL TRANSFORM AND DISTRIBUTION STATIC COMPENSATOR (A CASE STUDY OF YIRGALEM SUBSTATION)” and examined the candidate. This is therefore, to certify that the thesis has been accepted in partial fulfilment of the requirements for the degree.

Mr. Tewodros Tesfaye	_____	_____
Major Advisor	Signature	Date
_____	_____	_____
External Examiner	Signature	Date
<u>Dr. Milkias Berhanu Tuka (Ph.D.)</u>		<u>05.08.2022</u>
Internal Examiner	Signature	Date
_____	_____	_____
Chairperson	Signature	Date
_____	_____	_____
SGS	Signature	Date

Final approval and acceptance of the thesis is contingent upon the submission of the final copy of the thesis to the School of Graduate Studies (SGS) through the Department/School Graduate Committee (DGC/SGC) of the candidate's department through the department Graduate Committee (DGC) of Electrical and Computer Engineering.

Stamp of SGS: _____

ACKNOWLEDGEMENT

In the name of God, the Most Gracious and the Most Merciful. Above all, I am grateful to God for the strengths, patience and guidance to complete this thesis. Thereafter, without whose incalculable blessings and prayers of parents and family, none of this would be possible. It is my pleasure to attribute credit to the many people who have contributed to this research.

First, I would like to express my sincere appreciation and gratitude to Mr. Tewodros Tesfaye and Mr. Muluaem Tesfaye to them invaluable guidance and continuous encouragement during this research and preparation of the thesis.

Secondly, I want to express my sincere thanks to all my teachers, and all those from whom I have learnt and gained knowledge.

Lastly, I would like express my sincere thanks to my parents and family for their support, love and encouragement throughout this period where they have played an important role in helping me to reach this stage.

List of Abbreviation and Acronym

AC	Alternator Current
AI	Artificial Intelligence
ANN	Artificial Neural Networks
ANSI	American National Standards Institute
ASDs	Adjustable Speed Drives
CENELEC	European Union Standards Organization
CMBDs	Central Main Board Distribution
CPD	Customer Power Devices
CT	Current Transformer
CVT	Constant Voltage Transformer
DC	Direct Current
DFT	Descript Fourier Transform
D-STATCOM	Distribution Static Synchronous Compensator
DVRs	Dynamic Voltage Restores
EEP	Ethiopian Electric Power
EEU	Ethiopian Electric Utility
EMD	Empirical Mode Function
ESA	Ethiopian Standards Agency
FACTs	Flexible Alternator Current Transmissions
FCT	Field Controlled Thyristor
FES	Fuzzy Expert System
FFT	Fast Fourier Transform
FT	Fourier Transform
GA	Genetic Algorithm
GTO	Gate Turn Off
HCC	Hysteresis Current Control
HHT	Hilbert- Huang Transform
HT	Hilbert Transform
HVDC	High Voltage Direct Current

IEC/EMC	International Electro-Technical Commission
IEEE	Institute of Electrical and Electronics Engineers
IGBT	Insulated Gate Bipolar Transistor
IMFs	Intrinsic Mode Function
IRP	Instantaneous Reactive Power
KV	Kilo-Voltage
KW	Kilowatt
KWA	Kilowatt Ampere
LPF	Low Pass Filter
MATLAB	Matrix Laboratory
MDB	Main Distribution Board
MOSFET	Metal Oxide Field Effect Transistor
MRA	Multi Resolution Analysis
MVA	Mega-Voltage Ampere
NECE	National Electro-technical Committee of Ethiopian
NEMA	National Electrical Manufactures Association
PCC	Point of Common Coupling
PD	Power Demand
PI	Proportional and Integrate
PLC	Programmable Logic Controllers
PQD	Power Quality Disturbance
PU	Per-Unit
PV	Photovoltaic
RMS	Root Mean Square
SBD	Sub Distribution Board
SLG	Single Line to Ground
SMES	Super Conducting Magnetic Energy Storage
SRF	Synchronous References Frame
ST	Stockwell Transform
STFT	Short Time Fourier Transform
STS	Static Transfer Switches

SVM	Support Vector Machines
TDD	Total Demand Distortion
THD	Total Harmonic Distortion
THDI	Total Harmonic Distortion Current
UPSs	Uninterruptable Power Supplies
VSI	Voltage Source Inverter
WT	Wavelet Transform

Table of Contents

ACKNOWLEDGEMENT	i
List of Abbreviation and Acronym	ii
List of Tables	viii
List of Figures	ix
ABSTRACT	xiii
CHAPTER ONE	1
1. Introduction	1
1.1. Background	1
1.2. Statement of the Problem	4
1.3. Objective of the Thesis	5
1.3.1. General Objective	5
1.3.2. Specific Objectives	5
1.4. Significance of the Study	5
1.5. Scope and Limitations of the Study	5
1.6. Methodology Used in this Thesis	6
1.7. Structure of Thesis	7
CHAPTER TWO	9
2. Theoretical Background and Review of Literature	9
2.1. Theoretical Background	9
2.2. Review of Literature	11
2.2.1. Detection Algorithms	16
2.2.2. Classification Techniques Based on Artificial Intelligence	20
2.2.3. Power Quality Definitions	22
2.2.4. Power Quality Standards	32

CHAPTER THREE	38
3. Research Methodology and Modeling	38
3.1. Research Approach	38
3.2. Description of Study Area.....	38
3.3. Data Collection.....	38
3.4. Data Analysis	39
3.4.1. Electric Power Supply System to Awada Industry Zone	39
3.4.2. Electrical Power Distribution Network of Awada Industry	41
3.4.3. Power Quality Related Problems in the Industry Zone	43
3.5. Standards on Harmonics.....	48
3.6. Modelling of Distribution Network	48
3.6.1. Distribution Transformers	48
3.6.2 Installed Loads.....	50
CHAPTER FOUR.....	53
4. Proposed Algorithms Used for Power Quality Issues Identify and Classify	53
4.1. Proposed Algorithm to Identify Power Quality Issues.....	57
4.1.1. Stockwell Transform	57
4.2. Proposed Algorithm to Classify Power Quality Issues	69
4.2.1. Support Vector Machine Classifier	69
4.3. Comparison between the ST with WT, FT and HT Algorithms	81
4.3.1. Identification of power quality issues using wavelet transform	82
4.3.2. Identification of Power Quality Issues Using Fast Fourier Transform	85
4.3.3. Identification of Power Quality Issues Using Hilbert Transform	86
4.3.4. Computational Complexity Analysis	86

4.4. Comparison between the Proposed Classifier with DT, DS, KNN, ES	91
CHAPTER FIVE	95
5. The Existing Power Quality Issues and Mitigation Technique	95
5.1. Introduction	95
5.2. Custom Power Devices (CPDs)	95
5.2.1. Network Reconfiguring Type CPDs	96
5.2.2. Compensating Type CPDs	96
5.3. Current Harmonic Distortion Mitigation with D-STATCOM	97
5.4. Simulation of Awada Industry Distribution Network with D-STATCOM	99
5.4.1. Generating a Reference Current	100
5.4.2. Hysteresis Current Control	103
5.4.3. Voltage Source Inverter (VSI).....	104
5.5. Simulation Results and discussion with and without D-STATCOM.....	105
5.5.1. Modeling of Harmonic Current Distortion Caused by Induction Motor.....	105
5.3.2. Discussion and Summary	111
5.6. D-STATCOM Capacity, Specifications and Measured Values at the Factory	112
5.7. Cost and Payback Period of D-STATCOM	113
CHAPTER SIX.....	114
6. Conclusion, Recommendation and Future Work.....	114
6.1. Conclusion.....	114
6.2. Recommendation.....	115
REFERENCES	116
APPENDICES	124

List of Tables

Table 2. 1: IEEE current distortion limit for systems rated 120V through 69kV [60].	35
Table 2. 2: IEEE voltage distortion limits [60].	36
Table 3. 1: Number and capacity of ASD on each transforms [61].	43
Table 3. 2: Calculated values of R_{tr} and X_{tr} for T1-T4.	50
Table 3. 3: The active and reactive power of loads connected to each transformer [61].	51
Table 4. 1: Confusion matrix.	75
Table 4. 2: Classifier performance summary.	78
Table 4. 3: Correctly classified versus misclassified sample results.	78
Table 4. 4: Comparison computational complexity of feature extraction algorithms.	87
Table 4. 5: Comparison among FT, WT and HT, ST for PQ applications.	87
Table 4. 6: Identification accuracy of ST and WT, FT, HT.	89
Table 4. 7: Identification error comparison of ST and WT, FT, HT.	90
Table 4. 8: Confusion Matrix.	92
Table 4. 9: Characteristics of Classifier Types.	93

List of Figures

Figure 1. 1: Elements of a substation A: Primary power lines' side B: Secondary power lines' [1]	2
Figure 1. 2: Overview of Yirgalem substation [2]. (Source: on-site visit)	3
Figure 2. 1: Detection algorithms discussed in this thesis.	17
Figure 2. 2: Classification techniques using artificial intelligence [78].	21
Figure 2. 3: (a) Lightning stroke impulsive transient and (b) Oscillatory transient [54].	23
Figure 2. 4: Typical voltage waveform during sag caused by an SLG fault [54].	24
Figure 2. 5: Typical voltage waveform during swell caused by an SLG fault [54].	25
Figure 2. 6: Voltage Fluctuation Caused by an Arc Furnace [54].	27
Figure 2. 7: Fourier series representation of a distorted waveform [54].	28
Figure 2. 8: Voltage notching caused by a three-phase converter [54].	31
Figure 2. 9: Demarcation of the power quality issues defined by IEEE Std.1159- 2014 [54].	32
Figure 2. 10: In IEEE 519-1992, point of common coupling [60].	36
Figure 2. 11: In IEEE 519-2014, PCC at primary side of transformer [60].	37
Figure 3. 1: Single line diagram of Yirgalem substation.	40
Figure 3. 2: Schematic diagram of Yirgalem substation.....	41
Figure 3. 3: Single line diagram of Power Distribution Network of Awada industry zone [61]. ..	42
Figure 3. 4: Insertion of D-STATCOM for current harmonic distortion mitigation to CMDDB-1.47	
Figure 3. 5: SIMULINK model of Awada industry distribution system.	52
Figure 4. 1: Flow chart of proposed methodology.....	54
Figure 4. 2: Complete block diagram of proposed methodology.	55
Figure 4. 3: (a) demonstrates the sample of the instantaneous waveform of measured voltage and current at the PCC.....	55

Figure 4. 4: (a) Instantaneous waveform of measured voltage at bus 33kv.	56
Figure 4. 5: (b) instantaneous waveform of measured current at the PCC in bus 0.4kv.	56
Figure 4. 6: Flow chart ST Algorithm [65].....	59
Figure 4. 7: Instantaneous waveform of measured voltage at the PCC phase a.	60
Figure 4. 8: Contour plots of S- transform absolute value coefficients in phase a with harmonic.	60
Figure 4. 9: Signal contaminated with Instantaneous voltage and S- transform contours absolute value.....	61
Figure 4. 10: 3D mesh Time-Frequency-Amplitude.....	61
Figure 4. 11: Contour plots of S- transform absolute value coefficients in phase A swell.	62
Figure 4. 12: Signal contaminated with Instantaneous voltage and S-transform contours absolute value.....	63
Figure 4. 13: 3D mesh Time-Frequency-Amplitude.....	63
Figure 4. 14: Instantaneous waveform of measured voltage at the PCC phase a.	64
Figure 4. 15: Contour plots of S- transform absolute value coefficients in phase a.	64
Figure 4. 16: Signal contaminated with interruption voltage and S- transform contours absolute value.....	65
Figure 4. 17: 3D mesh Time-Frequency-Amplitude.....	65
Figure 4. 18: Support Vector Machine Classification Schematic [49].	71
Figure 4. 19: One vs. One SVM Binary Classification Schematic [49].	73
Figure 4. 20: Scatter plot of feature extracted data set.	74
Figure 4. 21: Confusion matrix.....	75
Figure 4. 22: Receiver Operating Characteristic (ROC) curve.....	80
Figure 4. 23: Parallel coordinate between correct and incorrect classes.	81

Figure 4. 24: The test waveforms together with corresponding in phase references: Top, original signal phase a, Bottom, histogram of signal a.	82
Figure 4. 25: The test waveforms together with corresponding in phase references: Top, approximation signal phase a, Bottom, histogram of signal a.	82
Figure 4. 26: The test waveforms together with corresponding in phase references: Top, details coefficient phase A, Bottom, histogram of phase a.	83
Figure 4. 27: MRA at level 3: Top, original signal phase a, middle, approximation phase a, Bottom, details coefficients phase a.....	84
Figure 4. 28: Instantaneous waveform at bus 0.4kv.	85
Figure 4. 29: FFT analysis of 0.4kv bus.	85
Figure 4. 30: Original Signal and its Hilbert transform.	86
Figure 4. 31: Identification accuracy of ST and WT, FT, HT.	88
Figure 4. 32: Identification error comparison of ST and WT, FT, HT.	89
Figure 4. 33: Performances Assessment of Classifier.	93
Figure 5. 1: General Classification of Custom Power Devices [66].....	96
Figure 5. 2: Single line diagram of (a) D-STATCOM and (b) DVR [66].	97
Figure 5. 3: SIMULINK model of Awada industry zone network with D-STSTCOM.	99
Figure 5. 4: Detail schematic diagram of IRP based D-STATCOM.	100
Figure 5. 5: MATLAB/SIMULINK model of IRP control.....	101
Figure 5. 6: MATLAB/SIMULINK model of Hysteresis Current Control.	104
Figure 5. 7: Induction motor starting/load Simulink model.	106
Figure 5. 8: Instantaneous voltage waveform at bus 33kv.....	107
Figure 5. 9: Harmonic current distortion waveform caused by the starting of 75 kW induction motor at 0.4 kV.	108

Figure 5. 10: Distribution result of T1 with and without D-STATCOM included in the system at 0.02 sec.	109
Figure 5. 11: Single-phase Vs, Is, Il and source voltage/current waveforms (from top to bottom).	109
Figure 5. 12: Harmonic Spectrum of the source current on transformer T1 (Case 1)	110
Figure 5. 13: Harmonic Spectrum of the source current on transformer T1 (Case 2)	110
Figure 5. 14: Harmonic Spectrum of the source current on transformer T1.....	111

ABSTRACT

Power quality has become a crucial concern recently due to the increase of the consumption of electrical load and the increment in the use of sensitive devices connected to power systems. In spite of that, complexity in modern daily life and the increased usage of semiconductors make non-linear load a real threat to power quality level. In order that maintain power quality and to ensure its reliability, power quality disturbances must be identified and classified correctly and precisely. Thus, identification algorithms support decision makers to identified and mitigate the disturbance, and protect the power network from a high level of financial loss. In this thesis study identification, classification and mitigation of power quality issues in Awada industry zone. The measured voltage and current harmonic distortion levels are compared with the IEEE 519-2014 and IEC 61000-2-2 / -3-4 standards. The harmonic voltage distortion level in the factory has found to be well under the limits set by these standards while the current harmonic distortion levels on one of the transformer among four transform exceeds the limits with a maximum percentage total harmonic distortion current value of up to 23.09%. First, an identification process covering the most important and common power quality issues for further analyzed and discussed. Then after, most of the powerful processing algorithms in addition to support vector machine technique was investigated and their results are discussed. SVM then classify complex data and enhancing the evaluation process. This method achieved a sufficient detection algorithm, which overcame the Wavelet, Fourier and Hilbert limitations and resulted in an overall accuracy of 91.08%, 88.91% and 86.8% respectively. This resulted in a substantial improvement in terms of overall accuracy, with more than 97.1% when using Stockwell transform. In addition to the average classification accuracy, other common performance measures computed from the confusion matrix also presented and highest average accuracy of SVM is 98.3%. For mitigating, the current harmonic distortion level in the industry a D-STATCOM in current control mode is designed. The performance of the D-STATCOM is evaluated by simulating the distribution network with and without D-STATCOM. The simulation results show that the source current becomes pure sinusoidal and in-phase with the source voltage within 0.02 second and THDI reduced to 4.36% after the enabled of the D-STATCOM in the system.

Keywords: Custom Power Devices, D-STATCOM, Harmonic Distortion, Instantaneous Reactive Power Theory, Power Quality, Power Quality Standards, MATLAB/SIMULINK.

CHAPTER ONE

1. Introduction

1.1. Background

Electric power distribution is the final stage in the delivery of electric power; it carries electricity from the transmission system to individual consumers. A typical power distribution system consists of power transformers, distribution conductors, distribution feeders, service main conductors. Along with these, a distribution system also consists of circuit breakers, protective devices, recloses, capacitor banks, voltage regulators, measuring equipment etc. Currently Ethiopian electric power corporation power system have 400kV, 230kV, 132 kV primary transmission systems and 66kV, 45kV as sub transmission system and 33kV and 15kV as distribution system. In general, the 66 or 45kV substations power transformers of various ratings like 50/ 25 /12 /6.3/3MVA are installed for step down of voltage to 15kV for feeding to distribution transformers. Most of the outgoing feeders are connected in radial fashion. Typically, 33kV and 15kV overhead conductors are used for feeding 60 to 70 distribution transformers from each 33kV and 15kV feeder lines.

The voltage is then further reduced by distribution transformers to the utilization voltages of 400 volts three-phase or 230 volts single-phase supply required by most users. Substations are fenced yards with switches, transformers and other electrical equipment's. Once the voltage has been lowered at the distribution substation, the electricity flows to industrial, commercial, and residential centers through the distribution system. Conductors called feeders reach out from the distribution substation to carry electricity to customers. At key locations along the distribution system, voltage is lowered by distribution transformers to the voltage of 400volts three-phase or 230 volts single-phase supply required by most users. Figure 1.1 shows the general topology of today's elements of a substation.

Power quality (PQ) holds an important role nowadays for modern electric power utilities and their customers, especially with regard to power quality disturbances. The significant increase in nonlinear load and the increase usage of sensitive electronic devices have made the power quality problems a more critical issue than ever.

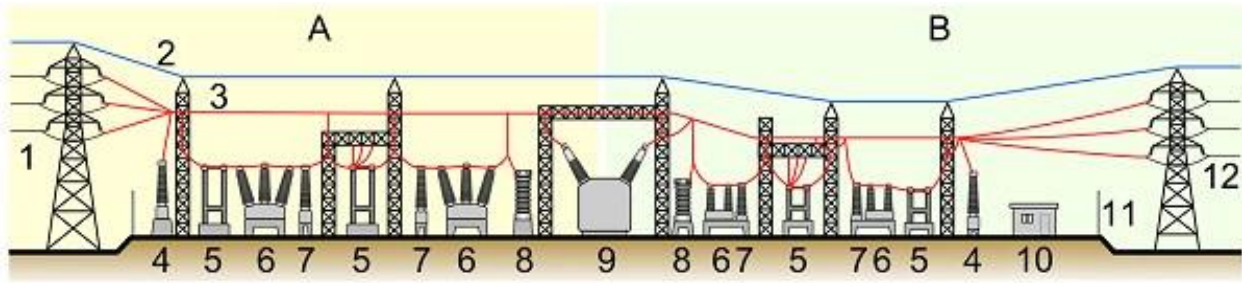


Figure 1. 1: Elements of a substation A: Primary power lines' side B: Secondary power lines' [1].

- | | |
|--|---------------------------|
| 1. Primary power lines | 8. Lightning arrester |
| 2. Ground wire/ communication line | 9. Main transformer |
| 3. Overhead power lines | 10. Control building |
| 4. Transformer for measurement of electric voltage | 11. Security fence |
| 5. Disconnect switch | 12. Secondary power lines |
| 6. Circuit breaker | |
| 7. Current transformer | |

Now a day, electric utilities, academic and research centers, and other end users of electric power have been interested to concern about the quality of electric power. This is because of mainly to high sensitivity of newer-generation load equipment to power quality variations, the increasing application of harmonic generating devices in power systems, increased awareness of end users about power quality issues, sever consequence of a power quality issues in interconnected power systems, and given high attention on maximizing efficiency and system performance. Electricity customers are exposed to power quality disturbances and hence could suffer from critical financial losses because of these problems. Large penetration of sensitive loads in industrial and commercial facilities has substantially increased their susceptibility to power quality disturbances. In Industries, especially at Awada industry zone electric power interruption is becoming a day-to-day circumstance. During connecting heavy induction machine is causing early failure of equipment, blackening of light bulbs, and decreased efficiency and performance of the industry.



Figure 1. 2: Overview of Yirgalem substation [2]. (Source: on-site visit)

In industries, power quality is increasing concern that requires higher quality service due to more sensitive electrical and electronic equipment. The effectiveness of a power system is measured in terms of efficiency, service continuity, and service quality in terms of voltage profile, stability and power delivery system performance.

Starting from the time of awareness and identification of power quality issues a lot of conventional solutions have been proposed and implemented to protect end used equipment's and utility power system equipment's. The evolution of power electronics controller devices has given to the birth of custom power applications, in which a wide range of flexible controllers using power electronics components are utilized to improve the power quality at distribution level. The Custom Power Devices (CPDs) refers to the use of power electronic controllers for distribution systems to improve the quality and reliability of power that is delivered to customers [66]. Many power quality assessments have to be conducted at different parts of the power system in order to evaluate the power quality level and take proper mitigation actions. In this thesis work, a power quality issues are identify and classify has be done on Awada industry zone and apply a proper way of mitigating the problem will be proposed.

1.2. Statement of the Problem

The most important purposes of the power system is to desire a sufficient electrical supply to its customers as economically as possible at normal level of quality. Electric power quality issue is occurring often that in industrial plants, governmental and non-governmental organizations, business centers, commercial centers, residences and other electric power users are facing challenges for the achievement of their goals. As every electric consumer in Ethiopia, Awada industry zone that get power from yirgalem substation through feeder six is injects harmonic current when connecting heavy induction machines to the system.

The factor to work on this thesis is the occurrence of harmonics pollution problem in the Awada industry. Harmonics pollution is increasing in the systems, causing power losses, sensitive equipment malfunctions, and consequent additional costs. Although the concern over the problem is noticeable, the solutions are not simple. The standards already define harmonics injection limits, but how utilities can enforce all customers to follow these standards is problematic. These injected harmonics are dangerous for the utility & end-users; the combined consequence of these facts makes the industry more disposed to power quality problems. A poor power quality has a great economic impact on the industrial consumers and a longer poor power quality may harm practically all operations of the industry. The increase in occurrence and variety of power quality issues and the impact to end users or customers necessitates the development of signal processing tools to monitor and analyze power quality issues. A good monitoring system should incorporate detection capabilities into the monitoring so that events of interest can be recognized and captured automatically. Recently, to detect, localize, and classify power quality disturbances, researchers have focused on signal processing techniques to decompose power signals into a set of features from where decision making becomes easier and more accurate than conventional methods. The majority of signal processing methods reported in the literature utilize time, frequency, and time-frequency domain representations of the disturbance waveform, based on which many specific features are derived in order to classify different types of PQ disturbances.

It has always been conventional devices to uses like capacitor bank and filters to improve harmonic pollution but in this thesis, using D-STATCOM had been designed to mitigate harmonic current problem. Therefore, this thesis found solutions to the identified and classified power quality issues using Stockwell transform and focused on appropriate mitigation device, mitigate the poor power

quality and improve profitability of the industry, which in effect helps the industry to stay competitive in the market by reducing productive wastage.

1.3. Objective of the Thesis

1.3.1. General Objective

The main objective of this thesis is to identify and classify the major power quality issue in Yirgalem distribution network on industry feeder and apply appropriate mitigation technique to overcome the problems using Stockwell transform and distribution static synchronous compensator.

1.3.2. Specific Objectives

The specific objectives of this thesis are:

- To collect and assess the distribution load data and the power quality problems that exists in the industry.
- To identify and classify the types of power quality problems using Stokwell Transform.
- To compare the results of identification and classification with Hilbert transform (HT), wavelet transform (WT), and Fourier transform (FT).
- To model the distribution system with and without D-STATCOM
- Draw relevant conclusions and recommendations.

1.4. Significance of the Study

The output of this thesis work addresses the existing power quality issues, to increases the efficiency, performance of their equipment, and saves the money they lost due to poor power quality, which causes production loss and damage to sensitive electronic devices.

1.5. Scope and Limitations of the Study

In this study voltage and current harmonic distortion levels, which are among the most common power quality disturbances in modern distribution system, were investigated in Awada industry zone distribution network. Data was initially gathered by reviewing different thesis and standards. Additional data were collected by reviewing different electrical installation documents and

weekly/monthly performance reports of the factory and through discussion with the factory engineers. It is unlikely to go through all the industries that face poor power quality, due to finance, capacity and time constraint, the study is limited on Awada industry zone by focusing identifying and classifying power quality issues because the industry zone is more convenient for this study. The research work after identified and classified the problems, only focus on the major problem parts to put the solutions. This research is done in modeling of D-STATCOM in current control mode was proposed as a mitigation technique and simulation of the factory distribution network with proposed D-STATCOM is done to see its performance.

Analysis and comparison of the measurement data with the IEEE 519-2014 and IEC 61000-2- 2 / -3-4 recommended harmonic distortion limits was carried out. The industry's distribution network was modeled in the MATLAB/SIMULINK environment. The model includes the distribution transformers, linear and nonlinear loads of the industry distribution network. A D-STATCOM in current control mode was proposed as a mitigation technique and simulation of the industry distribution network with proposed D-STATCOM is done to see its performance.

1.6. Methodology Used in this Thesis

To achieve the aforementioned objectives, various tasks were performed as state below first for gating brief and reliable information about power quality problems and mitigation techniques, many published and unpublished works related to this study, are deeply reviewed and analyzed. As sources of information books, conference s, articles, journals, lecture notes and other reading materials were employed. Due to the nature of the study, it is started by reviewing literatures related to the identification and classification of power quality problems, causes of those problems; eliminate techniques, and economic impacts of power systems. Recent and important information and data have been collected from the industry. The total task of data collection is accomplished through direct measurement, from recorded data, equipment/wiring specifications and by asking the personnel who works on the specific area of concern. The methodological approach of this study are both descriptive, exploratory approaches and based on design that described in:- Number, Percentage and Graphs etc.

Data have been collected from the load side of service transformer with respective ratings of 4.45MVA, 33/0.4KV and 5% impedance.

Generally, the following methodology have been followed to conduct this research work:

- Literature review: A number of published ideas about power quality problems, identifications and mitigation techniques in books, thesis, articles, journals and lecture note materials have been reviewed.
- Interview: Made an interview with electrical personnel to obtain detailed information about power quality problems.
- Data analysis: The collected data have been analyzed and compared to the IEEE Standard 519-2014.
- Propose solutions: Appropriate solutions for power quality problems are established accordingly.
- Modeling and Simulation: Using MATLAB/Simulink software modeling and simulation of power quality problems have been carried out for the modeled networks.
- Analysis of the result: Analyzed the results of the simulation obtained from the simulating software.
- Conclusion, recommendation and suggestions for future work: Significant approaches have made for generalization of the work, recommend for implementation and suggest the limitations for future work.

1.7. Structure of Thesis

This thesis presents the mitigation of harmonic distortion current in the distribution system using the D-STATCOM. It is also arranged into six chapters as follows.

Chapter One: discusses the introduction part in which the background, problem statement, objective, significance of the study, scope of the study and methodology are included.

Chapter Two: presents the summary of the research thesis and publication reviewed. This chapter also presents a brief definition of different power quality phenomena with possible ways of mitigation techniques. The available international standards and the availability of national standards on power quality are discussed.

Chapter Three: methodology and approaches of the study, data gathering and data analysis methods and modelling the distribution network.

Chapter Four: presents a brief description of proposed detection and classification algorithms using for power quality issues. Compare the results of identification and classification.

Chapter Five: simulation results and discussion of the existing power quality issues and mitigation techniques in distribution network with and without the proposed mitigation presented.

Chapter Six: presents conclusions, recommendations and suggest for future work.

CHAPTER TWO

2. Theoretical Background and Review of Literature

2.1. Theoretical Background

The IEEE Standard Dictionary of Electrical and Electronics defines power quality as “the concept of powering and grounding sensitive electronic equipment in a manner that is suitable to the operation of that equipment”. Power quality may also define as “the measure, analysis, and improvement of bus voltage, usually a load bus voltage to maintain that voltage to be a sinusoidal at rated voltage and frequency”. Another definition of power quality reported in the literature [4] is as follows:

Power quality is “the provision of voltage and system design so that the user of electric power can utilize electric energy from the distribution system successfully without interference or interruption”. A broad definition of power quality borders on system reliability, dielectric selection on equipment and conductors, long term outages, voltage unbalance in three-phase systems, power electronics and their interface with the electric power supply and many other areas. In an electrical power system, there are various kinds of power quality disturbances. They are classified into different categories and their descriptions are important in order to classify measurement results and to describe electromagnetic phenomena, which can cause power quality problems. The term electric power quality (PQ) is generally used to assess and to maintain the good quality of power at the level of generation, transmission, distribution, and utilization of AC electrical power. Since the pollution of electric power supply systems is much severe at the utilization level, it is important to study at the terminals of end users in distribution systems. There are a number of reasons for the pollution of the AC supply systems, including natural ones such as lightning, flashover, equipment failure, and faults (around 60%) and forced ones such as voltage distortions and notches (about 40%). A number of customer’s equipment also pollute the supply system as they draw no sinusoidal current and behave as nonlinear loads.

Therefore, power quality is quantified in terms of voltage, current, or frequency deviation of the supply system, which may result in failure or mal-operation of customer’s equipment. Typically, some power quality problems related to the voltage at the point of common coupling (PCC) where various loads are connected are the presence of voltage harmonics, surge, spikes, notches, sag/dip,

swell, unbalance, fluctuations, glitches, flickers, outages, and so on. These problems are present in the supply system due to various disturbances in the system or due to the presence of various nonlinear loads such as furnaces, uninterruptible power supplies (UPSs), and adjustable speed drives (ASDs). However, some power quality problems related to the current drawn from the AC mains are poor power factor, reactive power burden, harmonic currents, unbalanced currents, and an excessive neutral current in poly phase systems due to unbalancing and harmonic currents generated by some nonlinear loads. These power quality problems causes: failure of capacitor banks, increased losses in the distribution system and electric machines, noise, vibrations, overvoltage. Excessive current due to resonance, negative sequence currents in generators and motors, especially rotor heating, de-rating of cables, dielectric breakdown, interference with communication systems, signal interference and relay and breaker malfunctions, false metering, interferences to the motor controllers and digital controllers, and so on. These power quality problems have become much more serious with the use of solid-state controllers, which cannot be dispensed due to benefits of the cost and size reduction, energy conservation, ease of control, low wear and tear, and other reduced maintenance requirements in the modern electric equipment. Unfortunately, the electronically controlled energy efficient industrial and commercial electrical loads are most sensitive to power quality problems and they themselves generate power quality problems due to the use of solid-state controllers in them. Because of these problems, power quality has become an important area of study in electrical engineering, especially in electric distribution and utilization systems. It has created a great challenge to both the electric utilities and the manufacturers. Utilities must supply consumers with good quality power for operating their equipment satisfactorily and manufacturers must develop their electric equipment either to be immune to such disturbances or to override them.

A number of techniques have evolved for the mitigation of these problems either in existing systems or in equipment to be developed in the near future. It has resulted in a new direction of research and development (R&D) activities for the design and development engineers working in the fields of power electronics, power systems, electric drives, digital signal processing, and sensors. It has changed the scenario of power electronics as most of the equipment using power converters at the front-end need modifications in view of these newly visualized requirements. Moreover, some of the well-developed converters are becoming obsolete and better substitutes are

required. It has created the need for evolving a large number of circuit configurations of front-end converters for very specific and particular applications. Apart from these issues, a number of standards and benchmarks are developed by various organizations such as IEEE (Institute of Electrical and Electronics Engineers) and IEC (International Electro technical Commission), which are enforced on the customers, utilities, and manufacturers to minimize or to eliminate the power quality problems. The techniques employed for power quality improvements in existing systems facing power quality problems are classified in a different manner from those used in newly designed and developed equipment. These mitigation techniques are further sub classified for the electrical loads and supply systems, since both of them have somewhat different kinds of power quality problems. However, in many situations, the power quality problems may be other than those of harmonics such as in distribution systems, and the custom power devices such as distribution static compensators (D-STATCOMs), dynamic voltage restorers (DVRs), and unified power quality conditioners (UPQCs) are used for mitigating the current, voltage, or both types of power quality problems.

This thesis is aimed at providing an awareness of the power quality problems, their causes and adverse effects, an exhaustive exposure of the mitigation techniques to the customers, designers, manufacturers, application engineers, and researchers dealing with the power quality problems.

2.2. Review of Literature

To analyse power quality and its disturbances, it is necessary to detect and identify these disturbances in time, precisely and correctly. Furthermore, it is crucial to categorize them according to their standards, in order to act and solve these disturbances. Thus, an advanced algorithm is essential for detection, feature extraction and classification of this data in order to ensure an understanding of these events. Signal processing algorithms provide the mathematical solution to handle signals, especially in the electrical power system. The industrial, commercial sectors and the domestic environment are common area in using both sensitive equipment and non-linear loads and voltage sag and current harmonics distortion are big problems in the case study power system.

There are many different methods to mitigate voltage sags and current harmonic distortion, but the use of a custom power device (D-STATCOM) is considered the most efficient method. D-

STATCOM is a Custom Power Device used to eliminate voltage disturbances and current harmonics distortion. The voltage sag and current harmonic distortion detection are the primary concerns to improve the power quality by Distribution Static Synchronous Compensator (D-STATCOM), is used to improve power quality more than other FACTS devices due to, having the ability to control active power flow, having higher energy capacitive and Smaller in size, it is cost effective.

In this literature, several methodologies of signal processing algorithms and their capabilities, in terms of detection and feature extraction, are investigated and the following researches are some of the works that have done previously on power quality problems and mitigation techniques.

Hussein Mohamed El-Eissawi Fathi (2012) has done a PhD thesis submitted to AlAzhar University, on power quality Assessment of Egypt 2nd Testing Research Reactor (ETRR-2) center. Measurement and analysis of different power quality disturbances like transients, voltage sag, voltage swell, flicker, harmonics, voltage unbalance and frequency deviations have been done on the distribution system. The thesis tries to compare the measured data with international standards and also propose and design mitigation mechanisms for the disturbances, which exceed standard limits. For the disturbances captured during measurement a single tuned passive filter, Dynamic Voltage Restorer (DVR) and Uninterruptable Power Supply (UPS) has been proposed to be installed at different locations of the electrical distribution network. The costs and payback times of these mitigation techniques have been included in the . Finally, the recommends that power quality assessment have to be done continually with monitoring for longer period of time and with more number of monitoring points for sensitive projects like the one considered on the study [5].

Prafull A. Desale et al (2014) publish a brief review on the CPDs for power quality improvement. The gives a comprehensive survey of CPDs by presenting different application of these devices on a distribution network to compensate a number of power quality disturbances. The indicates that a D-STATCOM, being one of the compensating type CPDs, can be used effectively for harmonic current compensation, flicker effect compensation, power factor improvement and load current balancing in distribution systems. The presents sample simulation result only for voltage sag /swell compensation using DVR in a MATLAB/Simulink environment [3].

Shabana Urooj and Pikasha Sharma (2016) publish a on “Harmonic Elimination using D-STATCOM” on which the analysis and comparison of two D-STATCOM control theories are presented. The two control theories analyzed on this are IRP theory and SRF theory that are used for extracting reference currents to be compensated by D-STATCOM. The analysis is done by simulating the D-STATCOM with the two control theories connected to a sample network configuration with non-linear load, on a MATLAB environment using SIMULINK’s Simscape Power System toolbox. Finally, the presents different simulation results and indicates that both the control techniques are reliable and useful for eliminating harmonic distortion [6].

Gokulananda Sahu et al (2014) publish a on performance analysis of D-STATCOM. The presents the design and analysis of instantaneous P-q control based D-STATCOM for composite compensation, i.e. harmonic distortion and reactive power compensation. A simulation of D-STATCOM performance is done for balanced and unbalanced non-linear load cases using MATLAB’s SIMULINK [7].

Gunjan Varshney et al (2016) publish a on Photovoltaic (PV) based D-STATCOM in which the DC link voltage is regulated by the PV module. MATLAB/Simulink software is used to evaluate the performance of D-STATCOM in unity power factor and AC voltage control mode. This performs comparative analysis of three different control theories of D-STATCOM based on simulation results. The control theories are synchronous reference frame based control theory, instantaneous reactive power control theory and unit template based control theory [8].

Zia Hameed et.al (2016) Harmonic distortion is one of the major issues to maintain the power quality. From the results shown that harmonics are removed by using active shunt filters. Harmonics not only effects the power quality but also cut down the useful life of the power apparatus. Harmonics is all time concern present in the fundamental signal. Harmonics analysis is also very important to study all the effects. Innovative technology management by critical analyzing about power quality problems, issues, related international standards, and their effect in life and the corrective measures using different means are presented [9].

Sandesh Jain et.al (2012) Power quality is improved by power factor correction and harmonic reduction in which voltage source inverter (VSI) is used that injects current in to the system, which compensates the undesired load current. The filter circuit is incorporated in to the system design to filter out the harmonics and supply the reactive power without any interruptions. IEEE 519-

1992, Recommended Practices and Requirements for Harmonic Control in Electric Power Systems, established limits on harmonic currents and voltages at the point of common coupling (PCC), or point of metering [10].

Manila Garg et.al (2015) Power quality issues have become important to electricity consumers at all levels of usage. Sensitive equipment and non-linear loads are now more commonplace in both the industrial commercial sectors and the domestic environment. The interest in Power Quality (PQ) is related to all three parties concerned with the power i.e. utility companies, equipment manufacturers and electric power consumers. The power quality survey is the first, and perhaps most important step in identifying and solving power problems cited previously. In other words, it is thus designed to locate, identify and eliminate the electrical disturbances, which disrupt data collection networks. Different mitigation equipment's are used to improve power quality problems [11].

Shweta Gupta et.al (2015) Power Quality related issues are of most concern nowadays. The widespread use of electronic equipment, such as information technology equipment, power electronics such as adjustable speed drives (ASD), programmable logic controllers (PLC), energy-efficient lighting, led to a complete change of electric loads nature. Due to their non-linearity, all these loads cause disturbances in the voltage waveform. Several studies have been made to evaluate the costs of PQ problems for consumers. The assessment of an accurate value is nearly impossible; so, all these studies are based on estimates. The mitigation of PQ problems may take place at different levels: transmission, distribution and the end-use equipment [12].

Ogunboyo Patrick et.al (2018) Describes investigations of poor voltages, causes and large economic losses are analyzed. provides an investigative study on the typical 11/0.4 kV, low voltage electric power distribution network. The network was modelled with standard network parameters for low voltage typical electric power distribution network using MATLAB/Simulink Sim Power System toolbox. The summary of the gives recommendations on effective methods for enhancing voltage profile and correcting the unbalanced voltage to an allowable standard [13].

Muhammad Rusli et.al (2015) Deals the rise of harmonics in the 20 kV distribution systems because of non-linear loads supplied by the distribution system. Two types of harmonics are stated current harmonic distortion and voltage harmonics distortion. The study discovered current total harmonic distortion that are injected into the 20 kV distribution system reduced by using a

harmonic filter. There are an active filter and passive filter, with economic considerations passive filter is the best option to reduce the level of harmonics in the 20 kV distribution system. By changing the power factor of 0.86 to 0.95, individual harmonic distortion current 5th order can be reduced. Filter capacity needed to compensate harmonic 5th order of electricity supplier (20 kV) [14].

Milkias Berhanu (2010) has done an investigation of power quality problems in distribution network of Adama Spinning Factory. This thesis work focuses only on harmonic current distortion level of factory's distribution network and it was compared with the power quality standard levels stated on IEEE-1159 and IEC-61000. Out of the four-distribution transformer, monitoring of harmonic current distortion level was carried out only on three of them due to measurement device problem on one of the transformer. The research work tries to find out the parallel resonance frequency of the network by considering all the PFC capacitors. Then, the proposes a tuned passive filter to mitigate the current harmonics that was above the standard limits set by IEEE and IEC. Moreover, PSpice software was used for simulation of the network with and without the proposed tuned passive filter. The simulation results on this show that the addition of shunt tuned passive filter on the distribution network reduces the distortion of the current waveform significantly. The simulation was done by considering all the available PFC capacitor banks in the system, but in actual scenario, the capacitor banks are switched in to and out of the system automatically based on the power factor level of the system. This will make the electrical characteristics of the network to change dynamically and affect the performance of the proposed tuned passive filters [15].

T.Thomas et.at (2019) Explains about power quality problems and future works, thus power system or main grid capacity to provide a clean and steady supply of electricity is known as power quality. Due to strong demand of electronic equipment, the progress of electric power utilization and rising non- linear loads on electrical system network may leads to many power quality related issues. This reviews the miscellaneous power quality problems such as harmonics, voltage sags, transient, variation of voltage and swells, interruptions. To eliminate these problems, the better way is to restore the technology, selection of equipment's with less sensitivity and the use of the interfacing devices. The considerable power quality problems are voltage sag, voltage swell, fluctuations of voltage, voltage unbalance, flickering, harmonic distortions, voltage dips, variations in frequency, very short interruptions, electrical noise, under voltages, very long

interruptions, etc. Current harmonics and voltage sags are the major power quality issue and is termed as the integer multiple of fundamental frequency and reduction in voltage outside the normal tolerance for a short time less than few seconds [16].

2.2.1. Detection Algorithms

To discuss signal-processing algorithms effectively, it is important to understand advantages and disadvantages for each signal-processing algorithm in power quality studies. The features extraction process is the core stage of a detection algorithm, where each signal waveform has unique features, as will be discussed in detail in this thesis. Features, which can be obtained directly from the root, mean square measurements (RMS values), as well as through the detection algorithm, should be available to meet the event characterization and report the disturbance signal efficiently. The feature extraction process involves finding unique features from the obtained mathematical coefficients, which represent the original signals. In this literature, a set of effective signal processing algorithms is discussed, including Fourier Transform, Wavelet Transform, Stokwell Transform and Hilbert-Huang Transform, as shown in Figure 2-1. The extracted features of PQDs are then used for the classification technique system in order to achieve the highest level of accuracy.

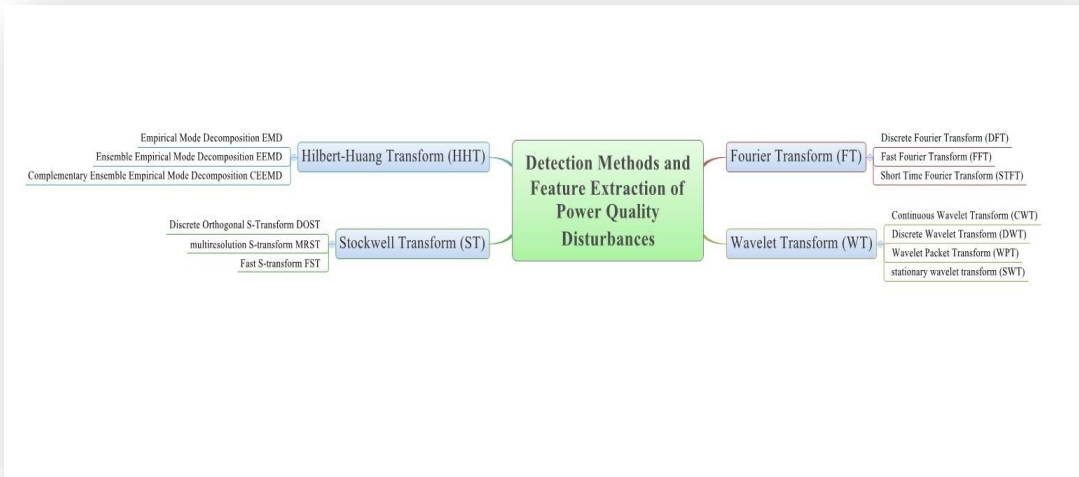


Figure 2. 1: Detection algorithms discussed in this thesis.

A. Fourier Transform

Fourier Transform (FT) is considered the basic algorithm to analyze signals in the frequency domain in many areas, such as engineering and physical sciences. FT is the base analysis method for the definition of power quantities in IEEE standard 1459-2010 [17]. FT stands on decomposing the signal into a summation of sinusoidal functions at specific frequencies. Fourier Transform can be divided into three main derivatives working in the power quality field: Discrete Fourier Transform (DFT), Short Time Fourier Transform (STFT) and Fast Fourier Transform (FFT). FT is broadly used for stationary signals, where it divides the signal into a sum of frequencies [18]. However, FT faces difficulty in collecting time information when the signal fluctuates. Therefore, developments to FT were conducted, which led to derivatives of FT, mentioned earlier. One of these derivatives is Discrete Fourier Transform (DFT), which is involved in detecting disturbances in power systems. DFT is unable to handle changes in power quality disturbances; it is a suitable algorithm for stationary PQDs only. Another derivative of FT, named Short Time Fourier Transform (STFT), has a role in detecting PQDs, where it has the ability to split the disturbed signal into small segments, and each of these segments is considered as a stationary signal, as in [19]. Authors introduced a relationship between the signal frequency and time [19], but it is still

difficult to detect non-stationary signals using STFT, as proved in [20]. Fast Fourier Transform (FFT) is sufficient for analyzing harmonics, as it is one of the steady state events, where it has the same results that can be achieved by DFT, but in less time. A developed version used windowed FFT to analyse power quality for harmonics only. However, the signal factors (amplitudes, frequencies and phases) could not be achieved precisely due to leakage reached by FFT [21].

B. Wavelet Transform

Wavelet Transform (WT) is an advanced signal processing algorithm that has a role in power quality studies. WT gains its power from the ability to detect and represent power signals in the time and frequency domain. WT can also decompose the signal in the frequency domain and find the wave coefficients, which is the key to recognizing the disturbance in the signal. Although WT was initially an interesting algorithm for researchers in the medical field, it became an interesting algorithm in power quality research. WT offers a powerful feature extraction process for distorted power signals, which has been proven in harmonic cases, as in [22]. In detail, signals are processed through a decomposition procedure, which decomposes the signal into several sums of short-term waveforms, called the mother wavelet. The main difference between WT and FT is that WT provides the signal information in the time–frequency domain, which gives WT an advantage in analyzing power quality disturbances. Moreover, WT has a mathematical coefficient, which is able to hold characteristics of the signal at different frequency bands. These coefficients hold more information about signals, such as the amplitude, energy level and standard deviation . In terms of detecting power quality disturbances, WT is able to detect non-stationary disturbances in short periods.

WT was classified originally into two main categories, Continuous Wavelet Transform (CWT) and Discrete Wavelet Transform (DWT). Authors introduced WT as a detection algorithm for power quality disturbances based on the multiresolution method. CWT is introduced to measure power quality disturbances. DWT is a powerful algorithm in detecting PQ disturbances, as can be seen in what is proposed to determine the magnitude of single event, which is voltage sag in [23]. Furthermore, authors applied a hybrid approach based on DWT with FFT to detect PQ disturbances [24], where DWT is responsible for detecting distorted signals and gaining the benefit of the process of features extraction. Based on the feature extraction process, DWT shows its ability to decompose the 10 cases of stationary and non-stationary power quality disturbances into 8

different levels of resolution in the time domain, as shown in [25]. Other derivatives of WT have effects in the field of power quality as well. Authors' proposal in [26] is produced based on WPT for power quality indices for balanced and unbalanced systems under operating conditions. In the wavelet network, combined ability of WT, SVM for analyzing non-stationary and for multiple signals in have been presented in a real-time environment [27] proposed a perspective for the IEEE standard 1459-2000 definitions using the stationary wavelet transform (SWT) to define power components.

C. Hilbert Transform

The HHT method has been developed in the recent year to study non-stationary PQ disturbances. Generally, this technique is the amalgamation of two techniques such as empirical mode decomposition and Hilbert transform. The empirical mode decomposition (EMD) is a technique in which the input signal is decomposed into a series of small components named as intrinsic mode functions (IMFs). Afterward, the IMFs are processed through Hilbert transform (HT) for extracting various features related to frequency, amplitude, and phase of the signal. HHT is initially implemented for voltage sag only which established the bath in power quality studies [28]. Automatic PQ events recognition using HHT and improved HHT have been presented in [29] , [30]. An islanding event has been accurately detected using HHT with wind energy [31] and PQ disturbances detected in the presence of distributed generation .

Another hybrid methodology was conducted to analyses power quality based on wavelet and Hilbert Transform, as introduced in [32]. Authors present two classification attempts, based on the HHT algorithm, to detect seven power quality events, which reach significant accuracy with 94.57% using support vector machine (SVM), as in [33]. HHT has no clear categories or derivatives, since it is a very recent algorithm and has been implemented for power quality in only a few publications.

D. Stockwell Transform

ST is a hybrid combination of the STFT and WT, which contains features of both and considered in a separate group. The R. G. Stockwell had introduced this in the year 1996. ST computes MRA of a signal in time domain and retains absolute phase of every frequency component. This has used a window, the width of which changes in inverse ratio of frequency. This effectively provides high

resolution of time for high frequencies and high resolution for lower frequencies [34]. Most of the complex PQ events are non-stationary and ST effectively extracts features using scalable and localized Gaussian Window, which is dilating, and translating. The continuous WT (CWT) of the function $h(t)$ is computed using below detailed relation. This is found as a best detection technique in a noisy environment. The other S-transform reported in the literature includes, discrete orthogonal S-transform [35], hybrid S-transform [36], generalized hyperbolic ST [37]. Modified ST with random forest tree [38], Multi-resolution S transform (MST) [39], and rule-based ST [40]. Recognition and assessment of various factors associated with wind turbines [41].

R. Naidoo and P. Pillay explains ST uses a window to localize the complex Fourier sinusoidal signal, similarly to STFT, but the width and height of the window scale with frequency is similarly to wavelets. Such description can be seen in detecting voltage sag and swell. S. Mishra et.al proposed the detection and classification of complex and single power quality disturbances using ST and a SVM with overall accuracy of 89%. Furthermore, S. He, K. Li and M. Zhang details explain a real-time approach to detect and classify distorted power signals was presented recently [42]. A derivative algorithm of ST named Discrete Orthogonal S-Transform is involved in five single disturbances, as mentioned in [43].

2.2.2. Classification Techniques Based on Artificial Intelligence

Artificial intelligence (AI) techniques can be identified as the automation of human thinking and actions such as learning, problem solving, estimation and decision-making. With such a powerful mathematical base, AI techniques became powerful tools to diagnose power quality disturbances correctly. Power quality suffers similarity in their shape, and each one of these distorted signals needs to be handled within a short time. Therefore, AIs are required in the classification of power quality disturbances. AI has proven its importance and ability to classify power signal disturbances, and handle data extracted from detection algorithms [44]. Figure 2-2 shows AIs discussed in this study.

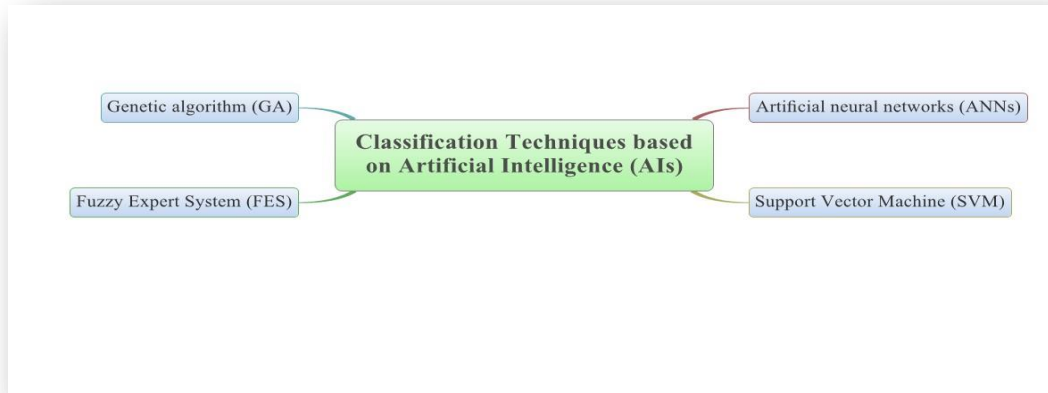


Figure 2. 2: Classification techniques using artificial intelligence [71].

Artificial Neural Networks

Artificial neural network is one of the main, robust AI techniques used in power systems as well as classification for PQDs. Authors in [45] proposed an early implementation of the neural network approach to classify distorted power waveforms. An approach to recognize the harmonics source is proposed, based on a neural network. Moreover, artificial neural network (ANN) is proposed to identify four cases of disturbances according to the faults in a transmission lines system [46]. Authors presented a robust ANN classifier for data extracted of power quality events in smart grids based on DWT algorithm [47].

A. Support vector machine

The principle of a support vector machine (SVM) was introduced by Vapnik [48]. An SVM is a supervised learning machine technique, which is applied for pattern recognition in many areas of sciences and classification systems techniques. Regarding power quality, SVM was used to identify voltage disturbances as a classifier in [49]. Pattern recognition is one of the approaches that relies on statistical learning theory and is applied to solve problems, and for forecasting and estimation. Five different power quality disturbances were detected by S-transform and classified by SVM, as presented in [50]. A. S. Cerqueira et al in (2008) presented a WT-based deletion algorithm to recognize distorted events with an SVM classifier. Five single power quality disturbances were detected by DWT and classified based on SVM in [51].

B. Fuzzy Expert System

The fuzzy expert system (FES) is one of the classical AI techniques, which is based on two decision choices for uncertain situations. It is driven by the calculation that human intellectual can apply models that do not have fixed boundaries. A fuzzy system is a task that plans objects at specified domain to their membership values, which is called the membership function. In power quality studies, an early approach to evaluate and quantify power quality based on fuzzy logic is proposed. Authors presented a fuzzy expert system using a group of fuzzy sets and rules as a replacement for Boolean sets to classify PQDs [52]. Another fuzzy classifier is implemented based on four levels of the decomposition process of WT, as in [53].

2.2.3. Power Quality Definitions

Power Quality can be defined as any power problem manifested in voltage, current, or frequency deviations those results in failure or miss-operation of customer equipment [54]. Power quality disturbances are usually caused by load switching, system faults, motor starting, load variations, non-linear loads, intermittent loads and arc furnaces. These results in many electrical disturbances like surge, sag, swell, harmonic distortions, interruptions, flickers, and signaling voltages. Categories & typical characteristics of different power quality phenomena, as defined and presented in IEEE Std 1159-2014: Recommended Practice for Monitoring Electric Power Quality, are listed in Appendix of this document. Each of these classes of power quality problem is defined and discussed herein after as presented by [54].

A .Transients

The term Transient/Surge denotes an event that is undesirable but momentary in nature that disappears during transition from one steady state operating condition to another. Based on the wave shape of voltage or current, transients can be classified in to two categories, impulsive and oscillatory.

Impulsive transient is a sudden; non–power frequency change in the steady-state condition of voltage, current, or both that is unidirectional in polarity (primarily either positive or negative). Impulsive transients are normally characterized by their rise and decay times, which can also be revealed by their spectral content. They are commonly caused due to lightning striking on a power system, poor grounding, switching of inductive loads, switching of power factor correction

capacitors, and utility fault clearing. Impulsive transients can excite the natural frequency of power system circuits and produce oscillatory transients.

Oscillatory transient is a sudden, non-power frequency change in the steady-state condition of voltage, current, or both, that includes both positive and negative polarity values. It is a brief, bidirectional variation of voltage/current and described by its spectral content, duration, and magnitude. Oscillatory transients are most commonly a result of switching, capacitor energization, and local system response to impulsive transients.

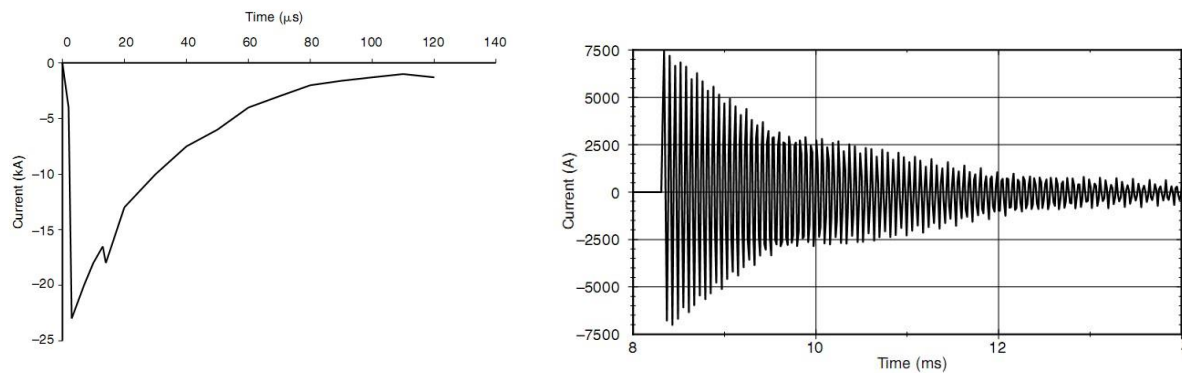


Figure 2. 3: (a) Lightning stroke impulsive transient and (b) Oscillatory transient [54].

Transients lead to equipment failure, nuisance tripping of adjustable-speed drives, system lock-up, data corruption and data loss. Different techniques and devices can be utilized to minimize and/or avoid transient problems:

- Surge arresters and transient voltage surge suppressors
- Synchronous closing breakers with pre-insertion resistors
- Line reactors
- Isolation transformers
- Low-pass filters
- Shielding on overhead utility line

Short Duration Voltage Variation

Short-duration voltage variations are caused by fault conditions, switching actions to isolate the faulted sections, the energization of large loads, which require high starting currents, or intermittent loose connections in power wiring. Depending on the fault location and the system conditions, the fault can cause either temporary voltage drops (sags or dips), voltage rises (swells), or a complete loss of voltage (interruptions).

Sag/dip is a decrease to between 0.1 and 0.9 PU in root mean square (RMS) voltage and current at the power frequency for durations from 0.5 cycle to 1 min and commonly caused by faults on the power system and starting of large loads such as motors. Voltage sag reduces the energy being delivered to the load and causes sensitive equipment to trip, computer systems to fail and lose their memory, adjustable-speed drive to shut down, motors to stall and over heat. Solutions to voltage sag problems include equipment such as Ferro resonant transformer (Constant Voltage Transformer, CVT), Motor-generator set, flywheel energy storage devices, Super conducting Magnetic Energy Storage (SMES) devices, automatic transfer switches, uninterruptible power supply (UPS) and DVR. A typical voltage wave form during sag caused by an SLG (Single Line to Ground) fault.

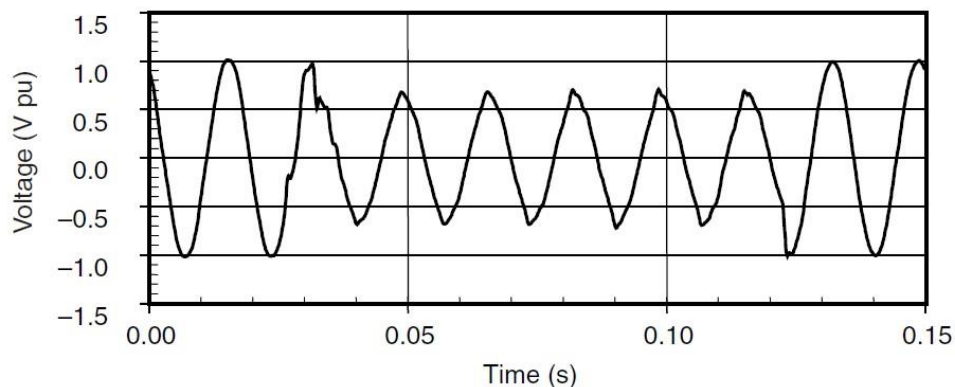


Figure 2. 4: Typical voltage waveform during sag caused by an SLG fault [54].

Swell is defined as an increase to between 1.1 and 1.8 PU in root mean square voltage or current at the power frequency for durations from 0.5 cycle to 1 min. As with sags, swells are usually associated with system fault conditions like the temporary voltage rise on the unfaulty phases

during a Single Line to Ground (SLG) fault, but they are not as common as voltage sags. Swells can also be caused by switching off a large load or energizing a large capacitor bank.

The increased energy from a voltage swell often overheats equipment and reduces its life. Solutions to voltage swell problems include equipment such as voltage regulator, motor generator set and uninterruptible power supply (UPS), automatic transfer switches. A typical voltage waveform during swell caused by an SLG fault.

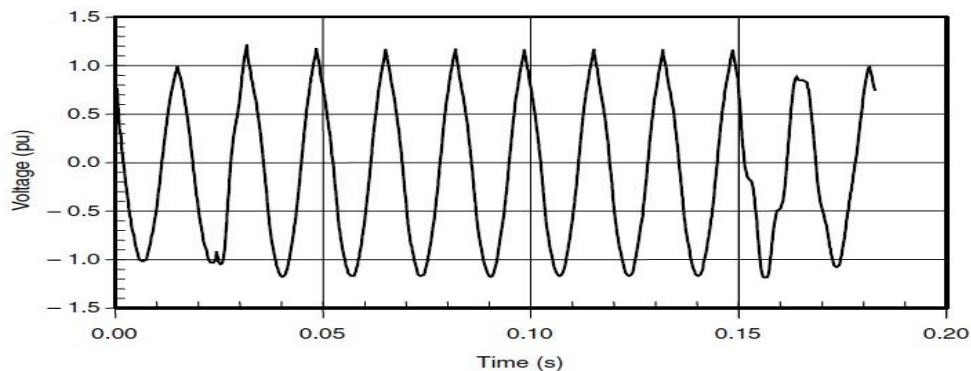


Figure 2. 5: Typical voltage waveform during swell caused by an SLG fault [54].

Interruption is an occurrence of the supply voltage or load current reduced to less than 0.1 PU for a period of time not exceeding 1 min. Interruptions can be a result of power system faults, the actions taken by utilities to clear transient faults, equipment failures, and control malfunctions.

Long Duration Voltage Variation

Long-duration variations encompass root-mean-square (RMS) deviations at power frequencies for longer than 1 min. Long duration variations can be under-voltages, over-voltages and sustained interruptions. Long duration voltage variation power quality problems can be mitigated by different voltage regulating devices like motor-generator set, tap changing regulators, Ferro resonant transformer, online Uninterruptible Power Supplies (UPS) and static VAR compensator.

Over-Voltage is an increase in the root mean square ac voltage greater than 110 percent at the power frequency for duration longer than 1 min. Over-voltages are usually the result of load switching (e.g., switching off a large load or energizing a capacitor bank).

Under-Voltage is a decrease in the root mean square ac voltage to less than 90 per- cent at the power frequency for duration longer than 1 min. A load switching on or a capacitor bank switching off may result in an under-voltage until voltage regulation equipment on the system can bring the voltage back to within tolerances. Overloaded circuits and the loss of major transmission support can also result in under voltages.

Sustained Interruption is a long duration voltage variation when disappearance of the supply voltage for a period in excess of one minute occurs.

Voltage Imbalance is sometimes defined as the maximum deviation from the average of the three-phase voltages or currents, divided by the average of the three-phase voltages or currents, expressed in percent.

$$\% \text{voltage unbalance ratio} = \frac{\text{maximum voltage deviation}}{\text{average voltage}} \times 100 \quad (2.1)$$

Imbalance is more rigorously defined in the standards using symmetrical components. The ratio of either the negative- or zero-sequence component to the positive-sequence component can be used to specify the percent unbalance. Voltage unbalance can be the result of single - phase loads on a three-phase system, blown fuses in one phase of a three-phase capacitor bank, different line impedances on long run lines, open circuit on the distribution system primary. Voltage unbalance can create a current unbalance 6 to 10 times the magnitude of voltage unbalance. Consequently, this current unbalance causes motors and transformer windings to overheat which may result in insulation failure.

Voltage Fluctuation

Voltage fluctuations are cyclical variations in the voltage root mean square values or a series of random voltage changes, whose magnitude does not normally exceed voltage ranges of 0.9 PU to 1.1 PU. Loads, which can exhibit continuous, rapid variations in the load current magnitude, can cause voltage fluctuations that are often referred to as flicker. The term flicker is derived from the impact of the voltage fluctuation on lamps such that they are perceived by the human eye to flicker. Arc furnace and welders are the most common causes of voltage fluctuations in utility transmission and distribution systems. Flickers can be mitigated by increasing the system capacity or by

implementing static capacitors and power electronic-based switching devices. Typical voltage fluctuation on a waveform caused by an arc furnace is shown in Figure (2.4).

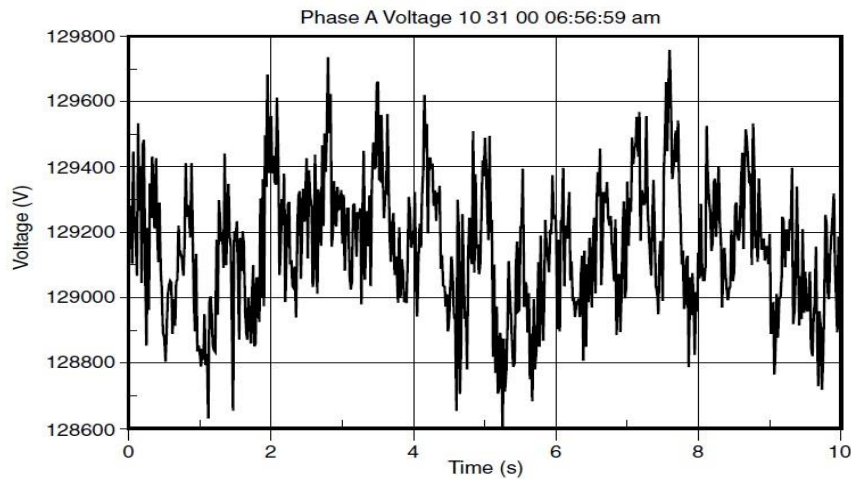


Figure 2. 6: Voltage fluctuation caused by an arc furnace [54].

Power Frequency Variation

Power frequency variations are defined as the deviation of the power system fundamental frequency from its specified nominal value (50 or 60 Hz). Frequency variations can be caused by faults on the bulk power transmission system, a large block of load being disconnected, or a large source of generation going off-line. Frequency variation is rare in an interconnected utility system. In isolated generation systems, the dynamic response of the control system (Governor of the generating system) to abrupt and huge load changes may not be adequate to regulate within the narrow bandwidth required by frequency-sensitive equipment.

Waveform Distortion

Waveform distortion is defined as a steady-state deviation from an ideal sine wave of power frequency characterized by the spectral content of the deviation. There are five primary types of waveform distortion: Harmonics, Inter-harmonics, DC offset, Notching and Noise.

Harmonics are sinusoidal voltages or currents having frequencies that are integer multiples of the frequency at which the supply system is designed to operate (termed the fundamental frequency; usually 50 or 60 Hz). Periodically distorted waveforms can be decomposed into a sum of the

fundamental frequency and the harmonics, using the Fourier series representation as shown in Figure (2.5) below. The equation for such waveform is given below.

$$V(t) = a_0 + \sum_{h=1}^{\infty} V_h \sin(h.2\pi f.t + \theta_h) \quad (2.2)$$

Where, a_0 is a dc component; V_h Is peak voltage level; f is fundamental frequency and θ_h is Phase angle.

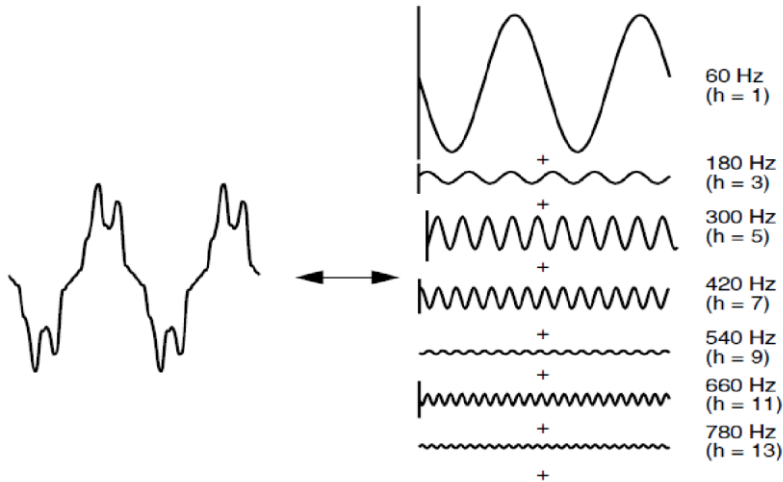


Figure 2. 7: Fourier series representation of a distorted waveform [54].

Harmonic current distortion originates from the nonlinear characteristics of devices and loads on the power system. Voltage distortion is the result of harmonic distorted currents passing through the linear, series impedance of the power delivery system. One of the major problems related to harmonic disturbances is harmonic resonance. The resonance can magnify harmonic distortions to a level that can damage the equipment or cause equipment malfunction. Power factor correction capacitors in distribution system are the main cause of harmonic resonance. Electric power system disturbances caused by harmonic effect include:

- Overload on distribution system (transformers, cables & capacitors) due to increase in root mean square value.
- Overload of neutral conductor due to third (triple) harmonic current
- Overload and torsional oscillation of motors and generators due to fifth harmonics

- Distortion of supply voltage capable of distorting sensitive loads like computer and control systems
- Premature failure or operation of protective devices (such as fuses)
- Disturbance of communication networks and telephone lines
- Flickering fluorescent lighting
- Inaccuracy of demand and watt-hour meter

Nonlinear loads in industrial and commercial facilities which are responsible for creating harmonic currents include Single-phase switch mode power supplies, AC/DC Adjustable speed drives, Discharge type lightings with magnetic and electronic ballasts, three phase power converters, saturated reactors, static VAR systems, inverters for distributed generation, Arc furnaces and arc welders. Harmonics in electric system can be controlled by adding different types of passive and active filters (to take out the harmonic current from the system, block the harmonic current from entering the system, or supply harmonic currents locally), reducing the harmonic currents produced by loads, modifying the frequency response of the system by filters, inductors, or capacitors.

The two most commonly used indices for measuring the harmonic content of a waveform are the Total Harmonic Distortion (THD) and the Total Demand Distortion (TDD). The THD is a measure of the effective value of the harmonic components of a distorted waveform relative to the fundamental. This index can be calculated for either voltage or current:

$$\text{THD}_V = \frac{\sqrt{\sum_{h=2}^{\infty} V_h^2}}{V_1} \times 100\% \quad (2.3)$$

$$\text{THD}_I = \frac{\sqrt{\sum_{h=2}^{\infty} I_h^2}}{I_1} \times 100\% \quad (2.4)$$

Where, V_h and I_h represent the rms voltage and current values at harmonic orders of h , respectively. V_1 and I_1 represent the fundamental rms voltage and current, respectively. Current distortion levels can be characterized more effectively by TDD factor, which is calculated relative to maximum

demand load current rather than the fundamental of the present sample. This is due the fact that a small current may have a high THD but not be a significant threat to the system.

$$\text{TDD} = \frac{\sqrt{\sum_{I_2}^{\infty} I_h^2}}{I_L} \times 100\% \quad (2.5)$$

Where I_L is the maximum demand load current at the fundamental frequency component.

Inter-harmonics are voltages or currents having frequency components that are not integer multiples of the frequency at which the supply system is designed to operate (e.g., 50 or 60 Hz). Inter-harmonics can be found in networks of all voltage classes. The main sources of inter-harmonic waveform distortion are static frequency converters, cycle-converters, induction furnaces, and arcing devices.

DC Offset occurs when there is the presence of a dc voltage or current in an AC power system. DC injection into the low-voltage and medium-voltage AC grids comes mostly from grid connected static power converters (caused by the delay mismatch in gating circuits and imperfections of power switches), HVDC transmission, and railway signaling equipment. Direct current in AC networks can have a detrimental effect by biasing transformer cores so they saturate in normal operation. This causes additional heating and loss of transformer life. Direct current may also cause the electrolytic erosion of grounding electrodes and other connectors. Active compensation methods can be advantageously used in suppressing the DC bias at grid connection points.

Notching is a periodic voltage disturbance caused by the normal operation of power electronic devices when current is commutated from one phase to another. During commutation, there is a momentary short circuit between two phases, pulling the voltage as close to zero as permitted by system impedances. A typical voltage notching caused by a three-phase converter is shown in Figure 2.6. Since notching occurs continuously, it can be characterized through the harmonic spectrum of the affected voltage.

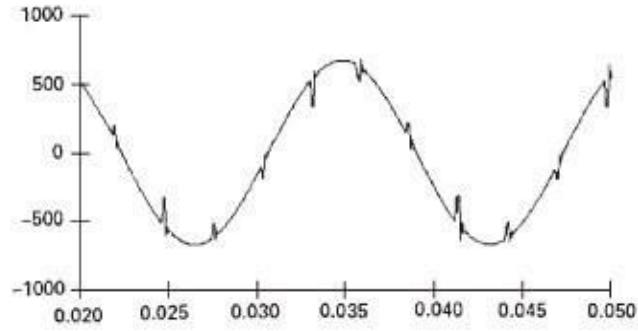


Figure 2. 8: Voltage notching caused by a three-phase converter [54].

Noise is defined as unwanted electrical signals with broadband spectral content lower than 200 kHz superimposed upon the power system voltage or current in phase conductors, or found on neutral conductors or signal lines. Power electronic devices, control circuits, arcing equipment, loads with solid-state rectifiers, and switching power supplies, can cause noise in power systems. The problem can be mitigated by using filters, isolation transformers, and line conditioners.

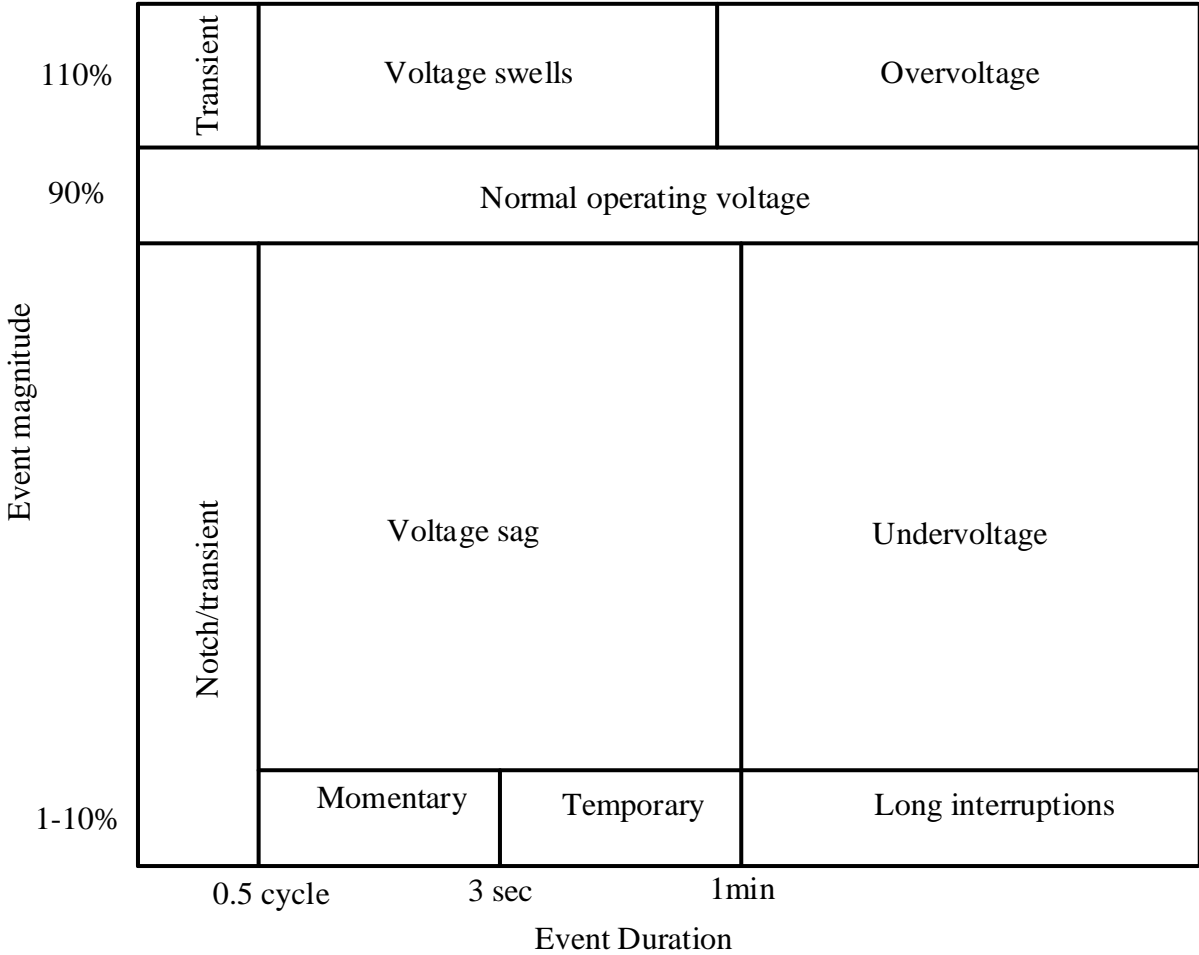


Figure 2. 9: Demarcation of the power quality issues defined by IEEE Std.1159- 2014 [54].

2.2.4. Power Quality Standards

The goal of producing power quality standards is to protect power utilities, providers and the end user or customer from any failure, dropdown or miss-operation when a voltage disturbance occurs [55]. Power quality standards provide limits, measurements and settings for voltage, current and frequency values when they deviate from nominal conditions [56]. Such standards draw lines and provide guidance regarding acceptable and unacceptable levels in the service provided for both providers and customers. It is important to provide customers with an acceptable level of disturbance events and variations where it is impossible to gain a healthy supply. As a result, many international standards related to power quality have been formulated by different standard organizations and put into work. Such organization includes Institute of Electrical and Electronics

Engineers (IEEE), European Union Standards organization (CENELEC), International Electro-technical Commission (IEC), American National Standard Institute (ANSI), National Electrical Manufactures Association (NEMA), and so on.

In this study, mostly the IEC and IEEE standards and definitions would be used for their widely usage in academic and research areas, and their high-level of completeness to characterize all the major electrical phenomena comprising power quality. Moreover, the position of Ethiopia's national standard on power quality issues will be addressed.

IEC standards

Founded in 1906, the IEC is the world's leading organization for the preparation and publication of international standards for all electrical, electronic and related technologies [57].

The IEC family, with 84 member countries and 87 affiliate member countries (developing countries), spread across more than 97% of the world's population. The European Committee has adopted IEC standards for Electro technical Standardization (CENELEC) and many other countries all over the world. The IEC has defined a category of standards called Electromagnetic Compatibility (EMC) Standards that deal with power quality issues. These standards are broken down into six parts: General (IEC 61000-1-x), Environment (IEC 61000-2-x), Limits (IEC 61000-3-x), Testing and Measurement Techniques (IEC 61000-4-x), Installation and Mitigation Guidelines (IEC 61000-5-x), Generic and Product Standards (IEC 61000-6-x). IEC standards for each power quality parameters are not given on a single publication; rather they are separated into several publications, which fall into different parts of the standard and for different levels of current and voltage. For example, the IEC standard relating to harmonics generally fall in parts 2 and 3, which includes:

- IEC 61000-2-2 (1993): Compatibility Levels for Low-Frequency Conducted Disturbances and Signaling in Public Low-Voltage Power Supply Systems,
- IEC 61000-3-2 (2000): Limits for Harmonic Current Emissions (Equipment Input Current Up to and Including 16 A per Phase),
- IEC 61000-3-4 (1998): Limitation of Emission of Harmonic Currents in Low-Voltage Power Supply Systems for Equipment with Rated Current Greater Than 16 A,

- IEC 61000-3-6 (1996): Assessment of Emission Limits for Distorting Loads in MV and HV Power Systems. Basic EMC publication.

IEEE Standards

The IEEE is a professional association formed in 1963 from a combination of the American Institute of Electrical Engineers and the Institute of Radio Engineers. The institute is the world's largest association of technical professionals with more than 420,000 members in over 160 countries around the world [58]. The IEEE Standards Association (IEEE-SA) is an organization within IEEE that develops global standards in a broad range of industries. Some of the standards developed by IEEE, which are related to power quality phenomena, are:

- IEEE Standard 1159-2009: Recommended Practice for Monitoring Electric Power Quality.
- IEEE Standard 1159.3-2003: Recommended practice for the transfer of power quality data.
- IEEE Standard 519-2014: Recommended Practices and Requirements for Harmonic Control in Electrical Power Systems.

Ethiopian Standards Agency

ESA is a governmental non-profitable organization and the sole national standards body that represents Ethiopian interest in economic, social and environmental aspects with regard to standard benefits across international and regional arena. ESA has three core business areas that mainly focus on the standard formulation, training and technical support and organizing and disseminating standards, conformity assessment procedures and technical regulation for the customers [59].

National Electro-technical Committee of Ethiopia (NECE) was established in November 2012 under ESA with an expert group from five different organizations: ESA, Addis Ababa University, Ethiopian Electric Utility, Ministry of Energy, and Ethiopian Conformity Assessment Enterprise. NECE, together with the Technical Committees on different fields, is the responsible body within the ESA, for the approval and adoption of IEC standards for national use. Ethiopia, as one of the affiliate plus member country of IEC, has adopted 251 IEC standards through NECE, out of the free 400 standards allowed for national adoption by such member countries. Unfortunately, NECE has not adopted the IEC 61000: EMC standards related to power quality phenomena as a national standard still now (when this research work is prepared).

IEEE std 519-2014

IEEE Recommended Practice and Requirements for Harmonic Control in Electric Power Systems. This standard includes recommended harmonic voltage limits and recommended current distortion limits for systems nominally rated 120V - 69kV, 69kV - 161kV and above 161kV. Recommended current distortion limits for systems nominally rated 120V - 69 kV: This current value is established at the PCC and should be taken as the sum of the currents corresponding to the maximum demand during each of the twelve previous months divided by 12. All values should be in percent of the maximum demand current, I_L . [60].

Table 2. 1: IEEE current distortion limit for systems rated 120V through 69kV [60].

Maximum harmonic current distortion (% of I_L .)						
Individual harmonic order (Odd harmonics) ^{i,ii}						
I_{sc}/I_L	$3 \leq h < 11$	$11 \leq h < 17$	$17 \leq h < 23$	$23 \leq h < 35$	$35 \leq h \leq 50$	TDD
< 20 ⁱⁱⁱ	4.0	2.0	1.5	0.6	0.3	5.0%
$20 < 50$	7.0	3.5	2.5	1.0	0.5	8.0%
$50 < 100$	10.0	4.5	4.0	1.5	0.7	12.0%
$100 < 1000$	12.0	5.0	5.0	2.0	1.0	15.0%
> 1000	15.0	6.0	6.0	2.5	1.4	20.0%

ⁱ Even harmonics are limited to 25% of the odd harmonic limits above.

ⁱⁱ Current distortions that result in a DC offset, e.g. half – wave converters, are not allowed.

ⁱⁱⁱ All power generation equipment is limited to these values of current distortions, regardless of actual I_{sc}/I_L , where, I_{sc} is maximum short circuit current at point of common coupling.

I_L is the maximum demand load-current (fundamental frequency component) at PCC. The short circuit current and rated current of 400V feeder at the point of common coupling.

I_{sc}/I_L Ratio is not more than in the range of < 20 . As a result, the TDD values of the current harmonics should not exceed 5% at the point of common coupling and the voltage distortion level limit is shown as in Table 2.2.

Table 2. 2: IEEE voltage distortion limits [60].

Bus voltage at PCC	Individual voltage distortion (%)	Total Voltage distortion, THD (%)
$v \leq 1\text{kv}$	5.0	8.0
$1\text{kv} < v \leq 69\text{kv}$	3.0	5.0
$69\text{kv} < v \leq 161\text{kv}$	1.5	2.5
$161\text{kv} < v$	1.0	1.5^{iv}

^{iv} High voltage systems can have up to 2.0% THD where the cause is an HVDC terminal whose effects will have attenuated at points in the network where future users may be connected. The maximum voltage and current harmonic contents of the electric power of Awada industry zone, when the industry is working at full load are measured. The current THD values obtained in the three phases are beyond the permissible range of the IEEE current distortion limits. The PCC is taken as the secondary side of the transformers serving the industry loads. The transformer is connected in delta-wye, so that the triple harmonics (the harmonics that are multiple of three) cannot enter to the primary side of the transformer that comes from the load side.

Point of Common Coupling (PCC) Differences between 519-1992 and 519-2014

In IEEE 519-1992, point of common coupling (PCC) is defined as follows: “Within an industrial plant, the PCC is the point between the nonlinear load and other loads.”

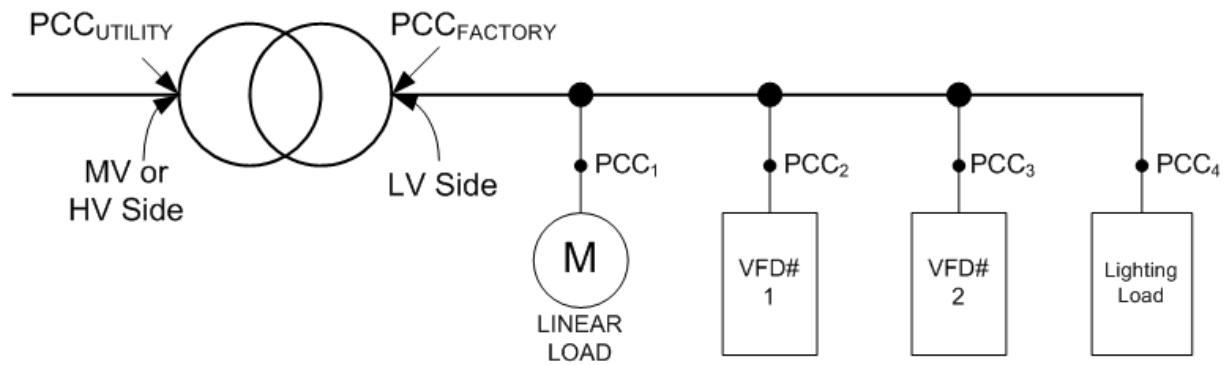


Figure 2. 10: In IEEE 519-1992, point of common coupling [60].

In IEEE 519-2014, PCC is: “Frequently for service to industrial users (i.e., manufacturing plants) via a dedicated service transformer, the PCC is at the HV side of the transformer. For commercial users (office parks, shopping malls, etc.) supplied through a common service transformer, the PCC is commonly on the LV side of the service transformer.”

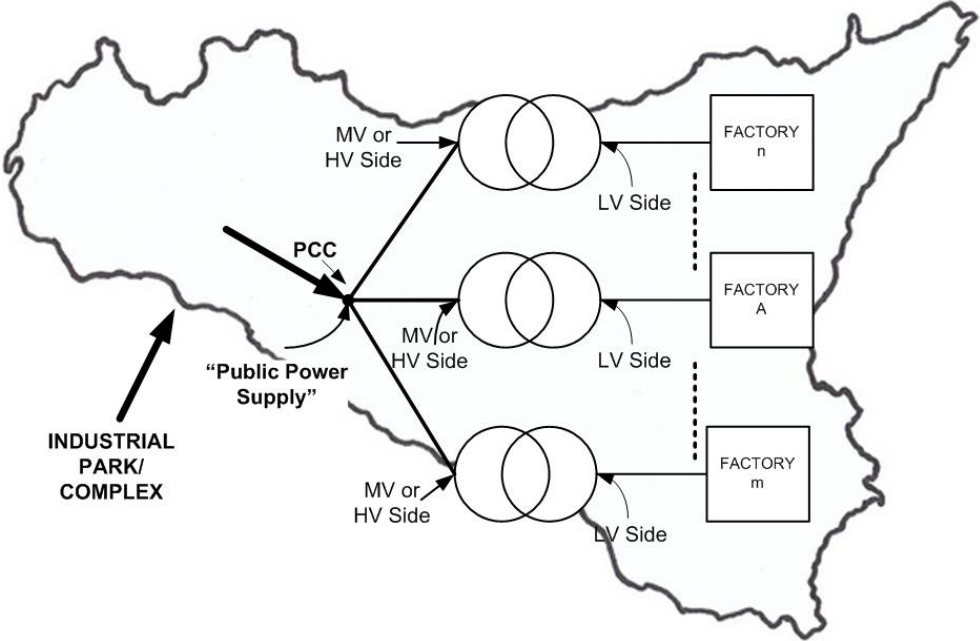


Figure 2. 11: In IEEE 519-2014, PCC at primary side of transformer [60].

CHAPTER THREE

3. Research Methodology and Modeling

3.1. Research Approach

The choice of research approach depends on the degree of precision by which the original research question can be formulated, and how much knowledge exists in the area of the chosen subject. This study had used both exploratory, descriptive approaches and based on design.

3.2. Description of Study Area

This study is conducted in the yirgalem substation in Sidaama region, Ethiopia. The Yirgalem substation is located in the Sidaama region about 314 km southern of Addis Ababa with a geographic reference and 42 km away from Hawassa. Distribution substation consists of 33 kV and 15kV middle voltage distribution line by step down transformer rated at 132/33kV and 132/15kV; low voltage customers are supplied by 400V or 220V with frequency of 50 Hz using 3-phase and 1-phase distribution line respectively. It incorporated many residential, industrial and commercial sectors.

3.3. Data Collection

For this thesis work, primary data and secondary data's would be collected from EEU, EEP and yirgalem substation. The data would be gathered through conducting interviews with the respective 47 personnel of the substations, Physical observation in the substations, past-recorded feeders loading (peak load and each hour load) data of the substation and distribution feeder roots, from Ethiopian Electric Utility (EEU) and Ethiopian Electric Power (EEP) engineering office. The collecting data would include line impedance, line reactance, line length, Bus connected ID (From Bus to Bus), bus description, bus nominal voltage, reactive and active power flow, transformers data, actual voltage level of the line and peak load data of the distribution network of case study. A general rule, it is necessary to test each location for at least 7 days at the points of common coupling (PCC) [60]. The electrical power of the factory is supplied to the installation via one incoming feeder from Yirgalem substation to keep good reliability.

1. Perform harmonic distortion level and voltage sag measurements for existing installation to characterize the sources on the system.

2. Evaluate the measured power quality issues levels with respect to selected standard limit/s. In addition, of the measurement data, different standards may require some additional parameters of the system under consideration. For instance, the short circuit ratio I_{SC}/I_L of the system needs to be calculated, in order to use the current distortion limits on IEEE std 519-2014.
3. If the system measurement does not meet the limits recommended by the selected standards, mitigation measures are necessary. Possible mitigation techniques for the problems would be identified; and the optimum one, which fits the system under consideration best, would be selected.
4. Evaluate the system again with the selected mitigation technique added to the system. Here different computer software can be utilized to model the system together with the selected mitigation technique and observe the overall response of the system.

3.4. Data Analysis

3.4.1. Electric Power Supply System to Awada Industry Zone

There are one incoming 132kv transmission lines from Hawassa substation to supply for Yirgalem substation. The incoming 132kv is stepped down and distributed by 33kv and 15kv feeders. The study area is served by three 132/33 kV, 25MVA and three 132/15 kV, 25MVA step down transformer (TR II and I) and the Substation consists of six outgoing feeders. Transformer one (TR I) power supplies for feeder 1, feeder 2 and feeder 3. Transformer two (TR II) power supplies for feeder 4, feeder 5, feeder 6 and its nominal voltage of the first three feeders is 15 kv and last three feeders is 33kv.

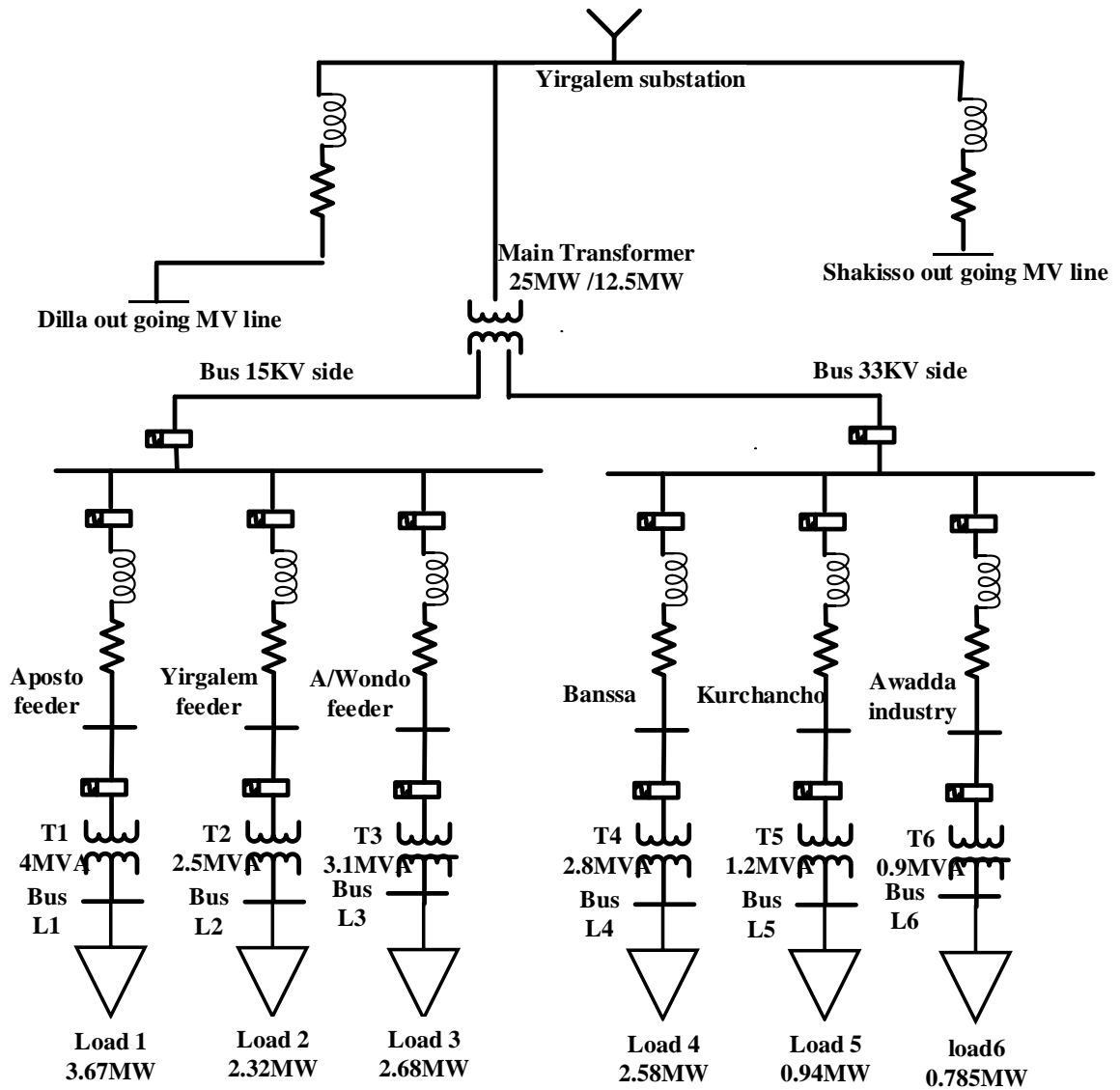


Figure 3. 1: Single line diagram of Yirgalem substation.

Among these feeders, Candidate feeder for possible study in this substation network was determined using load power quality analysis & load flow analysis algorithm to check presence of low level of power quality and harmonic pollution. In addition, harmonic pollution is increasing in power system causing power losses; sensitive equipment malfunctions and product wastage with recorded data were considered for this study.

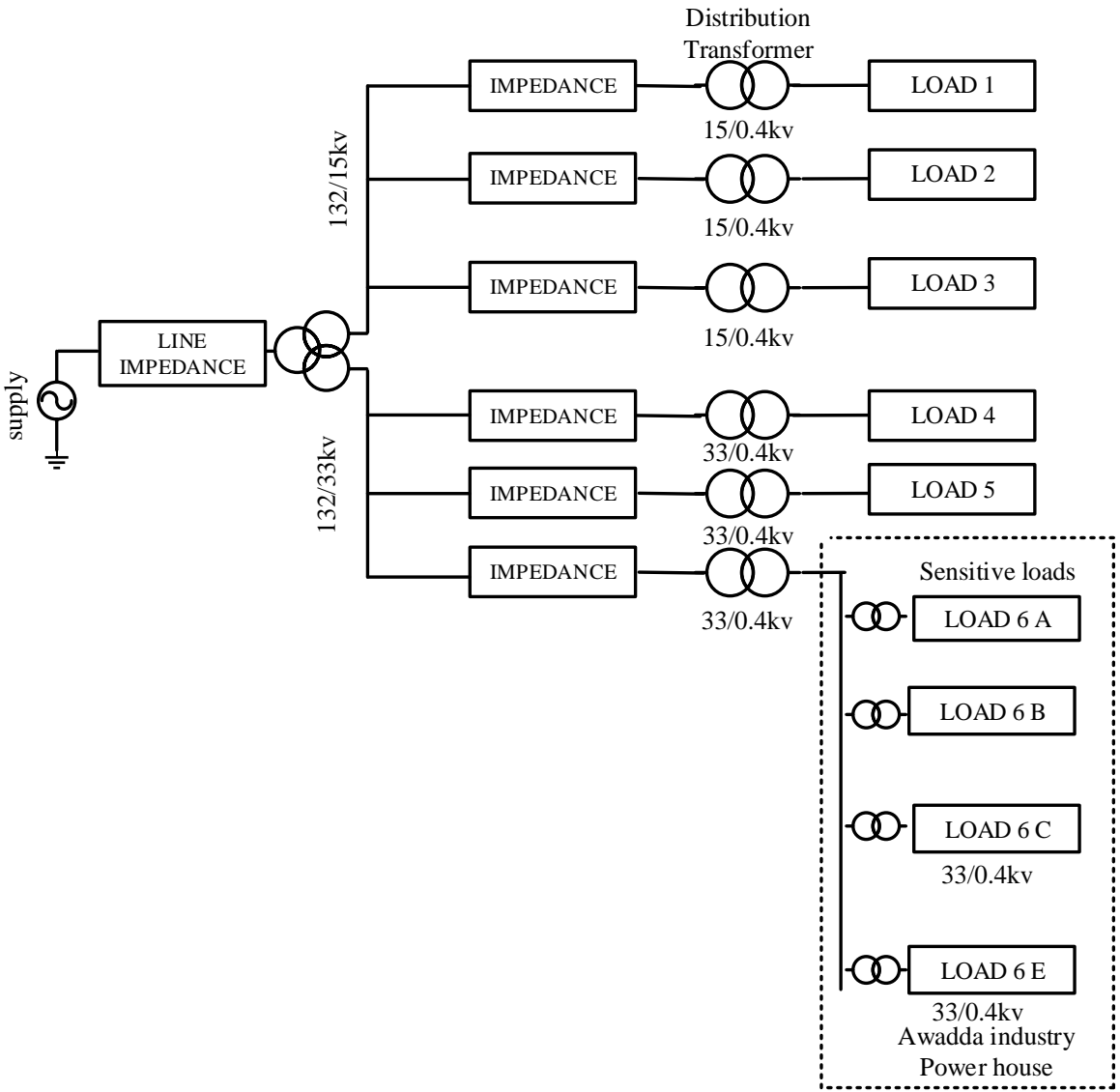


Figure 3. 2: Schematic diagram of Yirgalem substation.

3.4.2. Electrical Power Distribution Network of Awada Industry

The 33KV primary distribution feeder line from Yirgalem substation to Awada industry zone is an overhead distribution system. The industry is fed from a powerhouse, which is constructed within the plant. The distribution feeder line enters the powerhouse by underground system. As shown in figure 3.3, the 33kV feeder line is connected to three 33/0.4Kv, 1250kVA, %Z=5.05,

Delta-Wye and one 33/0.4KV, 800kVA, %Z=5.03, Delta-Wye step down net distribution transformers, through a common bus bar, to supply a maximum load of 2.85MW.

The electrical power in the factory is distributed through four Central Main Distribution Boards (CMDBs), as shown in Figure 3.3. These four CMDBs supply a number of different and scattered loads through Main Distribution Boards (MDBs) and Sub Distribution Boards (SDBs), placed at different locations in the plant near to the loads they fed.

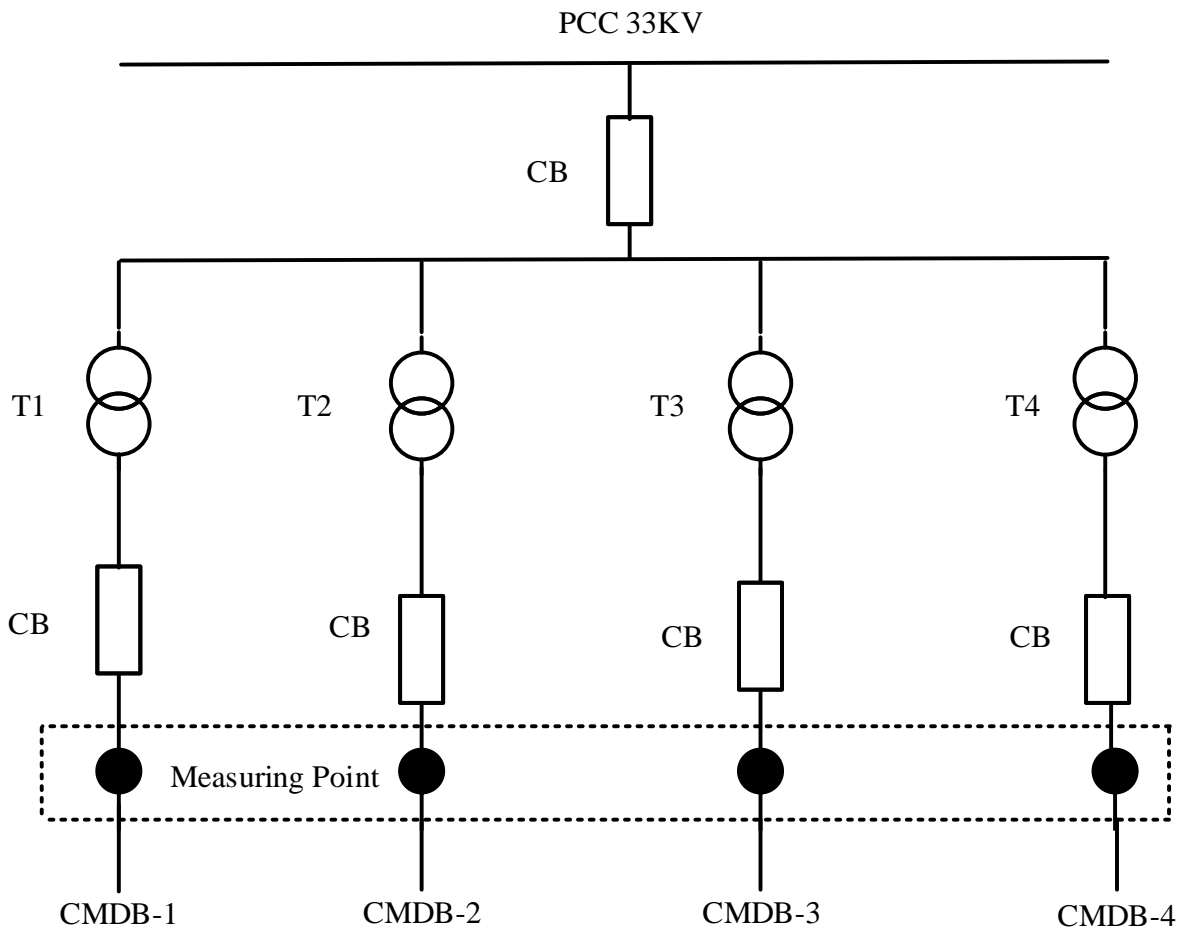


Figure 3. 3: Single line diagram of Power Distribution Network of Awada industry zone [61].

CMDB-1 supply power to the majority of the production machineries in the plant. On the other hand, the connected loads to CMDB-4 are mainly utility loads like huge Air Conditioning (AC) units, lighting loads, and office and kitchen equipment's. The factory has one 200KVA Stand-by Diesel generator connected to the emergency main distribution board (MDB-EM) via an Automatic Transfer Switch (ATS). This generator supplies power to administrative office, canteen,

stores, physical laboratory, compound lighting, and factory emergency lighting in the case of power interruption. The factory uses technologically advanced and energy efficient machineries, which are sensitive to small deviation in the supplied power quality and at the same time, have a tendency to distort the supplied pure sine wave. The loads in the industry can be categorized as follows.

- ASD (Inverters), Single and three phase Power Supplies, Microprocessor based controllers, Fluorescent lamps , Gas discharge lamps , Office equipment’s (computers, printers ...)

Of these load categories, the ASD and the AC induction motors are the most dominant loads in the industry. A total number of 155 ASD (frequency converters) with power ratings starting from 0.55 Kw up to 75 Kw are connected to the distribution network. The distribution of these ASDs on each distribution transformer is presented on Table 3.1. More harmonic distortion levels are likely to present on transformer T1 for the fact that higher total number and installed capacity of ASDs are connected to this transformer. In addition to the induction motors controlled by these ASD, there are many AC induction motors installed in the industry, which controlled by Direct on line (DOL) and Star-Delta starting methods.

Table 3. 1: Number and capacity of ASD on each transforms [61].

Transformer	Total number of ASDs (frequency inverters)	Total power estimated capacity of ASDs
T1	64	942 Kw
T2	21	202 Kw
T3	66	370 Kw
T4	4	56 Kw

3.4.3. Power Quality Related Problems in the Industry Zone

The weekly/monthly maintenance performance reports of the factory are reviewed in search of electrical problems happened in the industry because of power quality disturbances. Additionally, detail discussion with the factory engineers has been conducted to investigate additional problems related to power quality disturbance, which may not be recorded on reports due to different reasons. While conducting measurements for this study, a fire accident happens in CMDB-1 board,

all fuse boxes, and connecting cables of the capacitors have been damaged. The weekly/monthly maintenance performance reports indicate that this problem happens for the second time on the same CMDB board. Following are some of the problems, related to power quality and reliability, happened in the factory during the last couple of years.

a) Harmonics

The main industry standard used for harmonics in power systems is IEEE Standard. 519- 2014. This standard has been developed through the IEEE Industry Applications Society and the IEEE Power Engineering Society. Through the joint effort of these two societies, IEEE Standards. 519- 2014 suggests limits on the harmonic currents that a user can induce back into the utility power system and specifies the quality of the voltage that the utility should supply the user. The table below lists the harmonic current limits based on the size of the load with respect to the size of the power system to which the load is connected. The ratio I_{sc}/I_L is the ratio of the short circuit current available at the PCC [20] to the maximum fundamental load current.

The short circuit ratio (I_{sc}/I_L) is determined as follows:

- The three-phase short-circuit duty I_{sc} at the PCC may be obtained directly from the utility and expressed in amperes. If the short-circuit duty is given in MVA, it can be converted to an amperage value using the following expression:

$$I_{sc} = \frac{1000 \times \text{MVA}}{\sqrt{3} \times \text{kV}} \quad (3.1)$$

Where MVA and kV represent the three-phase, short-circuit capacity in mega-volt-amperes and the line-to-line voltage at the PCC in kV, respectively. Alternatively, the short circuit current in a circuit can be expressed as:

$$I_{sc} = \frac{V_{ph}}{Z_{sc}} \quad (3.2)$$

Assume that the impedance is purely reactive. This is a reasonably good assumption for industrial power systems for buses close to the mains and for most utility systems. Moreover, at utilization voltages, such as industrial power systems, the service transformer impedance often dominates the

equivalent system reactance. Therefore, the short circuit impedance can be approximated by the service transformer reactance.

We have the expression for percentage reactance, $\%X_{tr}$

$$\%X_{tr} = \frac{I_{FL} * X_{tr}}{V_{ph}} \times 100 \quad (3.3a)$$

$$X_{tr} = \frac{V_{ph}}{I_{FL}} \times \frac{\%X_{tr}}{100} \quad (3.3b)$$

Where I_{FL} the full is load current; V_{ph} is phase voltage; X_{tr} is reactance in ohms per phase of each transformer. Thus,

$$I_{sc} = \frac{I_{FL} * 100}{\%X_{sc}} = \frac{I_{FL} * 100}{\%X_{tr}} \quad (3.4)$$

The percentage reactance, $\%X_{tr}$, is calculated using equation 3.3 and 3.4, for T1, T2 and T3:

Equivalent utility reactance is 0.00634 ohms and 0.00987 ohms per phase at 0.4kv.

$$X_{tr(pu)} = X_{tr(old)} \left(\frac{KVA_{base}}{1000kv^2} \right)$$

$$\%X_{tr} = \frac{KVA * X_{tr}}{1000(kv^2)} * 100 = \frac{1250 * 0.00634}{1000(0.4^2)} * 100 = 4.95\%$$

$$I_{sc} = \frac{1804.22 * 100}{4.95} = 36448.9A$$

The percentage reactance, $\%X_{tr}$ for T4:

$$\%X_{tr} = \frac{KVA * X_{tr}}{1000(kv^2)} * 100 = \frac{800 * 0.00987}{1000(0.4^2)} = 4.94\%$$

$$I_{sc} = \frac{1154.7A * 100}{4.94} = 23374.5A$$

- The load average kilowatt demand PD for the most recent, Twelve months (April 2021- March 2022) harmonic distortion, and power factor data of each cost center is averaged for this analysis shown on Appendix B of this document. This report is prepared based on the measured value at the PCC for all four transformers and used for billing purpose by the

electric power utility. The average kilowatt demand PD for the period from (April 2021 to March, 2022) becomes:

Then, the average demand current calculated as follows:

$$I_L = \frac{\text{kw}}{\text{PF} * \sqrt{3} \times \text{kv}} \quad (3.5)$$

$$\text{PF} = \cos \left[\tan^{-1} \left(\frac{\text{total kvarh}}{\text{total kwh}} \right) \right] \quad (3.6)$$

$$\text{PF} = 0.8817$$

$$I_L = \frac{1270}{0.8815 * \sqrt{3} \times 0.4} = 2079.5\text{A}$$

The average demand current of each transformer is calculated based on the average percentage load share of the four transformers. The average percentage load share is calculated based on the monthly energy consumption by cost center report of the factory for the same duration from April 2021 to March 2022. The monthly percentage load share of each transformer is calculated by dividing the monthly energy consumption of each transformer to the total energy consumption of the four transformers. Then, 12 to get the average load share of each transformer divide the sum of the monthly percentage load share of the 12 (April, 2021 to March, 2022). Therefore, the average load share and corresponding average demand current becomes:

$$\text{T1: } 21.9\% \text{ of } I_L = 455.4\text{A}$$

$$\text{T2: } 24.1\% \text{ of } I_L = 501.2\text{A}$$

$$\text{T3: } 10.1\% \text{ of } I_L = 210.0\text{A}$$

$$\text{T4: } 43.9\% \text{ of } I_L = 912.9\text{A}$$

➤ Then, the short circuit ratio (I_{sc}/I_L) for each transformer found to be:

$$\text{For T1: } I_{sc}/I_L = 36448.9\text{A}/455.4\text{A} = 80 \quad \text{for T2: } I_{sc}/I_L = 36448.9\text{A}/501.2\text{A} = 72.7$$

$$\text{For T3: } I_{sc}/I_L = 23374.5\text{A}/210\text{A} = 111.3 \quad \text{for T4: } I_{sc}/I_L = 36448.9\text{A}/912.9\text{A} = 39.9$$

Therefore, as per the IEEE STD 519-2014, for the electrical system under consideration:

- Maximum acceptable voltage THD level of 8%, with a maximum percentage of 5% for individual harmonic components will be used for all the CMDB boards.
- Maximum acceptable current TDD level of 12%, 15%, and 8% with maximum percentage of 10%, 12%, and 7% for the individual harmonic components (3^{rd} to 11^{th}) will be used for CMDB-1.

Therefore, it is necessary to install D-STSTCOM for mitigation the current harmonic distortion to meet the IEEE standards values.

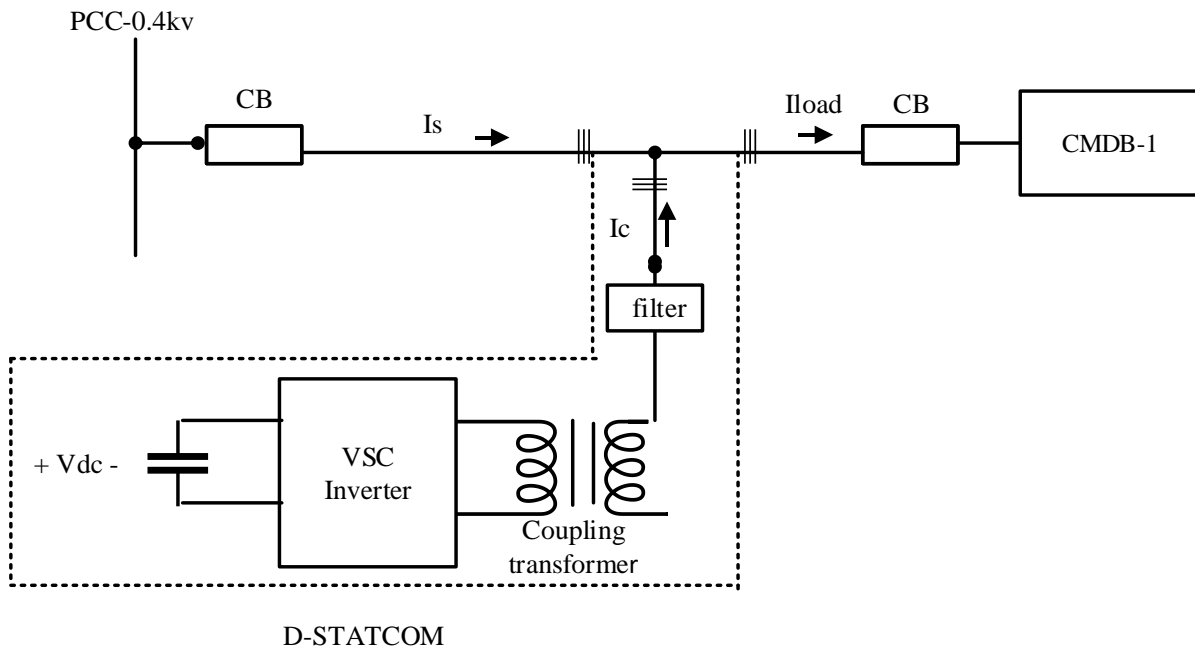


Figure 3. 4: Insertion of D-STATCOM for current harmonic distortion mitigation to CMDB-1.

Sources and Effect of Harmonics

Harmonic current emissions originate from all types of non-linear loads. Non-linear loads are loads, which draw non-sinusoidal current and voltage even when the supply voltage is perfectly sinusoidal. Non-linear loads include saturated magnetic circuits, such as those in power system transformers and rotating machines or induction motors in Awada industry zone, arc furnaces, fluorescent lighting and of course power electronic loads. Power electronic loads by far are the most significant harmonic contributors relative to the amount of energy they draw. Specifically, fifth and seventh harmonics are caused by static power converters used in adjustable speed drives

for motor control, switched mode power supplies and six-pulse static drives. Fifth and seventh harmonics creates a negative and positive torque, respectively on motors running from three-phase supply. Current distortion resulted from non-linear loads have significant adverse effects on both power system components and customer devices. These effects may result into permanent damage of the devices. The effects of harmonics in the industry range from false or spurious operations and trips of fuses and circuit breakers, overheating of transformers due to increased copper and core losses. The harmful effects of harmonics on transformers often unnoticed until an actual failure occurs and increased heating in motors due to additional copper losses and iron losses in the stator winding, rotor circuit and rotor laminations.

3.5. Standards on Harmonics

As discussed in chapter 2, Ethiopia has no national standard for limiting the level of harmonic distortion on electrical system. Moreover, the National Electro-technical Committee of Ethiopia (NECE) under the Ethiopia Standards Agency (ESA), which is responsible to approve and adopt international IEC standards to national standard, did not adopt the IEC 61000: EMC standards related to power quality phenomena for national use. As a result, the widely used and comprehensive international standards, IEEE and IEC harmonic distortion standards would be used as a reference for this study.

3.6. Modelling of Distribution Network

MATLAB/SIMULINK is a graphical programming environment for modeling, simulating and analyzing multi-domain dynamical system. This simulation software environment is used for simulating and analyzing the power quality performance of Awada industry distribution network. Its equivalent circuit (impedance diagram) models the distribution system. Calculations and assumptions taken in modeling different components of the distribution network are presented in the next sub-topics.

3.6.1. Distribution Transformers

Transformers are specified by their output voltage, kVA rating, percent impedance (percentage Z), and X/R ratio. Their series resistances and leakage reactance's model the transformers. The magnetizing current, shunt admittances and core losses are neglected, as is the case in most power

system analysis. The impedance of the transformer Z_{tr} can be calculated from the percentage impedance by using equation (3.7).

$$Z_{tr} = \frac{\%Z \times (KV)^2 \times 1000}{KVA * 100} \quad (3.7)$$

$$\%Z_{at \text{ new KVA}} = \frac{(\text{base KVA}_{\text{new}})}{KVA} \times \%Z_{at \text{ given KVA}} \quad (3.8)$$

The base KVA is selected to be 1250KVA. Normally, the X/R ratio of the transformers is not given on the nameplate. It can be requested from the manufacturer or can be calculated from transformer full load and no load loss values. Moreover, standard value of X/R ratio for different Transformer ratings is given on IEEE standard 141-1993 (Page 184), based on IEEE C37.010-1997. Since, no load and full load losses are specified only on one transformer nameplate, for uniformity of calculation, the standard values from IEEE STD 141-1993 is used for this study. From the graph, the X/R ratios for 1250KVA and 800KVA transformers are around 6.5 and 5, respectively. Then, the resistance and reactance values referred to the secondary side of the transformer are calculated for all the transformers as follows.

- I. Three transformers (T1, T2 and T4) of rating 1250 KVA, 50Hz, 33/0.4kv, $\%Z = 5.05$, $I_{pri} = 48.11A$, $I_{sec} = 1804.22A$, vector group: Dyn 5.

By using equation (3.1),

$$Z_{tr} = \frac{7.01 * (0.4)^2 * 1000}{1250 * 100} = 8.973 * 10^{-3} \Omega$$

$$Z_{base} = \frac{(V_{base})^2}{S_{base}} = \frac{(0.4)^2}{1.25} = 0.128 \Omega$$

By using the relation $Z^2 = R^2 + X^2$ and the X/R ratio of 6.5, the values of R_{tr} and X_{tr} of T1/T2/T4 become $R_{tr} = 0.625 * 10^{-3} \Omega$, $X_{tr} = 4.062 * 10^{-3} \Omega$.

- II. One transformer (T3) of rating 800 KVA, 50Hz, 33/0.4kv, $\%Z = 5.03$, $I_{pri} = 30.8A$, $I_{sec} = 1154.7$, vector group: Dyn 5, No load loss = 1508w, load loss = 723w.

Since the nameplate percentage Z value is given on the transformer's rating as a base KVA, it has to be converted to the selected base KVA, 1250KVA. The percentage Z on the base KVA of 1250 is:

$$\%Z_{\text{at new KVA}} = \frac{(1250\text{KVA})}{800\text{KVA}} \times 5.03 = 7.859\%$$

Similarly, by using equation (3.1),

$$Z_{tr} = \frac{7.859 * (0.4)^2 * 1000}{1250 * 100} = 1.006 * 10^{-2} \Omega$$

Again, by using the relation $Z^2 = R^2 + X^2$ and the X/R ratio of five, the values of R_{tr} and X_{tr} of T3 become $R_{tr} = 7.89 * 10^{-3} \Omega$, $X_{tr} = 39.4 * 10^{-3} \Omega$.

Table 3. 2: Calculated values of Rtr and Xtr for T1-T4.

Transformer	Transf. rating	R_{tr}	X_{tr}	L_{tr}
T1,T2 &T4	1250KVA	$2.037 * 10^{-2}$	$8.81 * 10^{-1}$	0.0202Mh
T3	800KVA	$8.8 * 10^{-2} \Omega$	$j4.5 * 10^{-1}$	0.0314Mh

3.6.2 Installed Loads

The electrical loads connected to the distribution boards are characterized as linear loads of active and reactive powers computed based on the actual power factor ($\cos \phi$) and the installed load data of each distribution board. The actual power factor of the loads is gathered from the factory's monthly energy consumption report of each cost centers. Twelve months (April 2021-March 2022) power factor data of each cost center is averaged for this analysis.

Table 3. 3: The active and reactive power of loads connected to each transformer [61].

Transformer category	Load category	Power (kw)	Reactive(Kvar)	Apparent power(KVA)
TR1	Load1	652.8	229.6	1250
	Load2	234.1	231.3	
TR2	Load3	392	319.2	1033
	Load4	255	106.0	
	Load5	82.1	306.4	
TR3	Load6	368.2	371.0	723
	Load7	200.6	75.7	
TR4	Load8	95.6	56.4	1135
	Load9	40.8	30.6	
	Load10	210.7	19.0	
	Load11	67	4.2	
	Load12	202.5	46.5	
	Load13	261	177.6	
	Load14	154	113.3	
	Load15	8.5	6.4	

In the model, the supplied voltage to the factory's distribution network is assumed to be balanced and pure sinusoid and represented by a balanced three-phase voltage source. Their equivalent winding resistances represent the distribution transformers and leakage reactance has connected in series. The magnetizing branch components are not considered in the model. The equivalent active and reactive loads connected to each transformer represent the installed electrical loads of the industry. The overall distribution network of the industry modeled in MATLAB/SIMULINK environment is presented in figure 3.5 below.

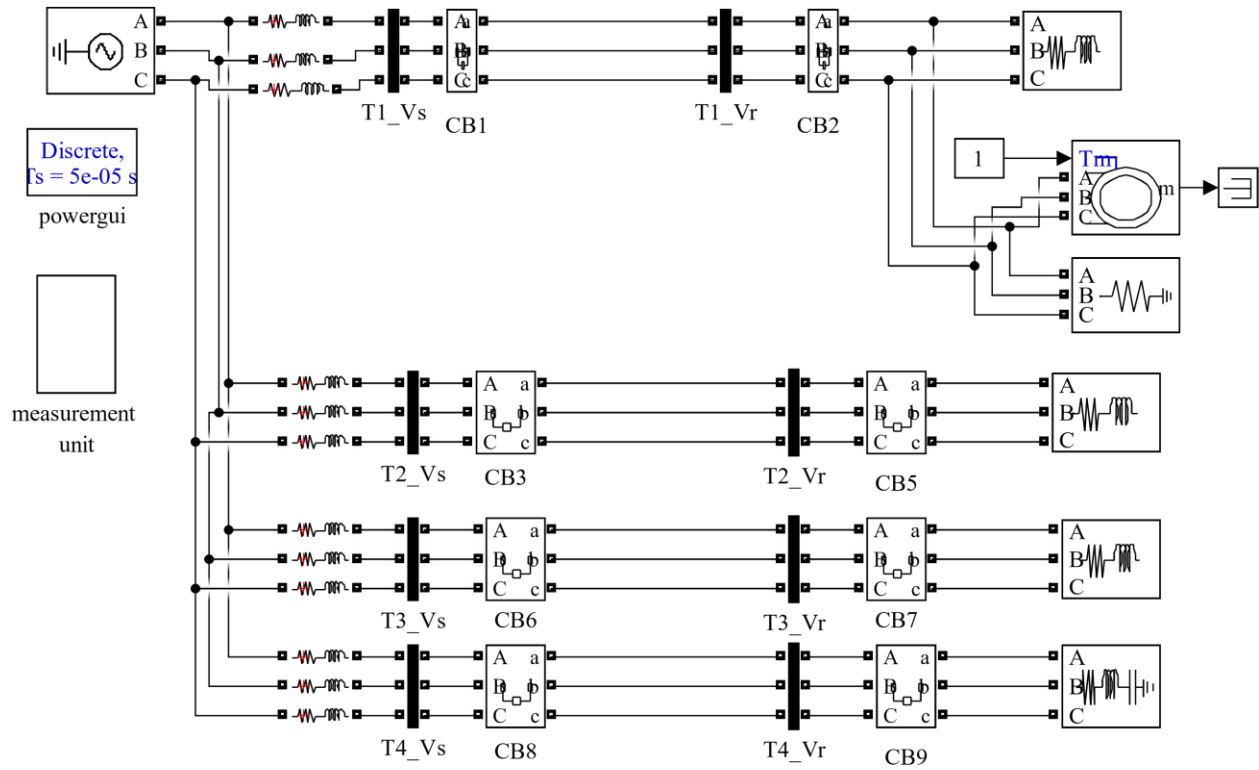


Figure 3. 5: SIMULINK model of Awada industry distribution system.

CHAPTER FOUR

4. Proposed Algorithms Used for Power Quality Issues Identify and Classify

In recent years, power quality (PQ) has become a significant issue for both utilities and customers. PQ issues and the resulting problems are the consequences of the increasing use of solid-state switching devices, non-linear and power electronically switched loads, unbalanced power systems, lighting controls, computer and data processing equipment, as well as industrial plant rectifiers and inverters. These electronic-type loads cause quasi-static harmonic dynamic voltage distortions, inrush, pulse-type current phenomenon with excessive harmonics, and high distortion. A PQ problem usually involves a variation in the electric service voltage or current, such as voltage sags and fluctuations, momentary interruptions, harmonics, and oscillatory transients, causing failure or inoperability of the power service equipment. Hence, to improve PQ, a fast and reliable detection of disturbances and sources and causes of such disturbances must be known before any appropriate mitigating action can be taken.

Digital signal processing, or signal processing in short, concerns the extraction of features and information from measured digital signals. A wide variety of signal-processing methods has been developed through the years both from the theoretical point of view and from the application point of view for a wide range of signals.

The algorithms for detection and classification of power quality disturbances (PQDs) are generally divided into three main steps:

(1) Generation of PQDs, (2) Feature extraction, and (3) classification of extracted vectors

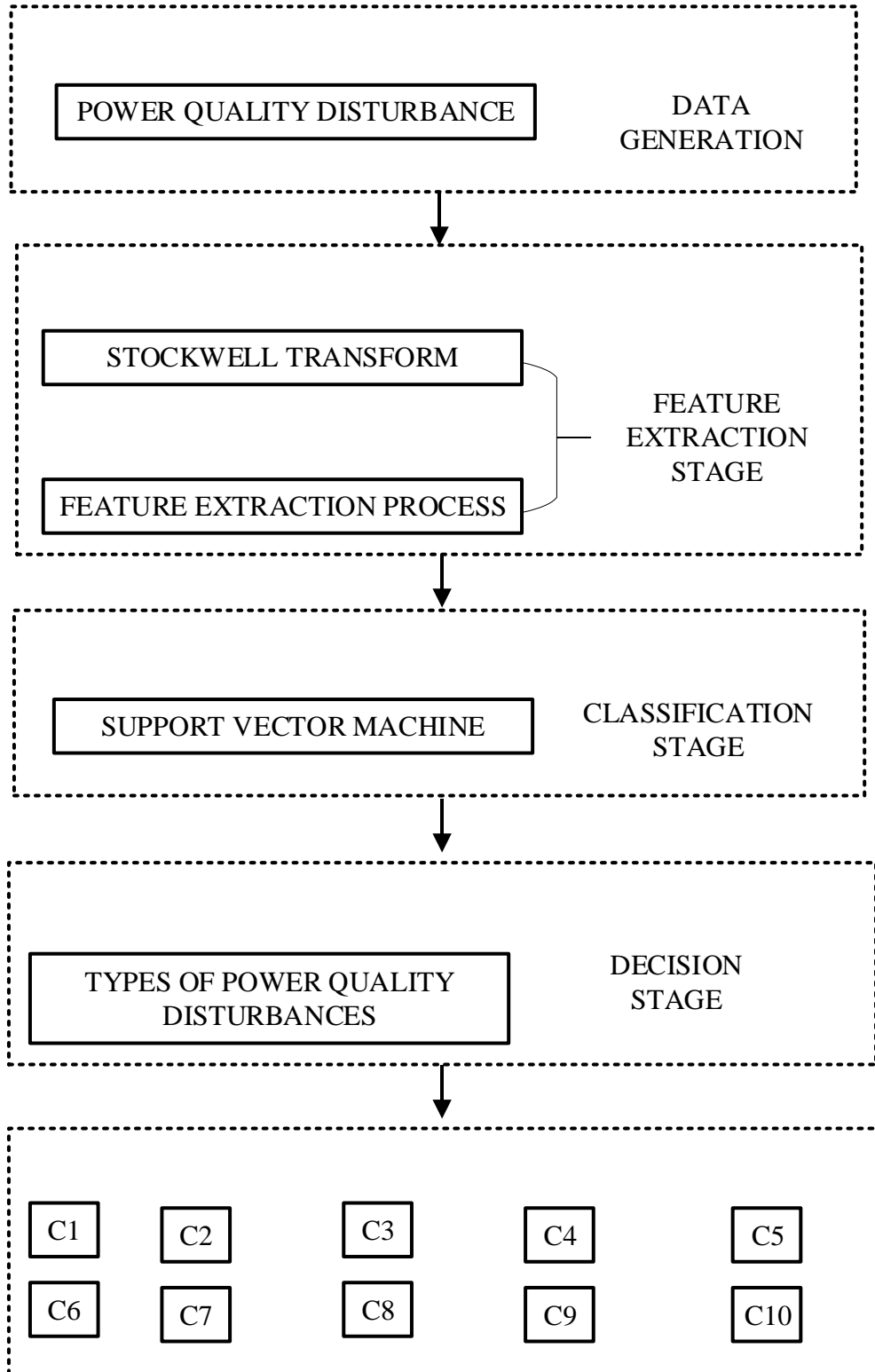


Figure 4. 1: Flow chart of proposed methodology.

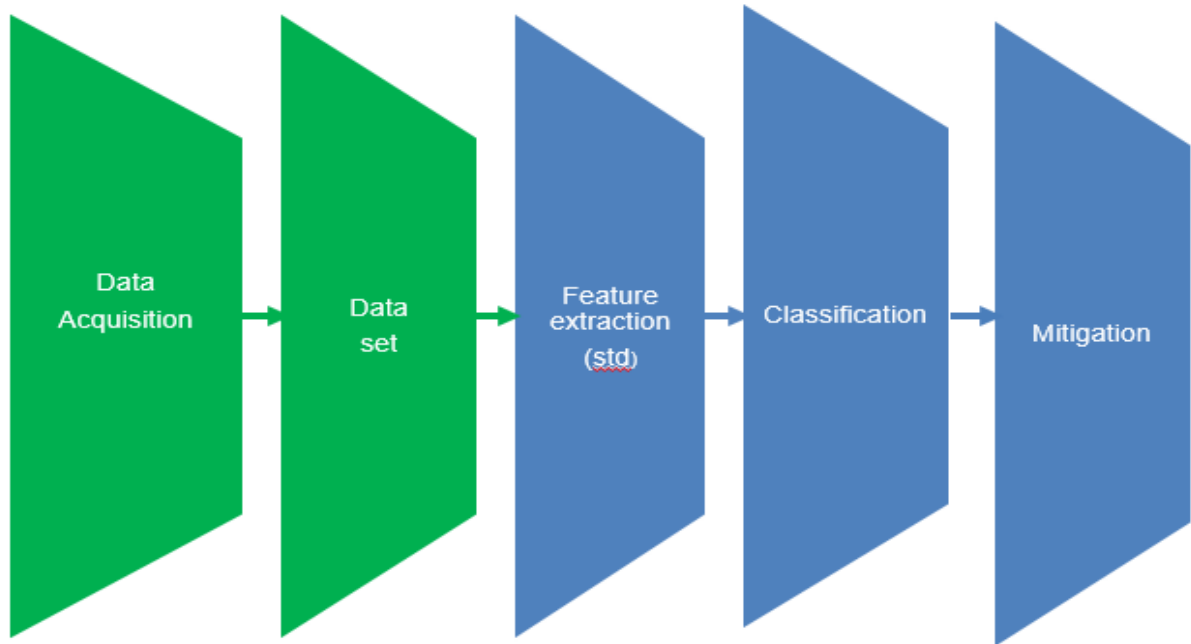


Figure 4. 2: Complete block diagram of proposed methodology.

1. PQ Disturbances Pattern Generation

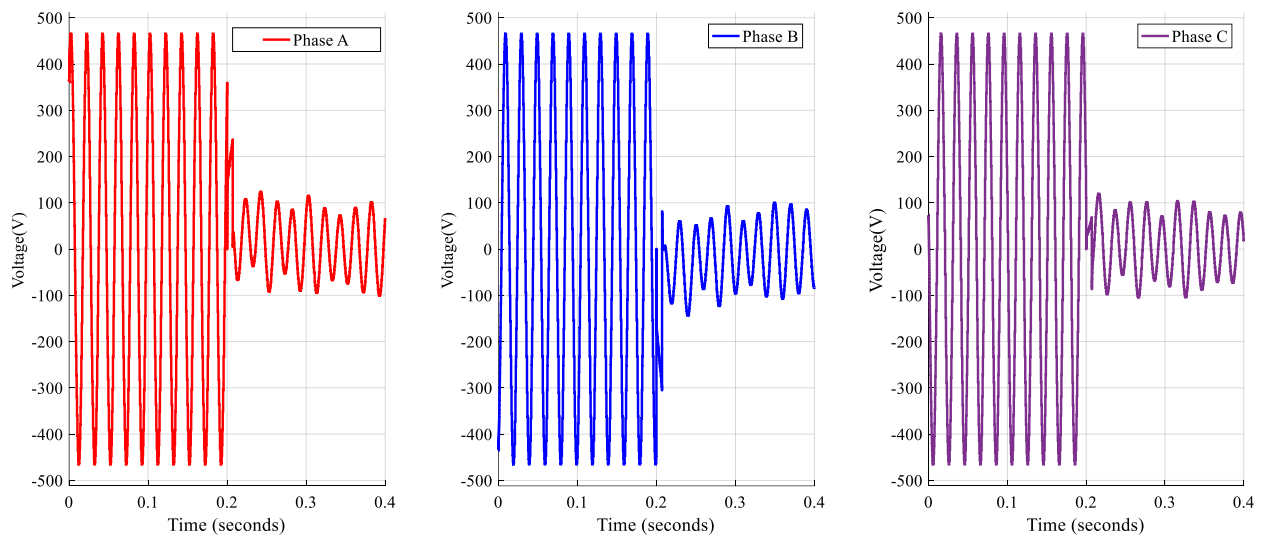


Figure 4. 3: (a) demonstrates the sample of the instantaneous waveform of measured voltage and current at the PCC.

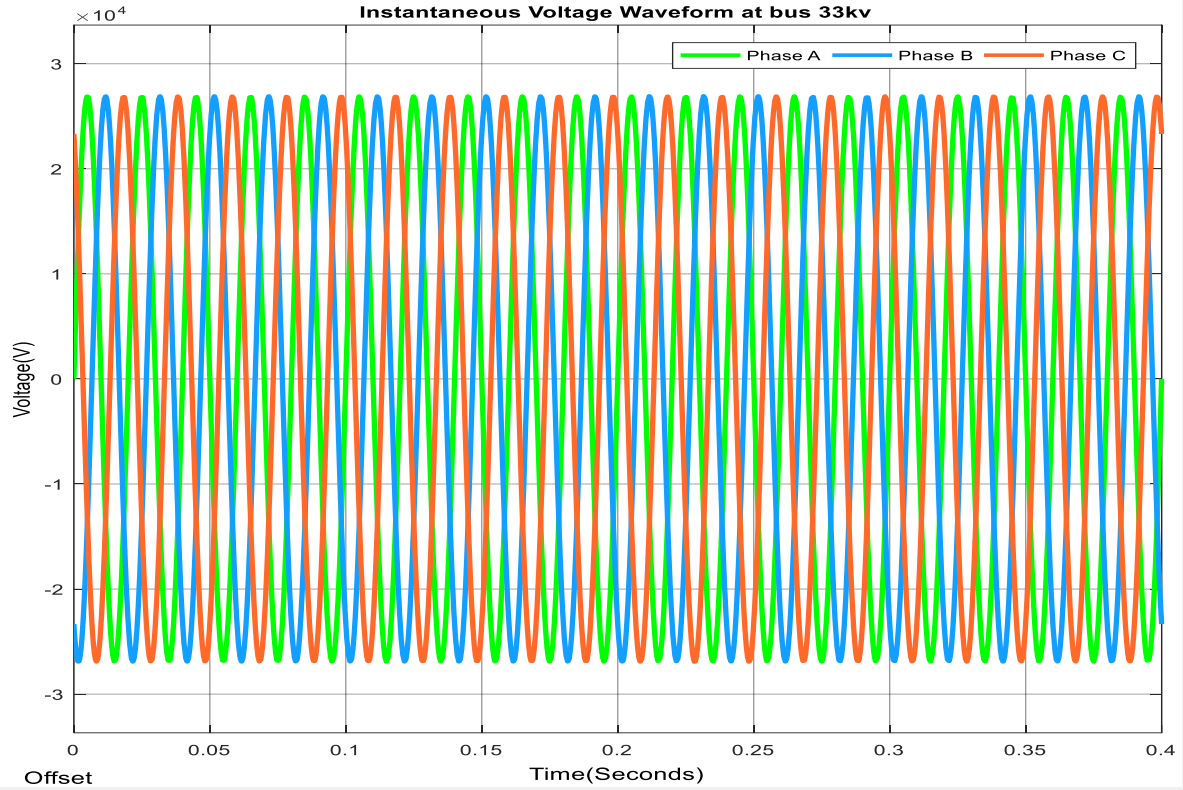


Figure 4. 4: (a) Instantaneous waveform of measured voltage at bus 33kv.

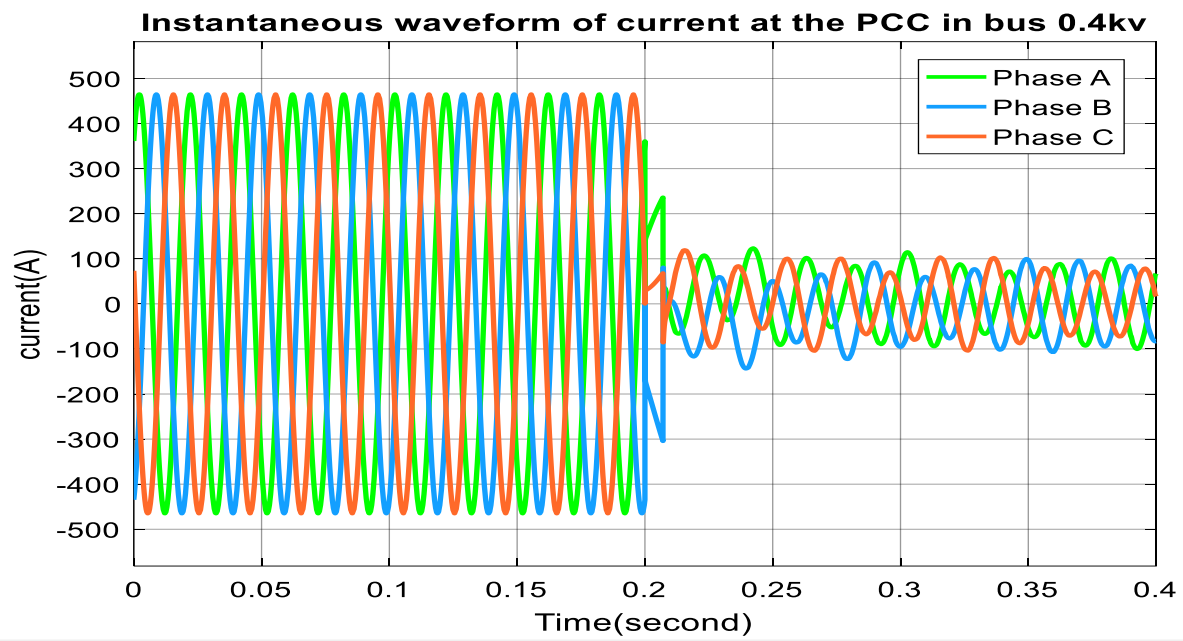


Figure 4. 5: (b) Instantaneous waveform of measured current at the PCC in bus 0.4kv.

4.1. Proposed Algorithm to Identify Power Quality Issues

4.1.1. Stockwell Transform

Detecting power quality problems is crucial to enhancing power quality level in electric power systems, and leads to effective decision making in handling these disturbances in the network. There are several ways to identify and classify power disturbances such as engineers capturing waveforms in the field. Unfortunately, manual capturing is almost impossible due to the data required to be sampled in modern power systems. Therefore, it is essential to investigate and study the waveforms of power quality disturbances, so they can be precisely detected and classified. Signal processing algorithms such as Fourier Transform, Stockwell Transform and Wavelet Transform have provided powerful mathematical algorithms for detecting power quality problems in electrical power systems, where they show significant successes in this field. Classification techniques support the detecting algorithm by testing, validating and training large amounts of power signals to ensure the effectiveness and efficiency of the chosen algorithm.

The multiresolution analysis (MRA) of the S-transform makes it as a suitable tool for time series analysis in power system environment [62]. Mathematically, the S-transform of a continuous time signal $h(t)$ has been presented in equation (4.1) as

$$S(\zeta, f) = \int_{-\infty}^{\infty} h(t) \frac{|f|}{\alpha\sqrt{2\pi}} e^{\left(\frac{-f^2(\zeta-t)^2}{2\alpha^2}\right)} dt \quad (4.1)$$

Where f is the frequency, t is the time and the ζ is the control parameter that controls the Gaussian window position on the t -axis. The factor α controls the time and the frequency resolution. As a result, the frequency resolution increases, when the parameter α value is above one. Similarly, if α decreases below one, the time resolution improves [63]. In this work, α is take as 0.5 for analysis of all these aforementioned signals.

A power signal $h(t)$, in discrete form is expressed as $h(kT)$, for $k = 1, 2, \dots, N - 1$ and the sampling time interval T . Mathematically, the discrete version of Fourier transform of the $h(kT)$, has been expressed [64] by equation (4.2)

$$H\left[\frac{n}{NT}\right] = \frac{1}{N} \sum_{k=1}^{N-1} h(kT) \cdot e^{\left(\frac{-i2\pi nk}{N}\right)} \quad (4.2)$$

Where $n = 0, 1, 2, \dots, N - 1$ The S-transform of a discrete time series $h(kT)$, is expressed by assuming.

$f \rightarrow n/NT$ and $\zeta \rightarrow jT$ is represented as

$$S\left[jT, \frac{n}{NT}\right] = \sum_{m=0}^{N-1} H\left[\frac{m+n}{NT}\right] G(m, n) e^{\frac{i2\pi mj}{N}} \quad (4.3)$$

And the $G(m, n) = e^{\frac{(i2\pi mj)^2}{N^2}}$, $n \neq 0$, where $j, m = 0, 1, 2, \dots, N-1$ and $n = 1, 2, \dots, N-1$. By assuming $n = 0$, equation (4.3) is given as in equation (4.4) as

$$s[jT, 0] = \sum_{m=0}^{N-1} h\left[\frac{m}{NT}\right] \quad (4.4)$$

The equation (4.4) provides zero frequency voice. The output of the S-transform is an $N \times M$ matrix is known as S-matrix. The row of the S-matrix represents the frequency and the column represent the time. Moreover, each element of the matrix is a complex value. The averaging of the amplitude of the S-matrix over time results in Fourier spectrum [64].

This matrix can be represented by below mentioned mathematical formulation.

$$S(\tau, f) = A(\tau, f)e^{-i\varphi(\tau, f)} \quad (4.5)$$

Here, $A(\tau, f)$: magnitude of amplitude, $\varphi(\tau, f)$: phase. Row and column of ST matrix correspond to frequency and time in respective order. Every column indicates frequency components of the signal at a moment of time. Every row indicates magnitude of a frequency component in respect to time which is indicated by samples ranging from 0 to $N - 1$. The S-matrix is used to compute the information related to magnitude, frequency and phase of a signal. Contour of magnitude represents a locus of maximum value computed from ST matrix at a time moment. For computing phase, regions of highest amplitude are examined from S-matrix, and respective phase is computed at these points. Frequencies of signal are computed from ST matrix and detailed by a contour known as frequency contour. ST-amplitude (STA) matrix is utilized for analysis of complex PQ events and computed using as $|S[jT, n/NT]|$.

The output of the S-transform is an $N \times M$ matrix is known as S-matrix. The row of the S-matrix represents the frequency and the column represent the time. Moreover, each element of the matrix is a complex value. The averaging of the amplitude of the S-matrix over time results in Fourier spectrum [30].

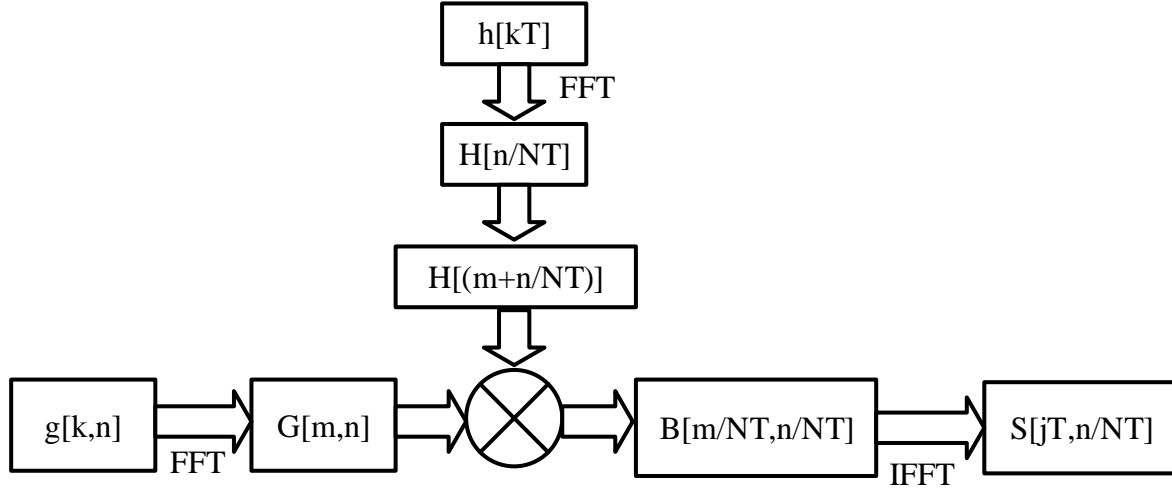


Figure 4. 6: Flow chart ST Algorithm [65].

The following steps are adapted for computing the discrete S-Transform [65].

- 1) Perform the discrete Fourier transform of the original time series $h(kT)$ (with N points and sampling interval T) to get $H\left[\frac{n}{NT}\right]$ using the FFT routine. This is only done once.
- 2) Calculate the localizing Gaussian $G(m, n)$ for the required frequency $\frac{m}{NT}$.
- 3) Shift the spectrum $H\left[\frac{n}{NT}\right]$ to $H\left[\frac{n+m}{NT}\right]$ for the frequency $\frac{m}{NT}$ (one pointer addition).
- 4) Multiply by to get $H\left[\frac{n+m}{NT}\right]$ by $G(m, n)$ to get $B\left[\frac{m}{NT}, \frac{n}{NT}\right]$ (N multiplications).
- 5) Inverse Fourier transform of $B\left[\frac{m}{NT}, \frac{n}{NT}\right]$ $\frac{n}{NT}$ to j to give the row of $S\left[jT, \frac{n}{NT}\right]$ corresponding to the frequency $\frac{n}{NT}$.
- 6) Repeat steps 3, 4, and 5 until all the rows of $S\left[jT, \frac{n}{NT}\right]$ corresponding to all discrete frequencies have been defined $\frac{n}{NT}$.

Harmonic power quality issues

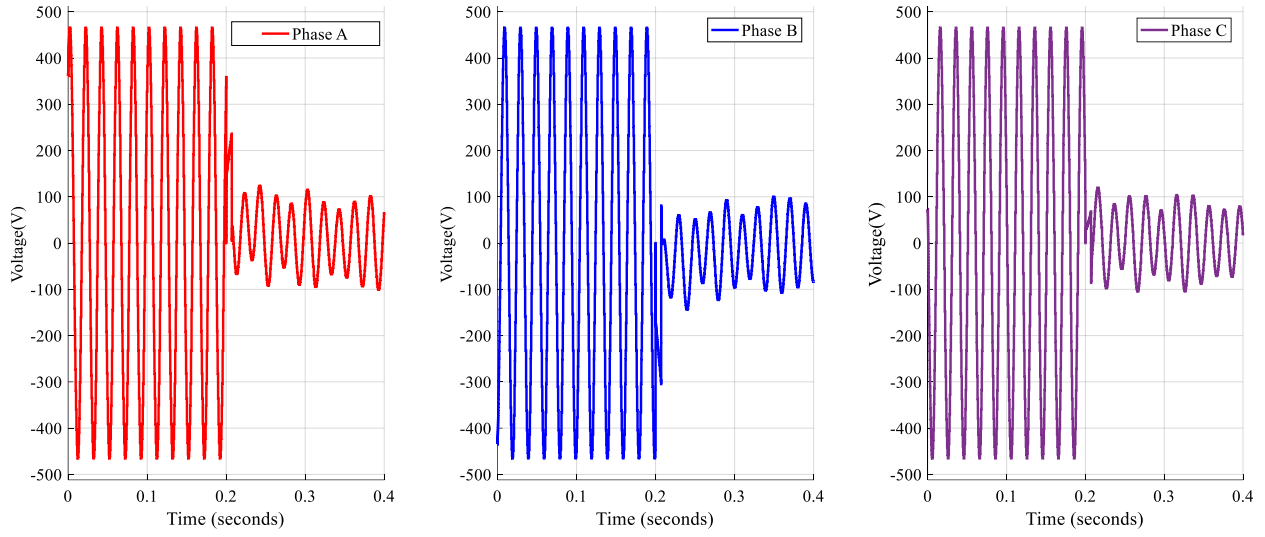


Figure 4. 7: Instantaneous waveform of measured voltage at the PCC phase a.

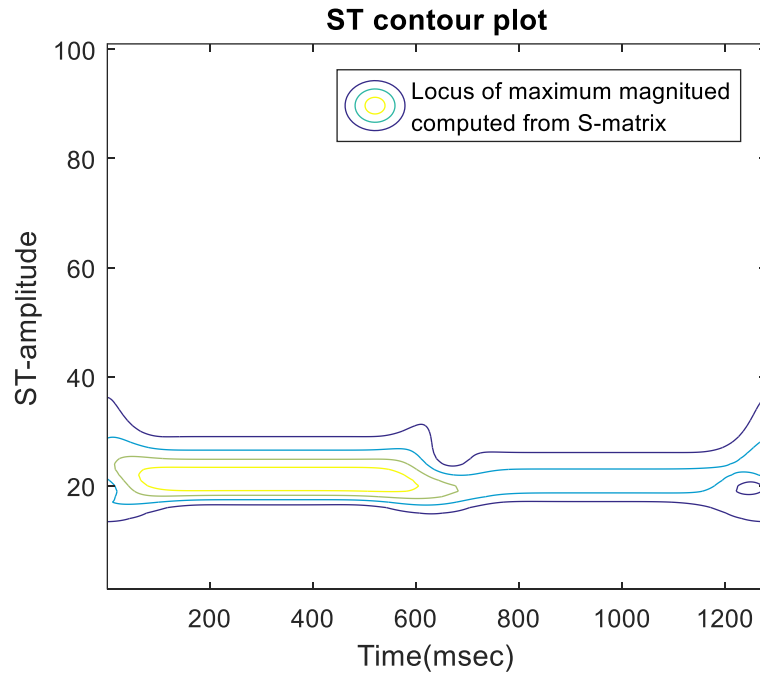


Figure 4. 8: Contour plots of S- transform absolute value coefficients in phase a with harmonic.

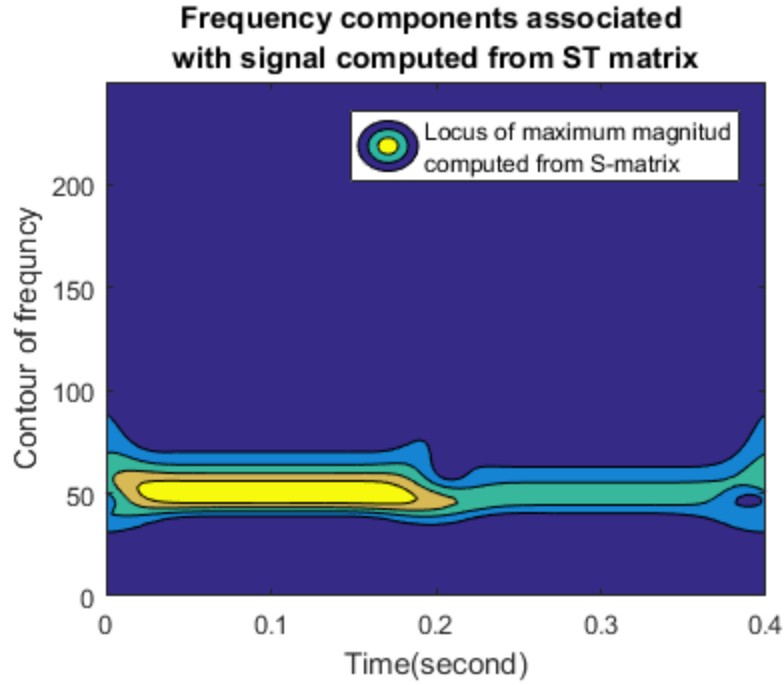


Figure 4. 9: Signal contaminated with Instantaneous voltage and S- transform contours absolute value.

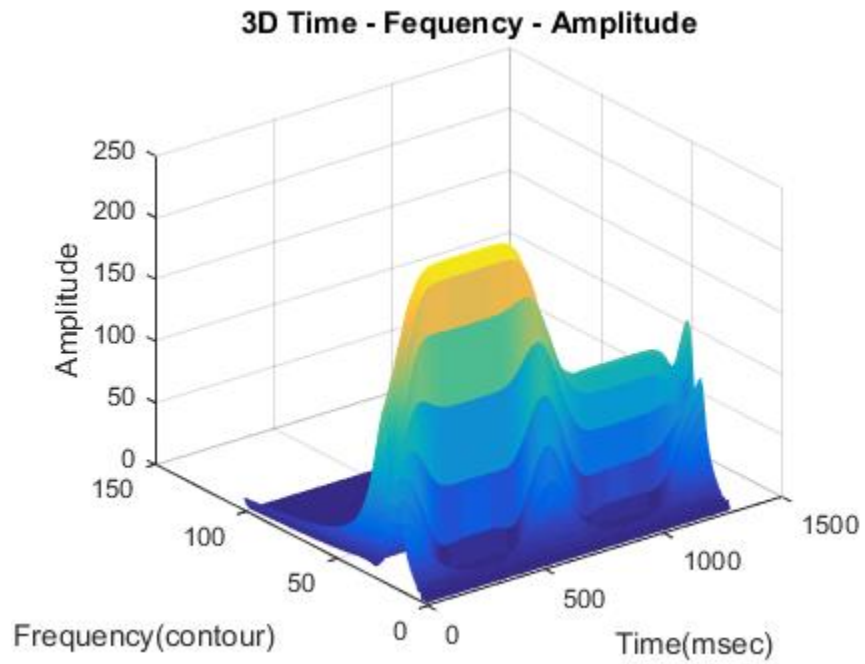


Figure 4. 10: 3D mesh Time-Frequency-Amplitude.

Swell power quality issues

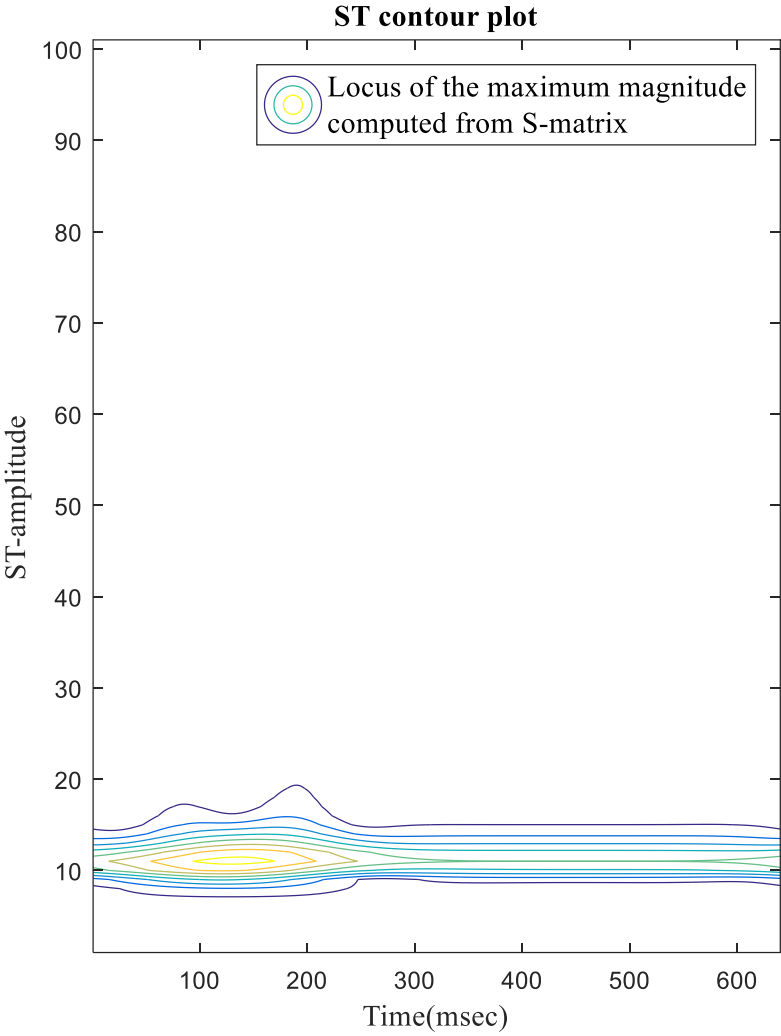


Figure 4. 11: Contour plots of S- transform absolute value coefficients in phase A swell.

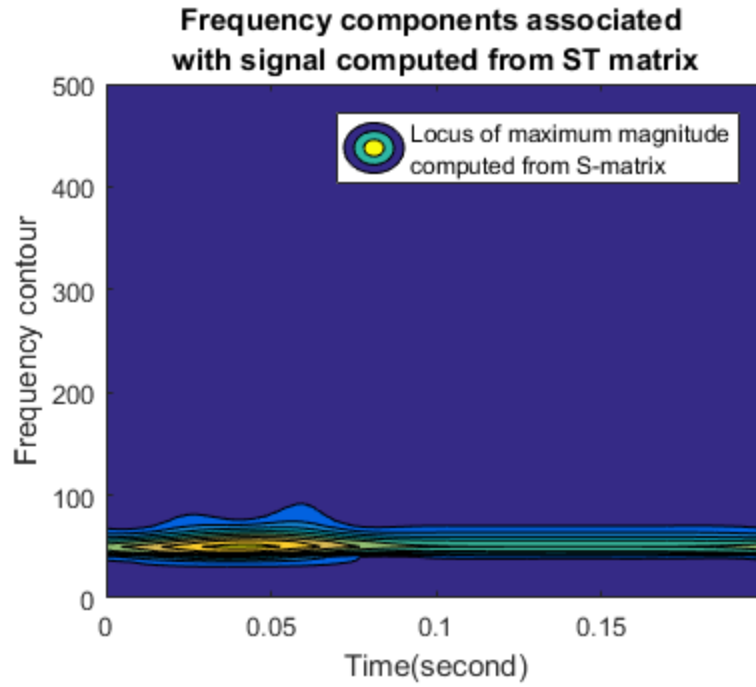


Figure 4. 12: Signal contaminated with Instantaneous voltage and S-transform contours absolute value.

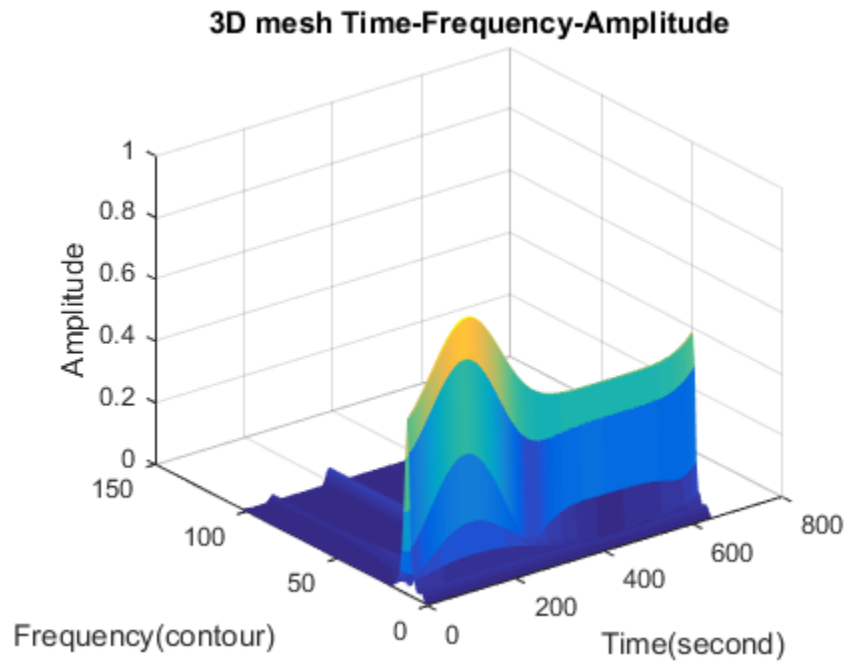


Figure 4. 13: 3D mesh Time-Frequency-Amplitude.

Interruption, power quality problems

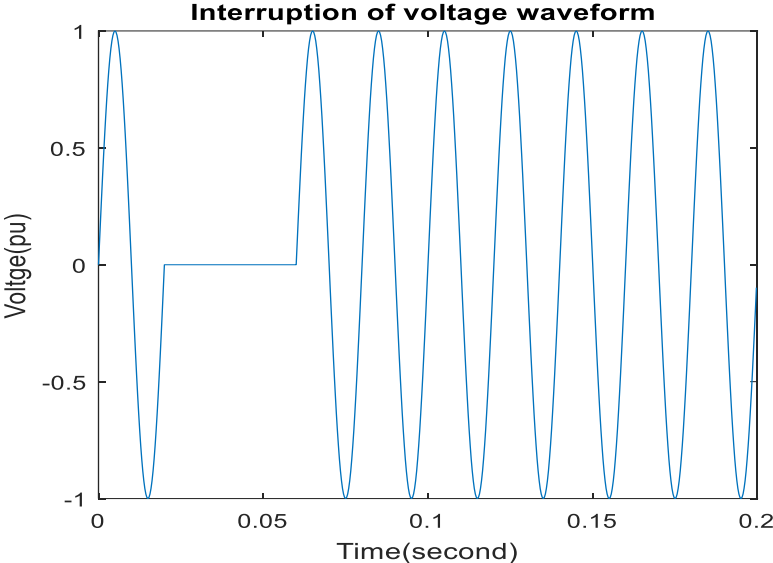


Figure 4. 14: Instantaneous waveform of measured voltage at the PCC phase a.

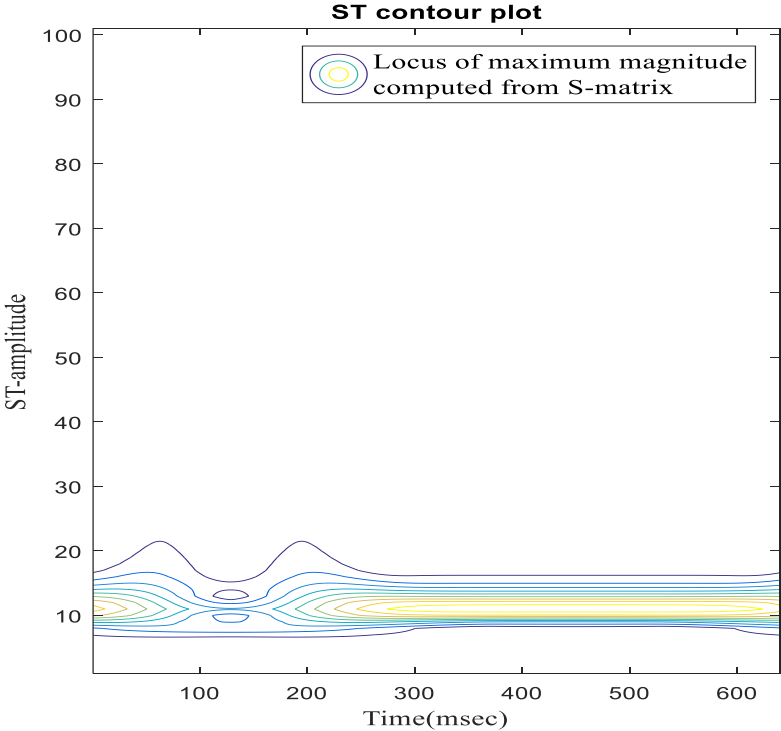


Figure 4. 15: Contour plots of S- transform absolute value coefficients in phase a.

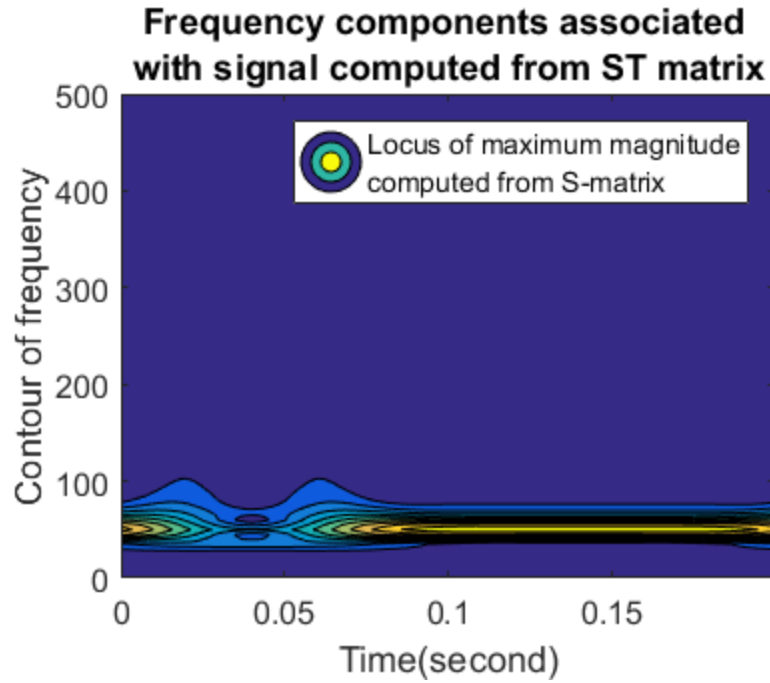


Figure 4. 16: Signal contaminated with interruption voltage and S- transform contours absolute value.

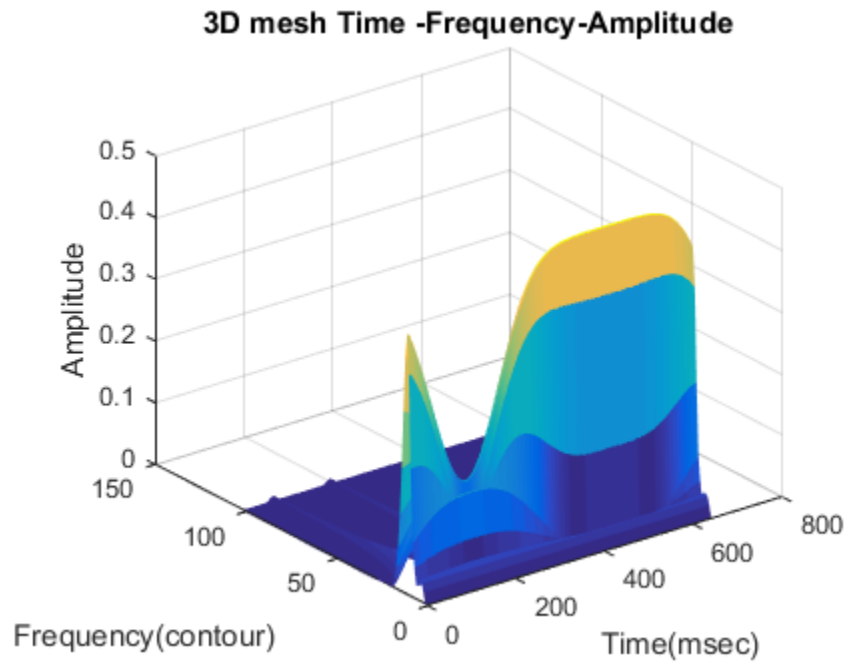


Figure 4. 17: 3D mesh Time-Frequency-Amplitude.

The S-transform will also generate time frequency contours, which can display the disturbance patterns for the respective single power quality disturbances. A single power quality disturbance and its' S-transform contours are shown in Figure 4.8.

In Figures 4.7 and 4.14, the Instantaneous waveform of measured voltage at the PCC phase a are displayed in its original waveforms respectively and in Figures 4.8, 4.11 and 4.15 the S-transform contours show the existence of the different voltage disturbance between the times of 0-600 and 600-1200 , 0 -250 and 0-100 , 100-200 milliseconds respectively.

From the graphical results in Figure 4.10, 4.13 and 4.17 it were shown that the S-transform contours could be used to detect both the single and multiple disturbances in 3D mesh Time-Frequency-Amplitude. The superior properties of the S-transform are because the modulating sinusoids are fixed with respect to the time axis while the localizing scalable Gaussian window dilates and translates. As a result, the phase spectrum is absolute in the sense that it is always referred to the origin or the time axis, the fixed reference point. The real and imaginary spectrum can be localized independently with a resolution in time, corresponding to the basis function in question, the changes in the absolute phase of a constituent frequency can be followed in long the time axis, and useful information can be extracted.

The main advantage offered by the technique is the use of the S-transform to decompose the power line signals into a set of time-frequency components in which simple and powerful feature extraction and feature selection can be performed. The choice of the S-transform was made due to its characteristics that can uniquely combine a frequency dependent resolution that simultaneously localizes the real and imaginary spectra of the original waveforms. The ST has provided the proper localization of the sag. These features are then used by classification technique to recognize the respective disturbance patterns in disturbance waveforms. The numerical results obtained with actual power quality data recorded in an industrial power system indicated that the new technique has perfect classification accuracy in the identification of multiple disturbances.

Figure 4.10, 4.13 & 4.17 shows the 3D ST plots for each signals used to determine the amplitude deviations of the frequency spectral elements within the signals. This model can support to realize all voltage deviations and the identification of the voltage change disturbance.

2. Feature Extraction

Feature extraction stage is the most important step for the machine learning based pattern recognition and classification of PQD problems. Extracted features are the measured data, obtained from the waveform samples to develop a feature vector. This feature vector should be dimensionally concise so that learning and generalization process in classifier algorithms for classification can be implemented effectively. Feature extraction stage consists of two sub stages.

A. Energy Feature:

The energy feature mining is according to the property which states that energy of the signal in time domain and in the frequency domain are equal, as frequency domain signal $X[n]$, i.e. Fourier transformed signal contains all the information about $X[t]$. This property is termed as Parseval's Theorem.

$$E_{sig}(t) = \frac{1}{T} \int_0^T |x(t)|^2 dt \quad (4.6)$$

$$E_{sig}(n) = \frac{1}{N} \sum_{n=1}^N |X[n]|^2 \quad (4.7)$$

Where t denotes the time and n is the sampling period of the signal waveform. The energy features of the PQDs are obtained from wavelet coefficients A_j and D_j , which are obtained at various frequency bands for each of the disturbance types. The energy feature vector consists of energy percentage corresponding to the respective wavelet coefficients, which are calculated by the relations shown in equation (4.8) and (4.9).

$$E_{Di} = \frac{1}{N} \sum_{j=1}^N |D_{i,j}|^2 \quad (4.8)$$

$i=1,2,3,\dots,L$

$$E_{Ai} = \frac{1}{N} \sum_{j=1}^N |A_{i,j}|^2 \quad (4.9)$$

$$E_i = [E_{A1} E_{A2} \dots E_{Al} E_{A1}, E_{D1} E_{D2} \dots E_{Dl} E_{Dl}] \quad (4.10)$$

E_{Dj} and E_{Dj} are the energies of wavelet-approximation and detail coefficients up to level j and E_i is the energy feature vector.

B. Entropy Feature:

Entropy parameter has been found suitable as a feature for PQD classification and recognition. In information theory, entropy is generally regarded as the precise indicator of disorder ness, imbalance and uncertainties relating to random variables that may be gained by the observations, whereas entropy is always greater than or equal to zero. Its outcomes can be generalized to provide information about specific events and outliers. Shannon entropy, a decreasing functions of a scattering of random variables and is maximum when all outcomes are equally to be expected. Following are the relations for Shannon entropy for detail and approximation level coefficients.

$$Ent_{Di} = - \sum_{j=1}^N D_{i,j}^2 \log(D_{i,j}^2) \quad (4.12)$$

$$Ent_{Ai} = - \sum_{j=1}^N A_{i,j}^2 \log(A_{i,j}^2) \quad (4.13)$$

Where A_i , and D_i , is the probability of the occurrence of feature values $\{D1.....8, A8\}$ and $i = 1....10$. Over all entropy, features obtained from the MRA based DWT for any PQ Signals are given by

$$Ent_i = [Ent_{D1} Ent_{D1} \dots Ent_{D1} Ent_{D1}, E_{D1} E_{D2} Ent_{A8}] \quad (4.14)$$

C. Standard Deviation:

Standard deviation feature measures the dispersion of an event frequency distribution or it can also be defined as a parameter that shows the way in which a probability function or probability density function is centered around its mean which is equal to the root of moment in which the deviation from mean is squared.

$$S. D_{D_j} = \sqrt{\frac{\sum_{j=1}^N (D_j - mean)^2}{N - 1}} \quad (4.15)$$

$$S.D_{A_j} = \sqrt{\frac{\sum_{j=1}^N (A_j - mean)^2}{N - 1}} \quad (4.16)$$

$$SD_i = E_i = [SD_{D_1} SD_{D_2} \dots SD_{D_l} SD_{D_l}] \quad (4.17)$$

$$Feature_i = [E_i Ent_i SD_{D_i}] \quad (4.18)$$

The feature vector obtained for i samples is used for the classification purpose in the classification stage for each of the PQDs type. Where half of the data is utilized for training the classifier and other, half is used for testing the classifier performance. Schematic diagram for the feature vector development is shown in Figure 4.7.

4.2. Proposed Algorithm to Classify Power Quality Issues

4.2.1. Support Vector Machine Classifier

The Support vector machine (SVM) tool, first presented by Vapnik (Vapnik, 1995), is a very powerful, high performance and computationally efficient family of supervised machine learning algorithm. It has wide application in classification and regression (time series prediction like estimation, forecasting, etc.) problems [48]. For PQD waveform pattern recognition, classification can be performed by utilizing various parameters. In literature, PQD classification is mostly based on statistical learning theory results [48]- [50]. For two or more categorized classes of disturbance data, it acts as discriminative classifier typically defined by an optimal hyperplane, separates all the categorized classes by the decision boundary, as shown in Figure 4.18. The hyperplane can be defined mathematically as:

$$g(x) = x'\theta + b = 0 \quad (4.19)$$

$\theta \in R$, for dimension d, comprises the coefficients expressing orthogonal vector to hyper plane. Hyperplane is a linear decision boundary that splits the space for classification into two parts. For inseparable and complex data, kernel functions are adopted. These functions transform data to large dimensional feature space where input data becomes more separable i.e. maximum margin hyper planes are established, related to original input feature space. Gaussian or radial basis function, sigmoid, polynomials, exponential radial basis functions, splines Etc. are the generally used types of Kernel functions in the literature [49]. In this thesis work, Gaussian kernel is adopted

for binary classification and feature mapping. The mathematical relation for Gaussian kernel is given as:

$$f(x_i, l_j) = \frac{\exp(-\|x_i - l_j\|^2)}{2\sigma^2} \quad (4.20)$$

In equation (4.20) x_i represents feature and l_j , landmark point whereas σ is a Gaussian kernel parameter, features $f(x_i, l_j)$ to vary more smoothly. For the classification let the training vector is $x_j \in R$, along with their categories $y_j = (-, +)$ where algorithm searches maximum margin length i.e. the region which contains no observations, for an optimal hyper plane and places the observations in the positive and negative class categories. From equation (4.19), for Separable class's classification, an objective is to minimize $\|\theta\|$ with respect to b and θ .

So that for all feature vectors (x_i, y_j) , $y_j g(x_j) \geq 1$. When support vectors x_j are on the boundary, $y_j g(x_j)$ is equal to one. To optimize and minimize the objective, SVM algorithm uses Lagrange multiplier, as shown in equation (4.21). To minimize the equation (4.21), subject to $\sum \alpha_j \cdot y_j$ is equal to zero.

$$0.5 \sum_{j=1}^a \sum_{k=1}^n \alpha_j \alpha_k y_j y_k G(x_j, x_k) - \sum_{j=1}^n \alpha_j \quad (4.21)$$

Where $\alpha_j \geq 0$ and $j = 1, 2, \dots, n$

$$\alpha_j [y_j g(x_j) - 1 + \delta_j] = 0 \quad (4.22)$$

$$\delta_j (C - \alpha_j) = 0$$

Whereas,

$$g(x_j) = \varphi(x_j)' \theta + b \quad (4.23)$$

In above equation φ is a kernel function. δ_j is entitled slack parameter and C is regularization parameter. For perfectly separable class's slack parameter, δ_j is equal to zero.

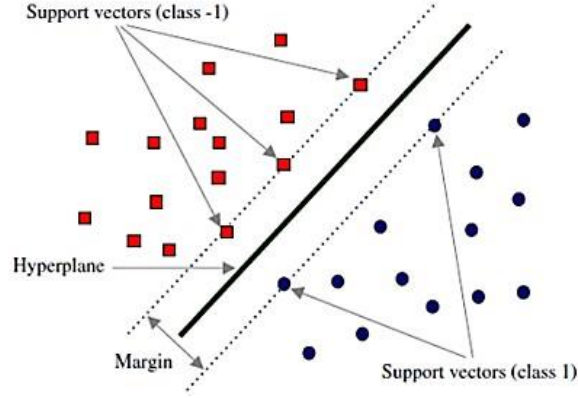


Figure 4. 18: Support Vector Machine Classification Schematic [49].

In case of inseparable classes, minimizing equation (4.24) with respect to θ , b and δ_j , subject to equation (4.16).

$$0.5\|\theta\|^2 + C \sum \delta_j \quad (4.24)$$

$$y_j g(x_j) \geq 1 - \delta_j \quad (4.25)$$

Where $\delta_j \geq 0$, except $0 \leq \alpha_j \leq C$, for all $j = 1, 2, 3, \dots, n$. SVM Score function is shown in equation (4.26) as:

$$\tilde{g}(x) = \sum_{j=1}^n \tilde{a}_j y_j x \cdot x_j + \tilde{b} \quad (4.26)$$

Where \tilde{b} the bias is estimate and \tilde{a}_j is j th vector estimate. The SVM classifies new observation z using $\text{sign}(\tilde{g}(z))$. Non-linear boundary in SVM works in transformed predictor space to get optimal hyperplane.

The dual formalization for nonlinear SVM is represented in equation (4.27) with respect to a_1, a_2, \dots, a_n , subject to $\sum \alpha_j y_j$ is equal to zero, where $0 \leq \alpha_j \leq C$

$$0.5 \sum_{j=1}^n \sum_{k=1}^n a_j a_k y_j y_k G(x_j, x_k) - \sum_{j=1}^n a_j \quad (4.27)$$

For all $j=1,2,\dots,n$. and the complementarity conditions. $G(x_j, x_k)$ are the elements of the Gram matrix. The resulting score function for SVM is given in equation (4.28).

$$\hat{g}(x) = \sum_{j=1}^n \hat{a}_j y_j G(x_j, x_k) + \hat{b} \quad (4.28)$$

SVM has better generalization ability (i.e. ability to learn a rule for classifying training data to ability of resulting rule to classify testing data.). It may handle large feature vector dimension space and has no over fitting issue for large classification problems as compared to logistic regression and neural network or other conventional classifiers. SVM training is much easier than training artificial neural networks [49].

3. Classification Stage

The Feature_i feature vector, developed in equation(4.18), comprises of 27 dimensions of feature dataset for 250 samples of each of the PQ disturbance class i.e. 27×250 . From 250 samples of each disturbance class, half of the data set has been used for training the SVM classifier and rest of data is for testing purpose. For classification training with SVM, one vs. one (1Vs.1) approach is adopted as shown in figure. Where in each SVM training node, i=1 class is trained against all classes. Similarly for next SVM training node that aforesaid i=1 class is replaced with i=2 class and training is done with all other classes. This process was iterated until all classes were passed through training. With this training process SVM develop algorithm functions i.e.(Cn), for binary data classification and outlier detection of n classes. Therefore 1 vs.1 approach may allow the SVM classifier to have a very upright training performance with this multi class classification problem. Testing of classifier, for each class, results the positive scores and negative scores for classified and misclassified class samples respectively. The label for classified disturbance sample was set to one and misclassified sample was set to 0. The input to the classifier is the time domain disturbance. Figure 4.19: shows the one vs. one SVM binary classification schematic diagram.

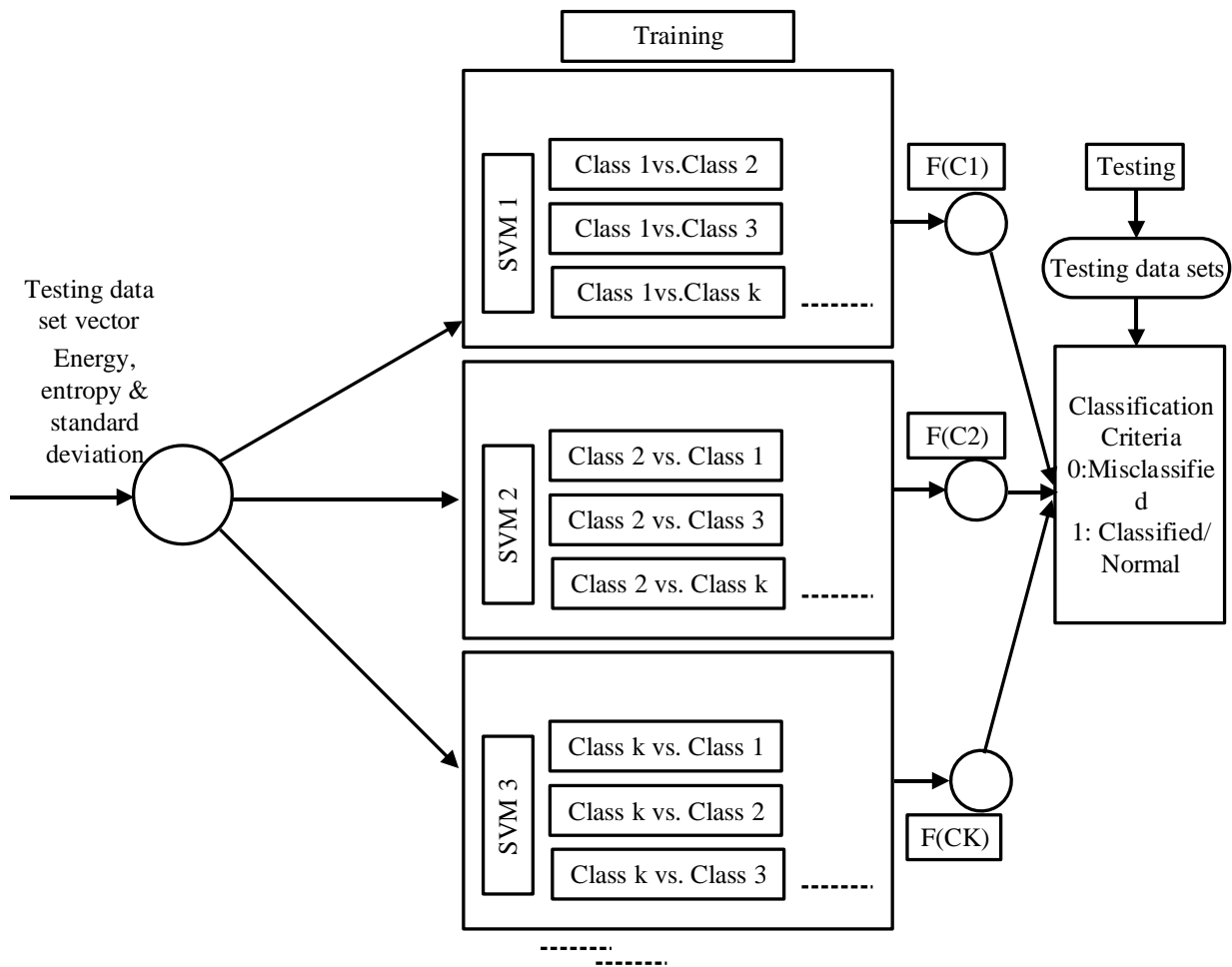


Figure 4. 19: One vs. One SVM Binary Classification Schematic [49].

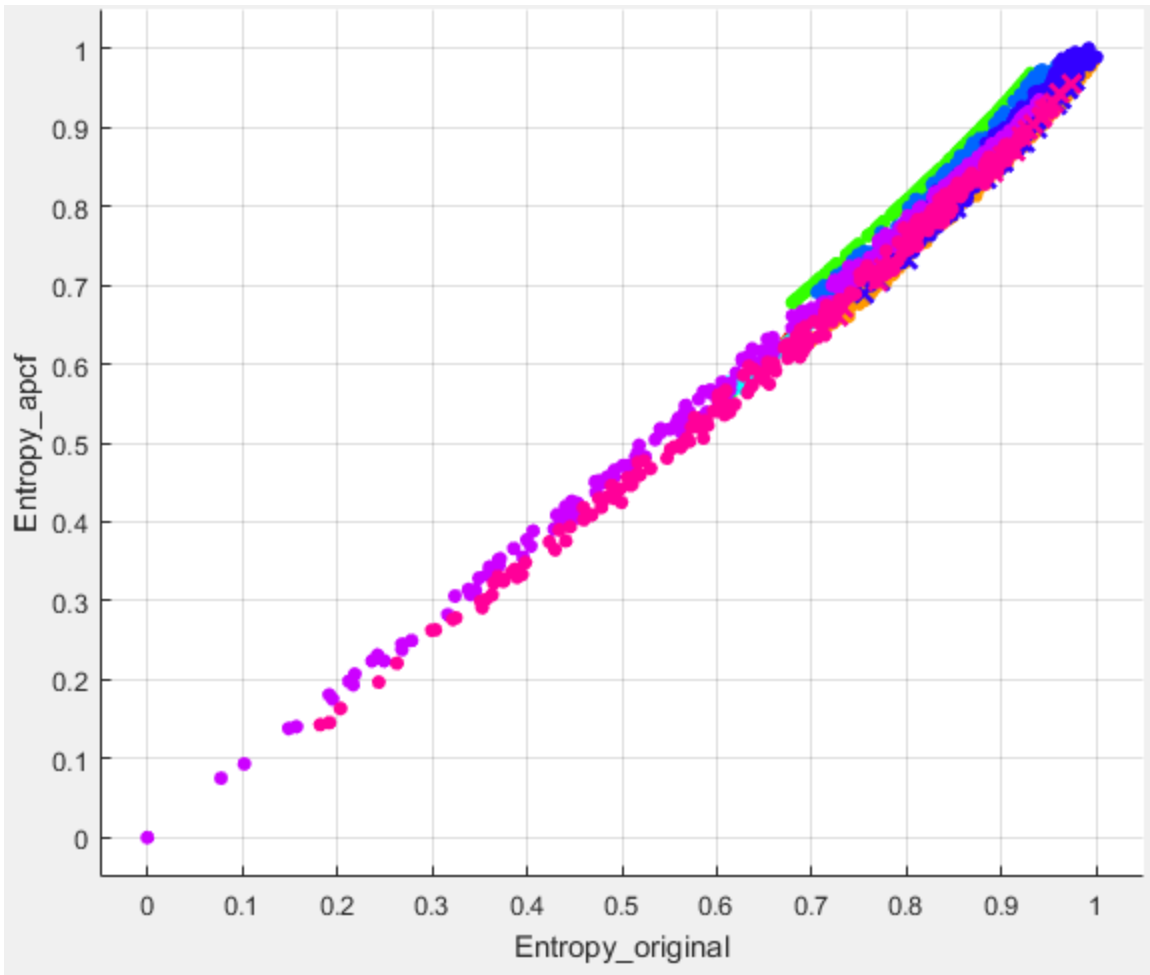


Figure 4. 20: Scatter plot of feature extracted data set.

C1 is a flicker power quality issues, C2 is a harmonic power quality issues

C3 is an impulse transient power quality issues, C4 is an interruption power quality issues

C5 is an oscillatory power quality issues, C6 is a pure signal power quality issues

C7 is a sag power quality issues, C8 is a sag harmonic power quality issues

C9 is a swell power quality issues, C10 is a swell harmonic power quality issues

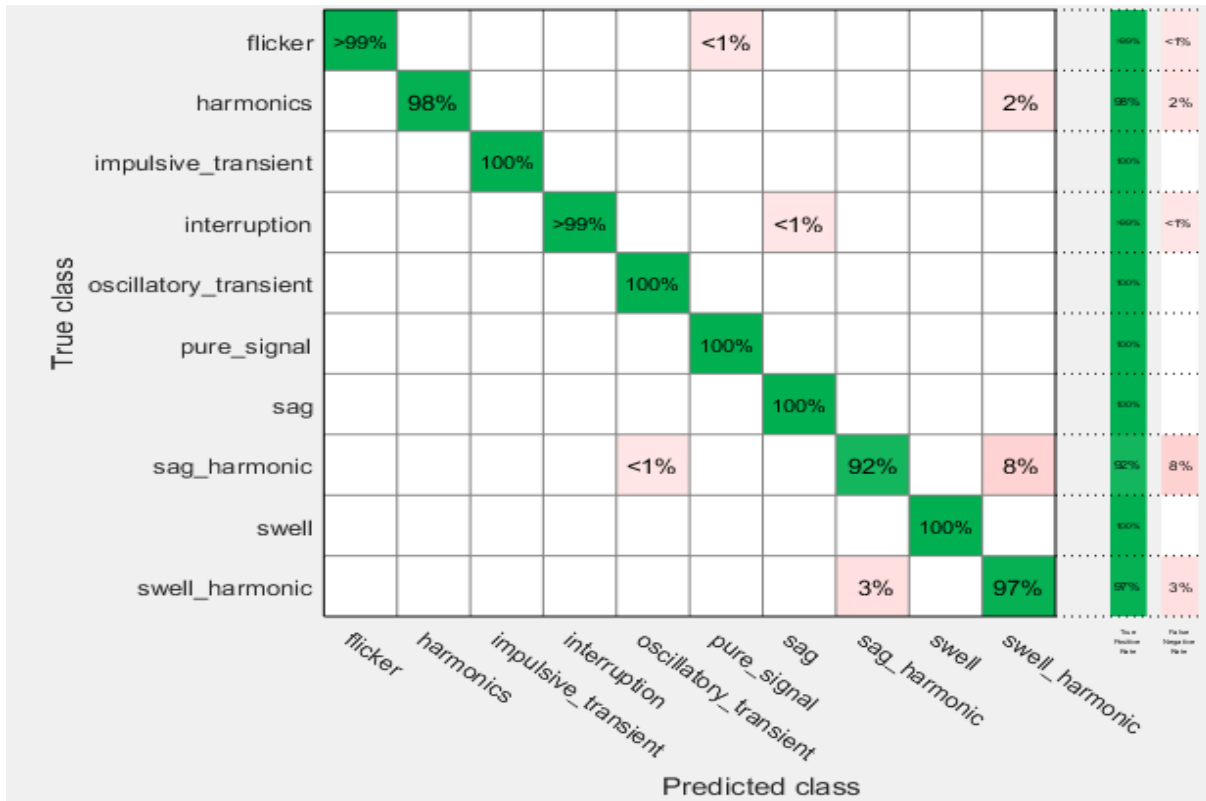


Figure 4. 21: Confusion matrix

Table 4. 1: Confusion matrix

Actual class in (%)		Predicted class in (%)									
		C1	C2	C3	C4	C5	C6	C7	C8	C9	C10
C1		247	0	0	0	3	0	0	0	0	0
C2		0	250	0	0	0	0	0	0	0	0
C3		0	0	250	0	0	0	0	0	0	0
C4		0	0	0	250	0	0	0	0	0	0
C5		0	0	0	0	249	0	0	1	0	0
C6		0	0	0	0	0	250	0	0	0	0
C7		0	0	0	0	0	0	250	0	0	0
C8		0	0	0	0	0	0	0	232	0	8
C9		0	0	0	0	0	0	0	0	250	0
C10		0	0	0	0	0	0	0	1	20	229

The diagonal elements in confusion matrix represent true positives (TP) i.e. correctly classified disturbances, whereas off diagonal elements shows misclassified disturbance samples. From matrix, all rows elements except diagonal element are false negatives (FN) i.e. sample is classified as predicted class but actually it is not. Similarly, all the column elements except diagonal elements are false positives (FP). From Figure (4.21):

- The columns show the predicted classes. In the top row, greater than 99% of the power quality issues from Flicker are correctly classified, so 97% is the true positive rate for correctly classified points in this class, shown in the green cell in the True Positive Rate column.
- The other power quality issues in the Flicker row are misclassified: less than 1% of the Flicker are incorrectly classified as from pure signal. Less than 1 % is the false negative rate for incorrectly classified points in this class, shown in the red cell in the False Negative Rate column.
- In the bottom up row, 98% of the power quality issues from harmonics are correctly classified, so 98% is the True Positive Rate for correctly classified points in this class, shown in the green cell in diagonal matrix cells in confusion matrix table in the True Positive Rate column.
- The other power quality disturbances issues in the harmonic row is misclassified: 2% of the power quality disturbances issues are incorrectly classified as from swell harmonics. 2 % is the False Negative Rate for incorrectly classified points in this class, shown in the pink cell in the False Negative Rate column.
- In the bottom row, greater than 99% of the power quality issues from interruption are correctly classified, so greater than 99% is the True Positive Rate for correctly classified points in this class, shown in the green cell in diagonal matrix cells in confusion matrix table in the True Positive Rate column.
- The other power quality disturbances issues in the interruption row is misclassified: less than 1% of the power quality disturbances issues are incorrectly classified as from sag. Less than 1 % is the False Negative Rate for incorrectly classified points in this class, shown in the pink cell in the False Negative Rate column.

- In the bottom up row, 92% of the power quality issues from sag harmonics are correctly classified, so 92% is the True Positive Rate for correctly classified points in this class, shown in the green cell in diagonal matrix cells in confusion matrix table in the True Positive Rate column.
- The other two power quality disturbances issues in the sag harmonics row is misclassified: less than 1% of the power quality disturbances issues are incorrectly classified as from oscillatory transient and 8% as from swell harmonic. Less than 1 % and 8% are the False Negative Rate for incorrectly classified points in this class, shown in the pink cell in the False Negative Rate column respectively.
- In the bottom up row, 97% of the power quality issues from swell harmonics are correctly classified, so 97% is the True Positive Rate for correctly classified points in this class, shown in the green cell in diagonal matrix cells in confusion matrix table in the True Positive Rate column.
- The other power quality disturbances issues in the swell harmonic row is misclassified: 3% of the power quality disturbances issues are incorrectly classified as from swell harmonics. 3 % is the False Negative Rate for incorrectly classified points in this class, shown in the pink cell in the False Negative Rate column.

Classifier performance summary is shown in Table 4.2, where positive rate of disturbance class refers sensitivity of classifier or recall rate. The overall accuracy is found 98.3%.

Table 4. 2: Classifier performance summary.

Classes	True positive Rates (%)	False negative Rates (%)	Positive predictive rate (%)	False discovery rate (%)
C1	>99	<1	100	-----
C2	98	2	100	-----
C3	100s	-----	100	-----
C4	>99	<1	100	-----
C5	100	-----	100	-----
C6	100	-----	99	1
C7	100	-----	>99	<1
C8	92	8	92	8
C9	100	-----	100	-----
C10	97	3	93	7
Overall accuracy			98.3%	

Table 4. 3: Correctly classified versus misclassified sample results.

Types of PQDs	Testing patterns	Correct Classified	Incorrect (misclassified)
C1	250	247	003
C2	250	250	0
C3	250	250	0
C4	250	250	0
C5	250	249	001
C6	250	250	0
C7	250	250	0
C8	250	232	018
C9	250	250	0
C10	250	229	021
Average	250	245.7	4.3

Tables 4.1, 4.2 and 4.3 clearly shows that proposed algorithms has effectively classified the eight distinct and two hybrid PQDs. Performance of classifier is found up to mark. As two hundred fifty disturbances, sample patterns for all ten-disturbance classes were employed for testing purpose in SVM classifier. In consequence, an average of 245.7 samples out of 250 is found correctly classified whereas 4.3 samples are found as misclassified. However, class wise correctly classified and misclassified samples numbers are also tabulated in Table 4.3. The classification results show that proposed algorithm is effective and due to its simplicity and less computational requirements.

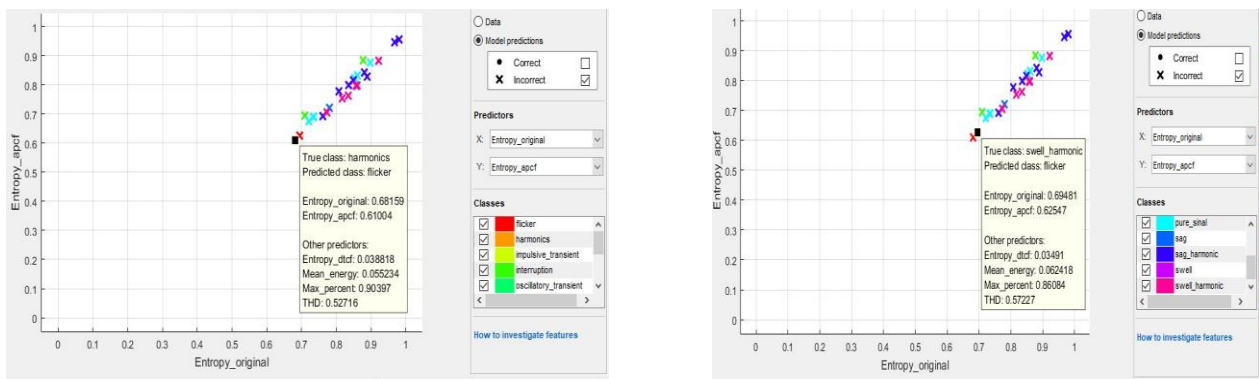
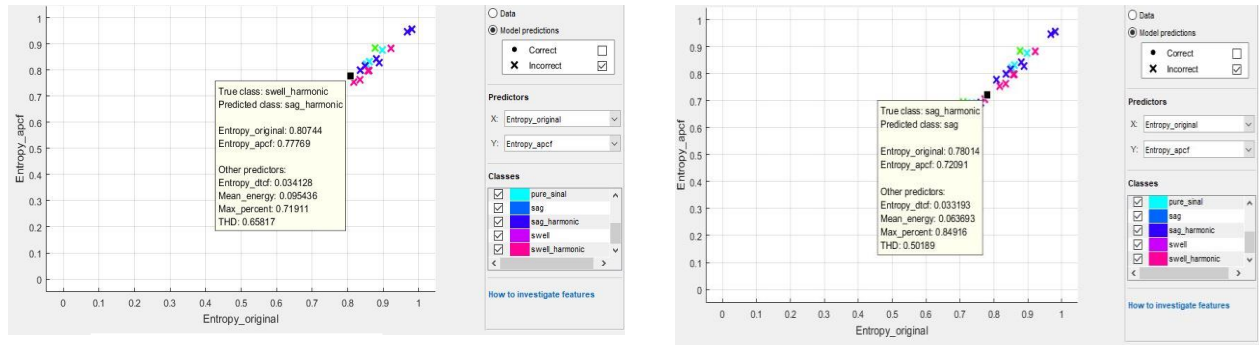


Figure 4. 1: (a) Incorrectly classified of flicker as harmonics and swell harmonic.



(a)

(b)

Figure 4. 2: Incorrectly classified of sag harmonic as swell harmonic

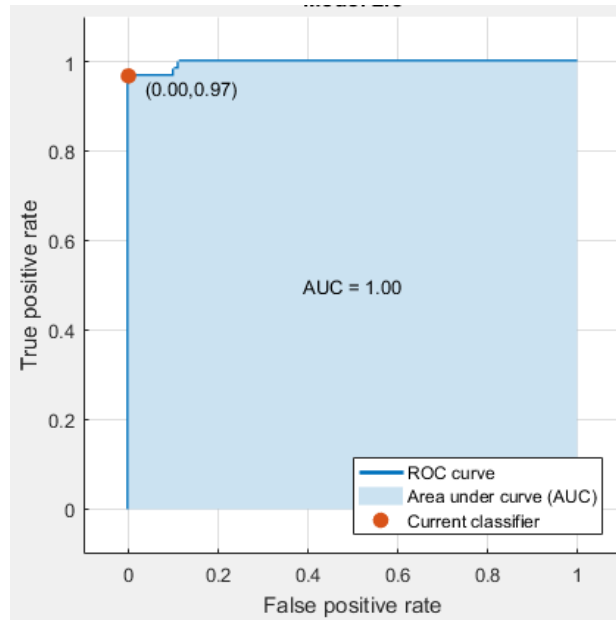


Figure 4. 22: Receiver Operating Characteristic (ROC) curve.

View the receiver operating characteristic (ROC) curve showing true and false positive rates. The ROC curve shows true positive rate versus false positive rate for the currently selected trained classifier. Can select different classes to plot. The marker on the plot shows the performance of the currently selected classifier. The marker shows the values of the false positive rate (FPR) and the true positive rate (TPR) for the currently selected classifier. For example, a false positive rate (FPR) of 0.03 indicates that the current classifier assigns 3% of the observations incorrectly to the positive class. A true positive rate of 0.97 indicates that the current classifier assigns 97% of the observations correctly to the positive class.

A perfect result with no misclassified points is a right angle to the top left of the plot. A poor result that is no better than random is a line at 45 degrees. The Area Under Curve number is a measure of the overall quality of the classifier. Larger Area Under Curve values indicate better classifier performance. Compare classes and trained models to see if they perform differently in the ROC curve.

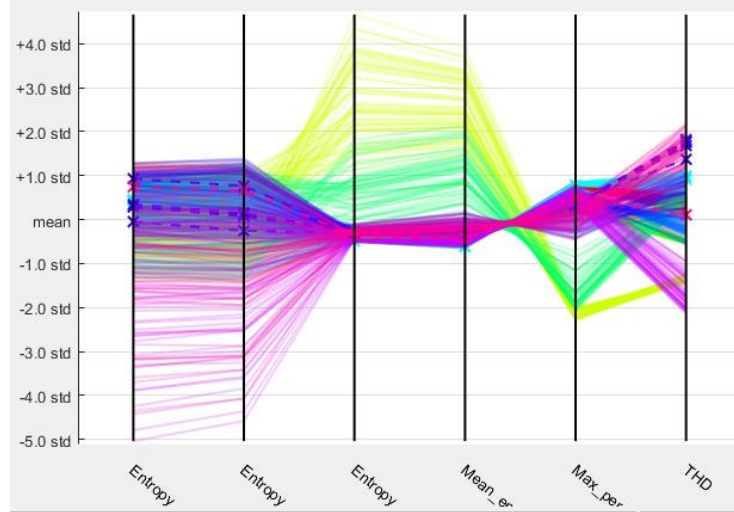


Figure 4. 23: Parallel coordinate between correct and incorrect classes.

To investigate features to include or exclude, use the parallel coordinates plot. You can visualize high dimensional data on a single plot to see 2D patterns. This plot can help you understand relationships between features and identify useful predictors for separating classes. You can visualize training data and misclassified points on the parallel coordinates plot. When you plot classifier results, misclassified points show dashed lines.

From the outcomes of this research, harmonics has been found out to be the most severe power quality issue, followed by voltage spike and fluctuation. The power quality monitoring techniques have been found to be employed for monitoring harmonics mainly, while D-STATCOM has been found out to be the most effective CPDs. It has been resolved that D-STATCOM can be a potential choice due to the advantages it offers.

4.3. Comparison between the ST with WT, FT and HT Algorithms

The ST is superior compared with other time-frequency representation such as FT, WT and HHT.

4.3.1. Identification of power quality issues using wavelet transform

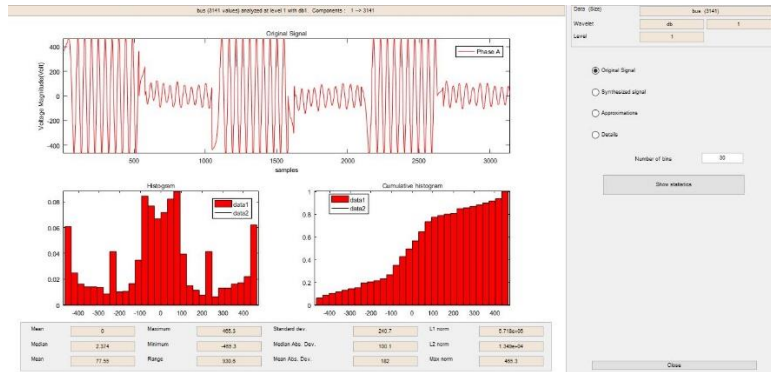


Figure 4. 24: The test waveforms together with corresponding in phase references: Top, original signal phase a, Bottom, histogram of signal a.

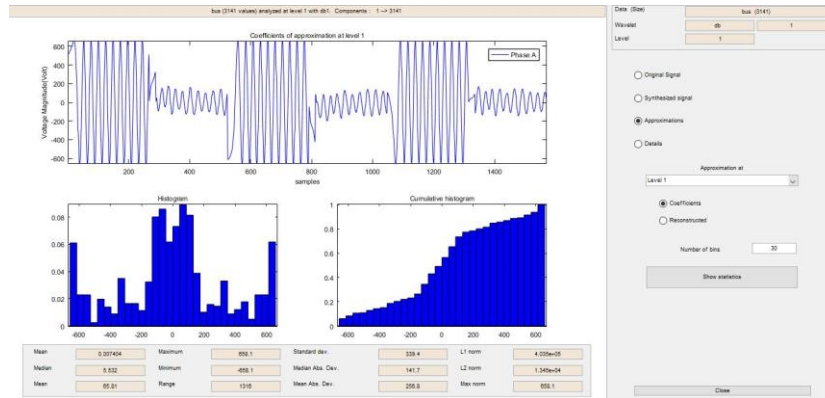


Figure 4. 25: The test waveforms together with corresponding in phase references: Top, approximation signal phase a, Bottom, histogram of signal a.

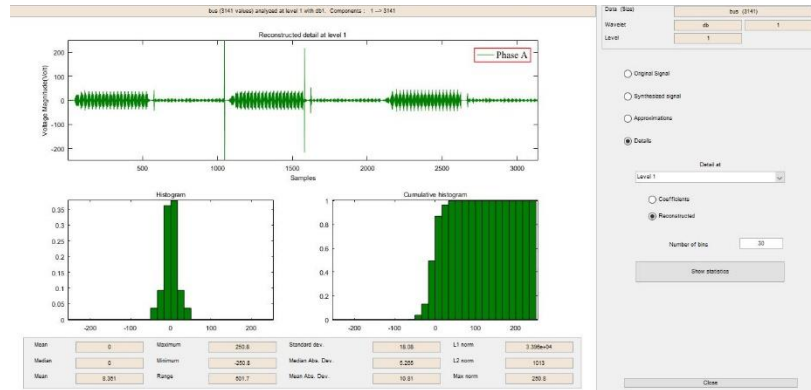


Figure 4. 26: The test waveforms together with corresponding in phase references: Top, details coefficient phase A, Bottom, histogram of phase a.

MRA can be described as the signal passing through a series of filters, which will split the signal into its low and high frequency components. This process is called decomposition, where the number of decomposition levels (filters) is related to the sampling frequency. For each decomposition level, there is an approximation of the signal and a number of details that correspond to the decomposition level. The signal can be synthesized from the approximation (low frequency) and the details (high frequency). The approximation and each detail represent a separate frequency range, which, therefore correspond to the series of filters. These coefficients have extracted unique parts of the signal from that frequency range, which make them useful in feature extraction. The three levels of decomposition for a target signal using the wavelet ‘db5’ can be seen in Figure 4.30 where the MATLAB Wavelet Toolbox was utilized to complete the decomposition.

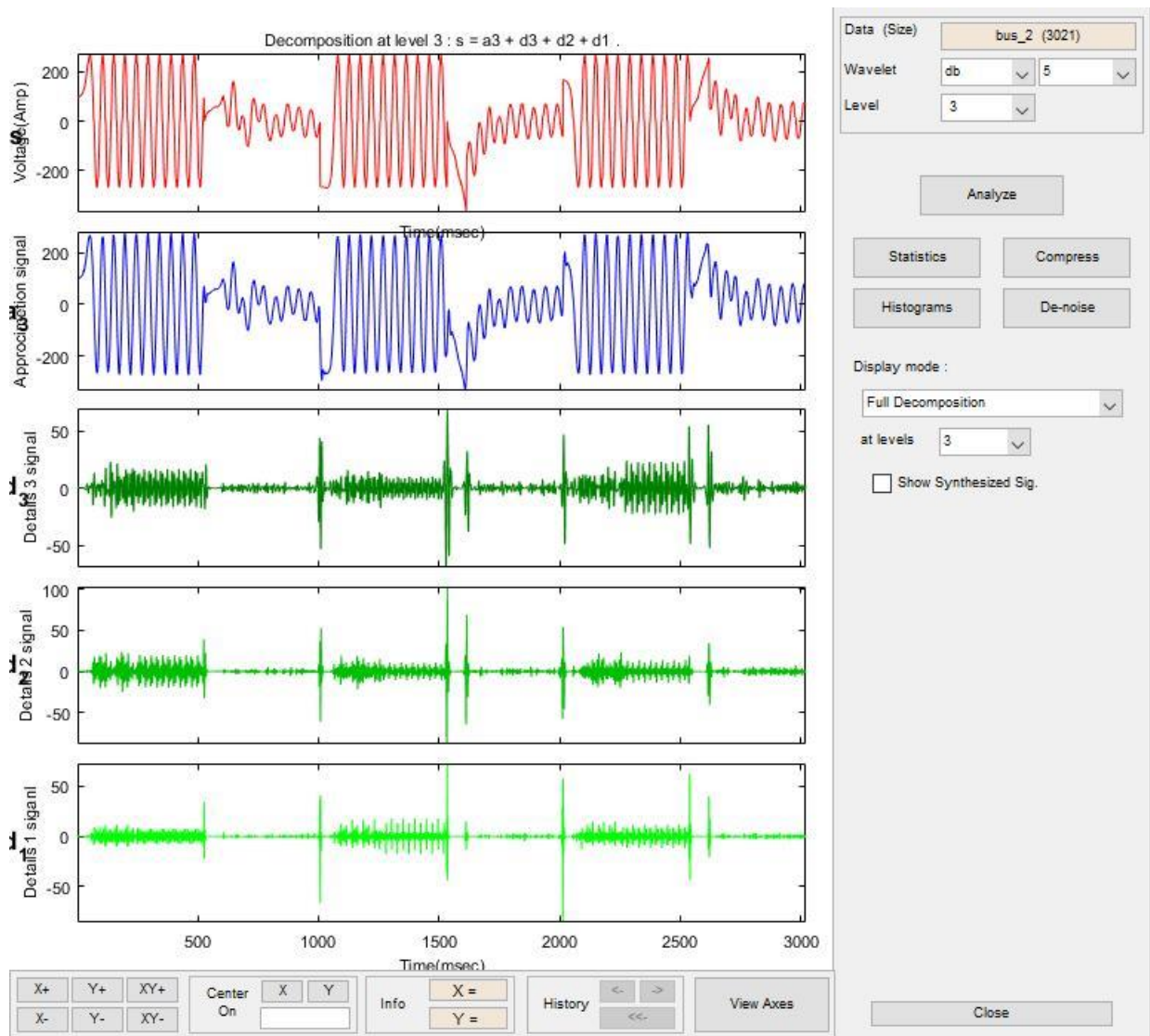


Figure 4. 27: MRA at level 3: Top, original signal phase a, middle, approximation phase a, Bottom, details coefficients phase a.

Wavelet transform analysis has been carried out on harmonic waveform distortion by considering debachies-1 mother wavelet up to one level decomposition. The one level decomposition gives one-detail coefficients. The standard deviations of detail coefficients are different for each power quality disturbance is for remaining disturbances are shown above Figure 4.29.

4.3.2. Identification of Power Quality Issues Using Fast Fourier Transform

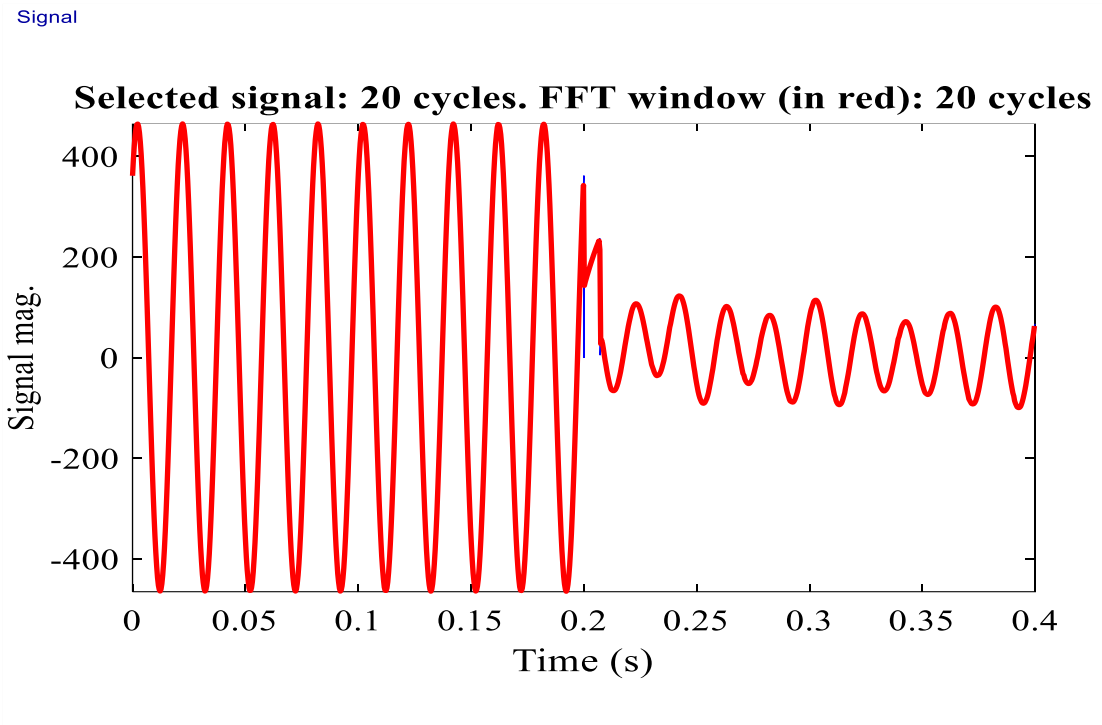


Figure 4. 28: Instantaneous waveform at bus 0.4kv.

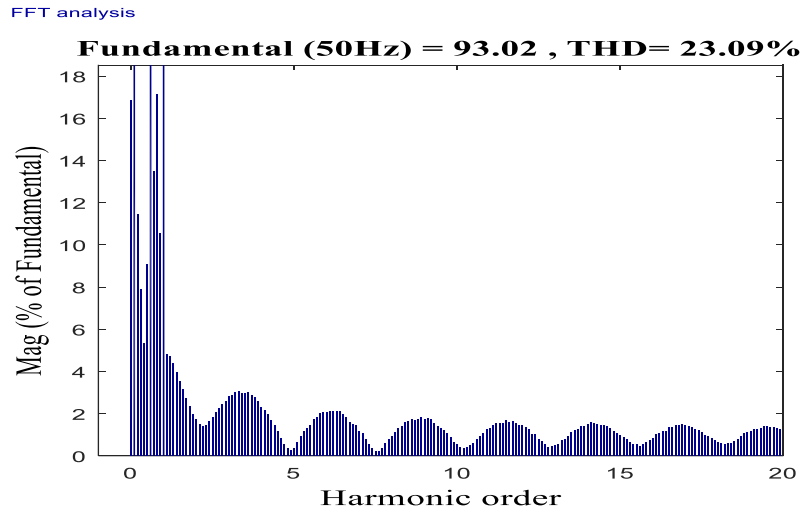


Figure 4. 29: FFT analysis of 0.4kv bus.

4.3.3. Identification of Power Quality Issues Using Hilbert Transform

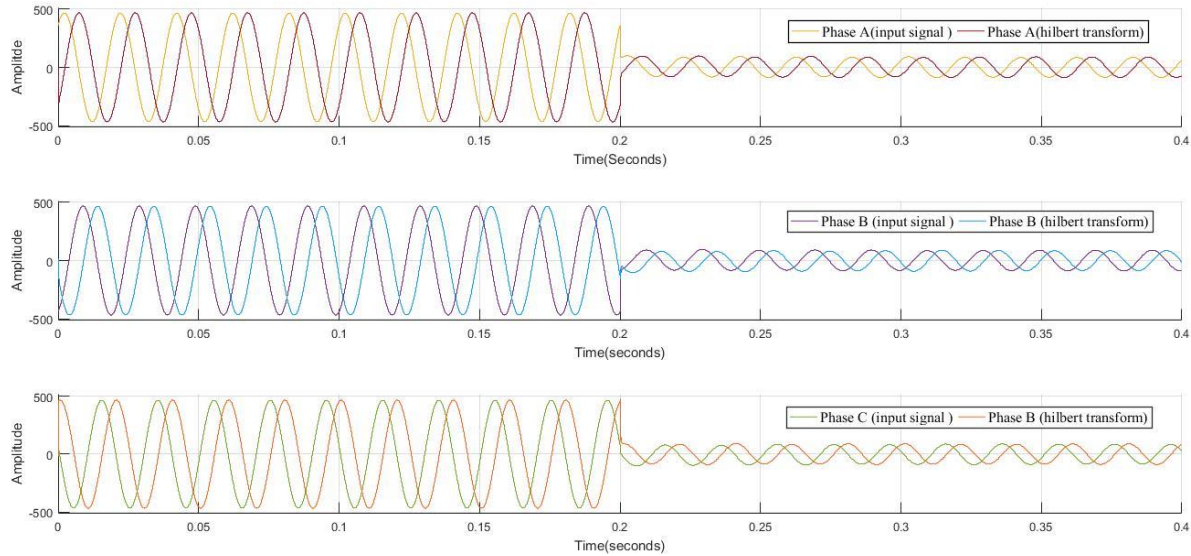


Figure 4. 30: Original Signal and its Hilbert transform.

This section shows the comparison among all transforms in terms of their operation and efficacy for detecting PQ problems in time of operation as given in Table 4.4 and 4.5.

4.3.4. Computational Complexity Analysis

In complexity calculations, the thing concerned is how the running time and memory requirements of the algorithm change and what are the implications and ramifications of that change as the size of the input to an algorithm increases. Let N be the size of the signal, M be the size of the moving window within the signal, and S be the step to move the window ($S \leq M$). Table 3.1 shows the computational complexity of algorithms discussed in this chapter. The S-Transform has high computational complexity. DWT has the lowest complexity. However, the real time implementations of the DWT are often computationally prohibitive. This is due to the computational requirement of the inner product calculations between the basic functions and the signal, which are required in order to find wavelet coefficients.

Table 4. 4: Comparison computational complexity of feature extraction algorithms.

Type of Algorithms	Algorithmic complexity
Discrete Fourier transform (DFT)	$O(N^2)$
Fast Fourier transform (FFT)	$O(N \log N)$
Windowed DFT	$O\left(\frac{M^2 N}{s}\right)$
Windowed FFT	$O\left(\frac{MN \log_2 M}{s}\right)$
Discrete wavelet transform (DWT)	$O(N)$
S-Transform	$O(N^2 \log_2 N)$

Table 4. 5: Comparison among FT, WT and HT, ST for PQ applications.

SI/No	Title	ST	WT	FT	HT
1	Window size	Adjustable depends up the input samples	Needs to be changed from small to large	Fixed	Linear
2	Measurement of time, frequency and magnitude simultaneously	Perfectly possible using S-matrix and 3D surface/mesh	Gives plot with respect to time, scale and magnitude	Not Possible	Partial Possible
3	Measurement of time and frequency accuracy	most accurate	No direct information about frequency	not accurate because fixed window size	not accurate
4	The time resolution and frequency resolution	Best time and frequency resolutions	Best time and frequency resolutions	Same for all spectral components	Same for all spectral components

Three TFR techniques as well as the traditional FFT were considered for analysis and visualization of time-varying waveform distortions. Main characteristics of the discussed techniques are

- 1) S-Transform provides good time-frequency representation of time-varying waveform distortions. Progressive resolution makes S-Transform track time variations better. However, the poor frequency resolution at high frequency is also induced by progressive resolution.
- 2) Due to the limitation of Heisenberg principle, TFR techniques are characterized with a tradeoff between time and frequency resolution. The TFR techniques, such as the FT, the Wavelet Transform, and the S-Transform are capable of executing amplitude tracking to some extent, but it is difficult for them to meet strict accuracy requirements in both frequency and time domains.
- 3) FFT may break down for time-varying waveform distortions and has no time information.
- 4) FT is not suitable for time-varying waveforms with both high and low frequency components due to the fixed time resolution.
- 5) DWT gives a time-scale representation of a signal, which is not enough for accurate analysis and measurement of time-varying waveform distortions. Simulation results also show the DWT may not have enough resolution to separate neighboring harmonics.

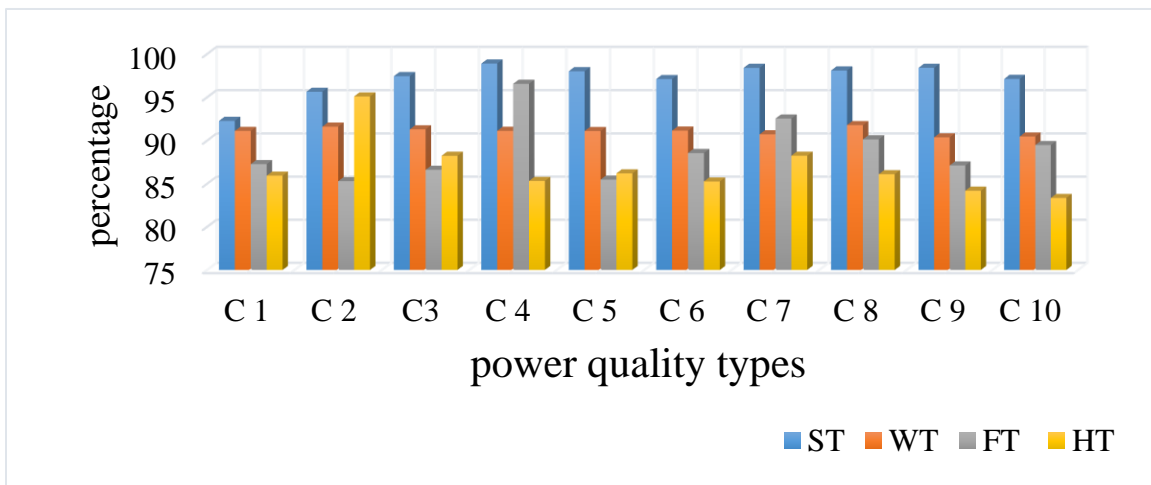


Figure 4. 31: Identification accuracy of ST and WT, FT, HT.

Table 4. 6: Identification accuracy of ST and WT, FT, HT.

	ST	WT	FT	HT
C 1	92.28	91.128	87.28	85.95
C 2	95.642	91.614	85.31	95.1
C3	97.45	91.3	86.63	88.25
C 4	98.904	91.129	96.56	85.33
C 5	98.015	91.114	85.49	86.21
C 6	97.109	91.157	88.57	85.27
C 7	98.402	90.729	92.55	88.26
C 8	98.101	91.79	90.15	86.12
C 9	98.409	90.38	87.13	84.2
C 10	97.128	90.472	89.49	83.36
Overall accuracy	97.144	91.0813	88.916	86.805

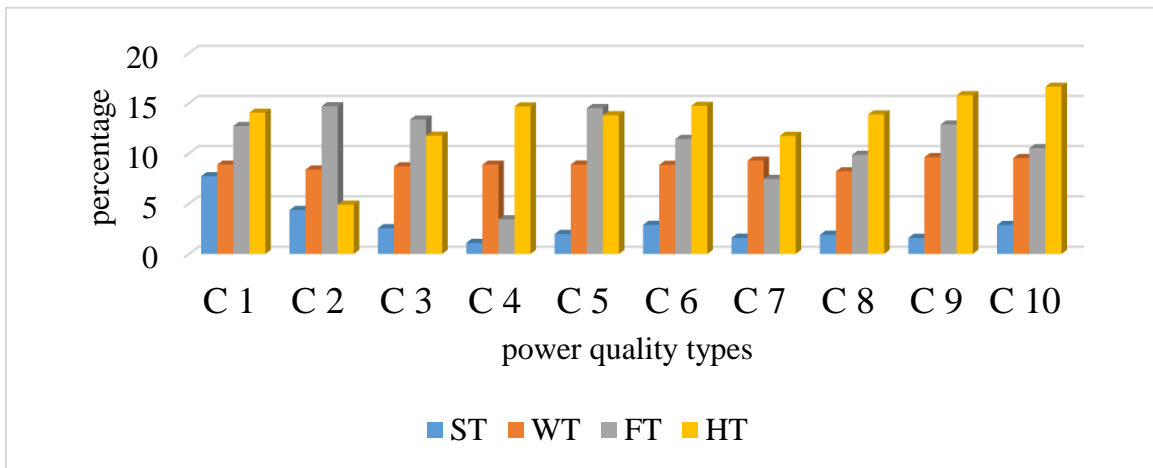


Figure 4. 32: Identification error comparison of ST and WT, FT, HT.

Table 4. 7: Identification error comparison of ST and WT, FT, HT.

	ST	WT	FT	HT
C 1	7.72	8.872	12.72	14.05
C 2	4.358	8.386	14.69	4.9
C 3	2.55	8.7	13.37	11.75
C 4	1.096	8.871	3.44	14.67
C 5	1.985	8.886	14.51	13.79
C 6	2.891	8.843	11.43	14.73
C 7	1.598	9.271	7.45	11.74
C 8	1.899	8.21	9.85	13.88
C 9	1.591	9.62	12.87	15.8
C 10	2.872	9.528	10.51	16.64
Error rate	2.856	8.9187	11.084	13.195

From Table 4.6 and Figure 4.34, it can be concluded that when detecting power quality disturbances, discrete wavelet transform is a powerful algorithm of non-stationary analysis for single cases and multiple disturbances, where accuracy was not less than 90% for each disturbance and overall accuracy. However, it is noticeable that WT and consequently DWT suffer from being sensitive to noise in some PQDs, especially disturbances with the appearance of harmonics and flickers. This could also be the reason for the inappropriate results of the classifier accuracy, as proven previously in figure. It is also noticed that the computational cost for DWT is still at high level. Nevertheless, detecting power quality disturbances based on a detection algorithm named Stockwell (ST) proved the ability to recognize these disturbances and detect them correctly. Moreover, in this analysis's presents a significant change in terms of accuracy for each disturbance in the classification technique, where they were no less than 92%. The overall accuracy shows another remarkable change as well, exceeding 97%. Nevertheless, another advantage of the proposed algorithm is the reduction of data size without losing the disturbance characteristics. Therefore, a significant reduction in memory space during operations and a decrease of computation cost result. Justification of using Stockwell transform includes:

- 1) ST is an effective and advanced algorithm in signal processing technique, which to analyses non-stationary signals when time is important.
- 2) It offers an improved time and frequency representation of a signal.
- 3) It exclusively combines a frequency-dependent resolution that at the same time localizes the real and imaginary spectra.
- 4) The fixed modulating sinusoids respecting the time-axis plus the scalable and movable Gaussian window properties of the ST can be used for better recognition of PQ events.
- 5) It is multi-resolution and non-destructive reversible time-frequency analysis method.
- 6) The ST is the phase correction of the WT and is a good candidate for the analysis of signals.
- 7) Due to the Excellency of the time-frequency resolution, the S-transform has been used for the analysis of the different type of PQ disturbances.

4.4. Comparison between the Proposed Classifier with DT, DS, KNN, ES

The performances of the classifier models were assessed in terms of classification accuracy, which is a relative factor of correct predictions for a dataset provided by the classifier. Confusion matrix of size 2×2 , which is used for the analysis of classifier performance, is given in Table 4.8. In the confusion matrix, the true positive (TP) represents the different type of power quality disturbances which are predicted as pure signal and one belong to other disturbances. The reliability of the decision support system mostly depends on FNs. The effectiveness of the proposed system is mostly represented by classification accuracy, which is defined as the rate of correct predictions for a dataset provided by the classifier. Classification accuracy can be computed as:

Table 4. 8: Confusion Matrix.

		ACTUAL VALUES	
		POSITIVE	NEGATIVE
PREDICTED VALUES	POSITIVE	TP	FP
	NEGATIVE	FN	TN

$$\text{Classification accuracy} = \frac{TP+TN}{TP+TN+FP+FN} \quad (4.29)$$

Classification accuracy for each cross validation fold and overall accuracy for the selected five best-known classifiers are shown in figure below. The highest average accuracies of 98.3 and 93.4% are obtained for cubic SVM and ensemble classifiers, respectively. In addition to the average classification accuracy, other common performance measures computed from the confusion matrix are also presented. The additional performance measures namely sensitivity (TP rate, TPR), specificity (TN rate, TNR), positive predicted value (PPV) or precision, error rate or misclassification rate (MCR), harmonic mean of precision and sensitivity (*F*-score) and quality index (QI) are illustrated with the following equations:

Sensitivity / True Positive Rate / Recall

$$\text{Sensitivity} = \frac{TP}{TP + FN} \quad (4.30)$$

Sensitivity tells us what proportion of the positive class got correctly classified.

A simple example would be to determine what proportion of the actual sick people were correctly detected by the model.

Specificity / True Negative Rate

$$\text{Specificity} = \frac{TN}{TN + FP} \quad (4.31)$$

Specificity tells us what proportion of the negative class got correctly classified.

Taking the same example as in Sensitivity, Specificity would mean determining the proportion of healthy people who were correctly identified by the model.

$$\text{Precision} = \frac{TP}{TP + FP} \quad (4.32)$$

$$\text{Error rate} = \frac{FP + FN}{\text{total}} \quad (4.33)$$

$$F - \text{Score} = \frac{2}{\left(\frac{1}{PPV}\right) + \left(\frac{1}{TPR}\right)} \quad (4.34)$$

$$QI = \sqrt{\text{sensitivity} \cdot \text{specificity}} \quad (4.35)$$

In the proposed algorithm, the sensitivity and specificity offered by SVM classifier are 98.3% and 95.3%, respectively. The sensitivity < 100 percentage indicates that the algorithm might have misclassified some power quality disturbances. A few FPs are detected, in the case of less specificity. In this thesis, the misclassification rate of SVM classifier is only 1.7%.

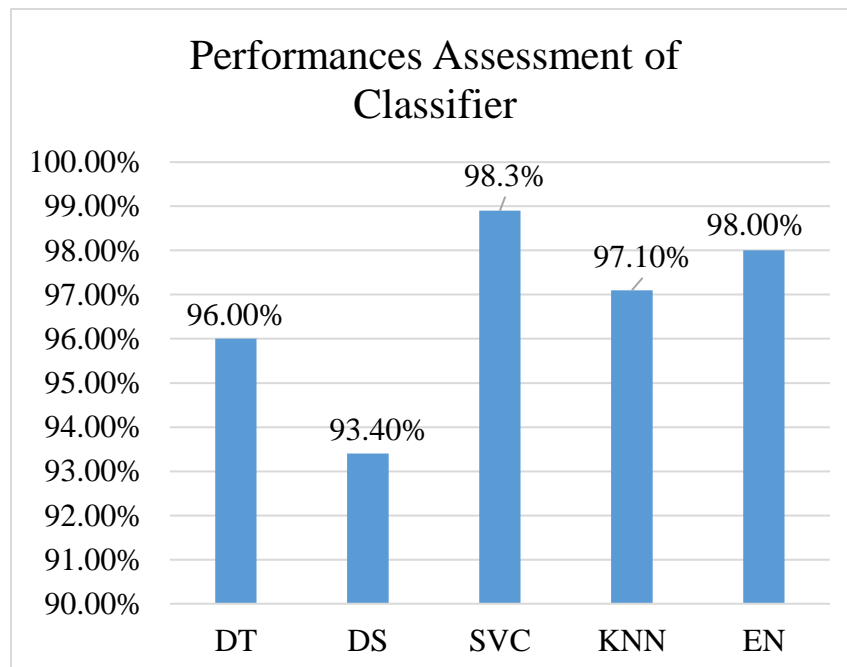


Figure 4. 33: Performances Assessment of Classifier.

Table 4. 9: Characteristics of Classifier Types.

Classifier	Prediction Speed	Memory Usage	Interpretability
Decision Trees	Fast	Small	Easy
Discriminant Analysis	Fast	Small for linear, large for quadratic	Easy
Support Vector Machines	Medium for linear. Slow for others.	Medium for linear. All others: medium for multiclass, large for binary.	Easy for Linear SVM. Hard for all other kernel types.
Nearest Neighbor Classifiers	Slow for cubic. Medium for others.	Medium	Hard
Ensemble Classifiers	Fast to medium depending on choice of algorithm	Low to high depending on choice of algorithm.	Hard

CHAPTER FIVE

5. The Existing Power Quality Issues and Mitigation Technique

5.1. Introduction

The power quality problems in power distributions systems are not new, but the awareness of the customer, utilities and equipment manufacturers has increased in recent years. Starting from the time of awareness and identification of power quality problems many conventional solutions, which typically use passive elements, have been proposed and implemented in different parts of the world. In spite of these solutions have existed for a long period in the field of electrical power engineering, they do not always respond correctly and perform as expected on the modern power system. Passive filters consisting of tuned L-C component have been widely used to suppress harmonic distortions. Although these passive filters have low initial cost and high efficiency, they also have various drawbacks like instability, fixed compensation, resonance with supply as well as loads and utility impedance.

The evolution of power electronics controller devices has given to the birth of custom power applications, in which a wide range of flexible controllers using power electronics components are utilized to improve the power quality at distribution level.

5.2. Custom Power Devices (CPDs)

The term custom power refers to the use of power electronic controllers for distribution systems to enhance the quality and reliability of power that is delivered to clients. These power electronics controllers are called CPD. They have good performance at medium distribution levels and most are available as commercial products [66]. The CPDs are of two types' network reconfiguring type and compensating type. The complete classification of CPDs is shown in the Figure 5.1.

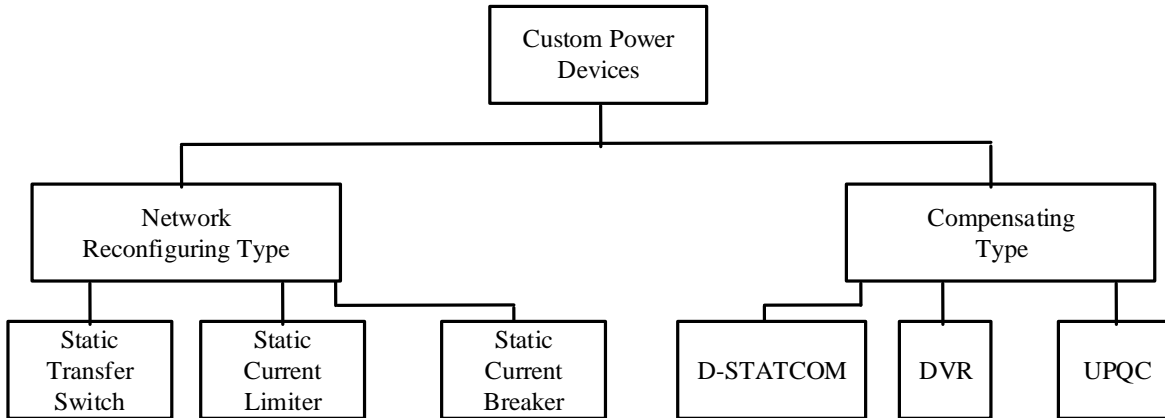


Figure 5. 2: General Classification of Custom Power Devices [66].

5.2.1. Network Reconfiguring Type CPDs

The network reconfiguring equipment can be normal thyristor or gate turn-off thyristor base. The Static Current Limiter/ Static Circuit Breaker are usually used for fast current limiting and current breaking during faults. On the other hand, the Static Transfer Switches (STS) are used to promptly transfer load to an alternate feeder to protect a load from voltage sag/swell or fault in the supplying feeder. Uninterruptable Power Supply (UPS) is also categorized as a network reconfiguring type CPD, which is used to mitigate voltage dip and short duration interruption.

5.2.2. Compensating Type CPDs

The compensating CPDs are used for active filtering, load balancing, power factor improvement and voltage regulating (sag/swell). These devices are mainly three types: Distribution STATCOM, Dynamic Voltage Restorer and Unified Power Quality Conditioner.

Distribution Static Compensator (D-STATCOM) is a shunt connected device, designed to inject unbalanced and harmonically distorted current to distribution line via coupling inductor to eliminate unbalance or distortions in the load current or the supply voltage. It can also perform voltage regulation when connected to a distribution bus. In this mode, it can hold the bus voltage constant against any unbalance or distortion in the distribution system. Generally, D-STATCOM s can be used in distribution networks for load current balancing, flicker effect compensation, current harmonic distortion compensation and voltage regulating (sag/swell). The single line diagram of D-STATCOM is shown in Figure 5.2.

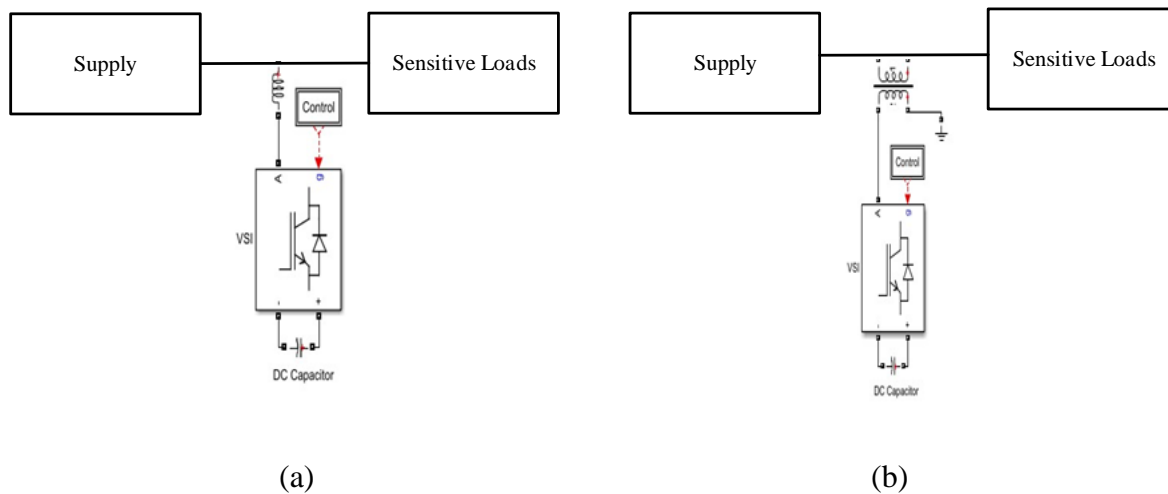


Figure 5. 3: Single line diagram of (a) D-STATCOM and (b) DVR [66].

Dynamic Voltage Restorer (DVR) is a series connected CPD, designed to inject a dynamically controlled voltage in magnitude and phase in to distribution line via coupling transformer to correct load voltage. The main purpose of this device is to protect sensitive loads from sag/swell, interruptions in the supply side. Since this is a series device, it can also be used as a series active filter. Generally, DVRs can be used in distribution networks for voltage regulation, flicker attenuation and voltage balancing. The single line diagram of DVR is shown in Figure 5.2.

Unified Power Quality Conditioner (UPQC) is a very versatile device that can inject unbalanced and distorted current in shunt and voltage in series simultaneously in a dual control mode. Therefore, it can perform both the functions of load compensation and voltage control at the same time. Applications of UPQC include VAR compensation, harmonic suppression, current balancing, active/ reactive power control, voltage balancing and voltage regulation. Most widely known custom power devices are D-STATCOM, UPQC, DVR among them D-STATCOM is very well known and can provide cost effective solution for the compensation of reactive power and unbalance loading in distribution system [66].

5.3. Current Harmonic Distortion Mitigation with D-STATCOM

Harmonic distortion is present to some degree on all power systems. Mitigating techniques has to be implemented on a system when the distortion levels exceed the limits set by different standard

organizations in order to avoid failure of equipment's both in the utility and customer premises. The analysis of measurements carried out in Awada industry zone network in the previous chapter shows that current harmonic distortion levels which exceeds the limits set by IEC and IEEE standards, are present on transformer T1. As presented in the previous sub-topics, CPD has a great advantage over the traditional passive and active harmonic filtering techniques in mitigating harmonic distortions. As a result, D-STATCOM is proposed for compensating the current harmonics in Awada industry zone distribution network, as it is capable of mitigating both these disturbances as presented in the previous sub topic.

There are two modes of D-STATCOM operation namely load compensation in current-control mode and voltage regulation in voltage-control mode. Since the main concern of this study are harmonic distortion, the D-STATCOM in current control mode is used in this study for load compensation, i.e. current harmonic compensation, power factor improvement and load balancing. Figure 5.3 shows a schematic diagram of the distribution network of Awada industry zone with a single D-STATCOM in Current Control Mode (CCM) is connected to transformer T1. The desired performance from the compensator is that it generates a current I_{comp} such that it cancels the reactive component, harmonic component and unbalance of the load current. Assuming the load current vector has real, reactive and harmonic components, for unity power factor operation, the source supplies only the real component. The compensator will inject the remaining part. The performance of the designed D-STATCOM for compensating the harmonic current distortion in Awada industry distribution network is analyzed by simulating the network with and without the D-STATCOM in MATLAB's SIMULINK environment. The following subtopic explains the working principles, simulation and results of the proposed D-STATCOM for Awada industry zone.

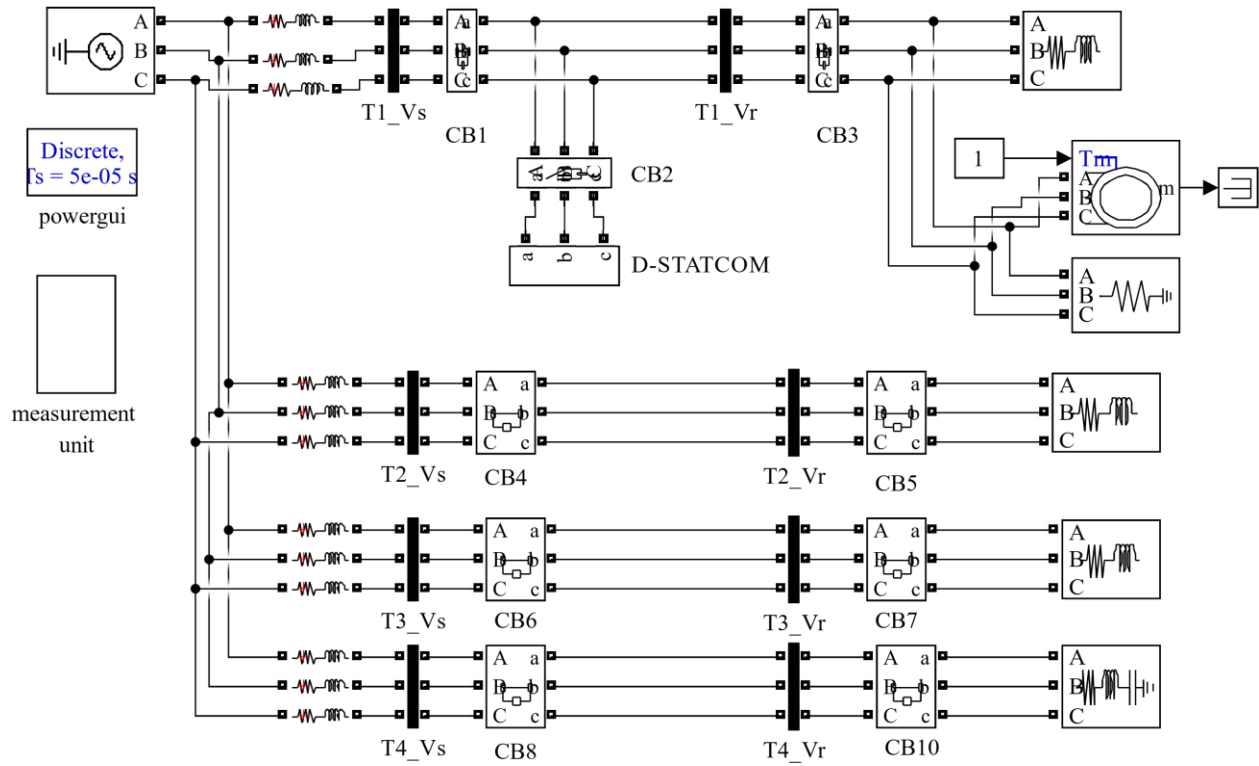


Figure 5. 4: SIMULINK model of Awada industry zone network with D-STSTCOM.

5.4. Simulation of Awada Industry Distribution Network with D-STATCOM

The main building blocks of the D-STATCOM used in the simulation are VSI (Voltage Source Inverter) with DC link capacitor, control unit for generating the reference current and control technique for generating the pulses for driving the VSI. The detail schematic diagram of a D-STATCOM used for this study is shown in Figure 5.4.

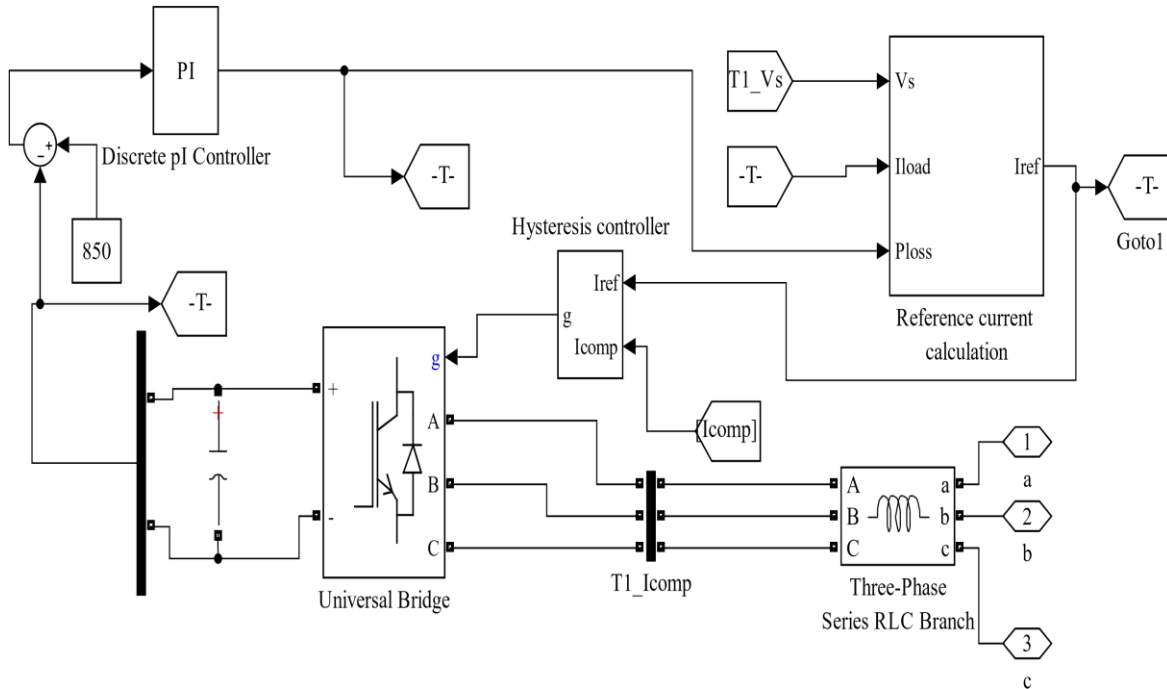


Figure 5. 5: Detail schematic diagram of IRP based D-STATCOM.

5.4.1. Generating a Reference Current

There are various theories and techniques available for generating the three phase reference currents, which have to be generated by the D-STATCOM in order to accomplish load compensation. Some of these theories are Synchronous Reference Frame (SRF) based control theory, Instantaneous Reactive Power (IRP) control theory, Unit Template based control theory and Synchronous Detection Mode (SDM) based theory. SRF and IRP based controls are the most commonly used control theories with D-STATCOMs and different researches show that they have a better compensating performance than other theories. The analysis done by [67] and [68] shows that, even though the source current THD level with the SRF theory is slightly lower than with the IRP theory, both control theories are equally reliable and applicable to reduce the THD levels to the acceptable range set by IEEE and IEC standards. A D-STATCOM with IRP based control theory is used in this study, for its simplicity in simulation of the control technique.

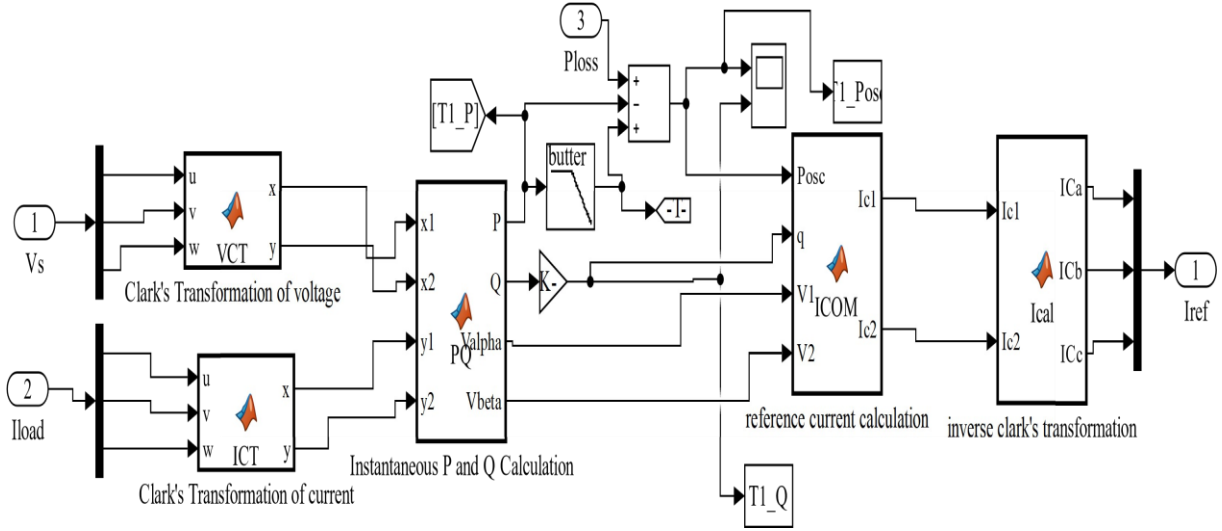


Figure 5. 6: MATLAB/SIMULINK model of IRP control [67].

In this technique, the reference current for the control of D-STATCOM is obtained from the instantaneous active and reactive power components in the α - β coordinate. The Simulink model of IRP based controller for generating the reference current is shown in Figure 5.5. In the model different MATLAB function block are shown. These function blocks are used for transforming the voltages and currents in to the α - β coordinate, calculating the instantaneous active and reactive powers, calculate the reference currents and transferring back it to the a-b-c coordinate. The snapshot of the codes used by each of the function blocks are shown in Figure 5.6 below. As shown in Figure 5.5, initially, the source voltage and load current waveforms in the a-b-c coordinate are transformed to the stationary orthogonal α - β coordinates using Clark's Transformation according to the given matrix in equation 5.1.

$$\begin{bmatrix} I_0 \\ I_\alpha \\ I_\beta \end{bmatrix} = \sqrt{\frac{2}{3}} \begin{bmatrix} 1 & 1/\sqrt{2} & 1/\sqrt{2} \\ 1 & -\frac{1}{2} & -\frac{1}{2} \\ 0 & \frac{\sqrt{3}}{2} & -\frac{\sqrt{3}}{2} \end{bmatrix} \begin{bmatrix} I_a \\ I_b \\ I_c \end{bmatrix} \quad (5.1)$$

$$\begin{bmatrix} V_0 \\ V_\alpha \\ V_\beta \end{bmatrix} = \sqrt{\frac{2}{3}} \begin{bmatrix} 1 & 1/\sqrt{2} & 1/\sqrt{2} \\ 1 & -\frac{1}{2} & -\frac{1}{2} \\ 0 & \frac{\sqrt{3}}{2} & -\frac{\sqrt{3}}{2} \end{bmatrix} \begin{bmatrix} V_a \\ V_b \\ V_c \end{bmatrix} \quad (5.2)$$

Then,

$$\begin{bmatrix} I_\alpha \\ I_\beta \end{bmatrix} = \sqrt{\frac{2}{3}} \begin{bmatrix} 1 & -\frac{1}{2} & -\frac{1}{2} \\ 0 & \frac{\sqrt{3}}{2} & -\frac{\sqrt{3}}{2} \end{bmatrix} \begin{bmatrix} I_a \\ I_b \\ I_c \end{bmatrix} \quad (5.3)$$

$$\begin{bmatrix} V_\alpha \\ V_\beta \end{bmatrix} = \sqrt{\frac{2}{3}} \begin{bmatrix} 1 & -\frac{1}{2} & -\frac{1}{2} \\ 0 & \frac{\sqrt{3}}{2} & -\frac{\sqrt{3}}{2} \end{bmatrix} \begin{bmatrix} V_a \\ V_b \\ V_c \end{bmatrix} \quad (5.4)$$

Then, the product of the voltage obtains the instantaneous active and reactive power and current waveforms in the α - β coordinate according to the given matrix in equation 5.2.

$$\begin{bmatrix} p \\ q \end{bmatrix} = \begin{bmatrix} V_\alpha & V_\beta \\ V_\beta & -V_\alpha \end{bmatrix} \begin{bmatrix} I_\alpha \\ I_\beta \end{bmatrix} \quad (5.5)$$

Instantaneous active and reactive powers p and q can be decomposed into an average (dc) and oscillatory components as:

$$p = \bar{p} + \tilde{p} \quad (5.6)$$

$$q = \bar{q} + \tilde{q} \quad (5.7)$$

As shown in Figure 5.5, the constant (dc) term of the instantaneous active power is extracted using 5th order LPF (Low Pass Filter). The source has to supply the constant term (\tilde{p}) and the power loss (P_{loss}) due to switching losses and coupling inductor loss. These losses force the DC capacitor to discharge. In order to maintain a constant stored DC voltage in the capacitor, additional power has to be drawn from the source to compensate the losses. Thus, the oscillating component of the instantaneous active power (\tilde{p} , presented as P_{osc} in Figure 5.5) is obtained by extracting the constant term (\bar{p}) and the power loss (P_{loss}) from the instantaneous active power (p). On the other hand, both the constant and oscillatory instantaneous reactive powers have to be supplied by the D-STATCOM compensator in order to maintain unity power factor at the source. Therefore, the total instantaneous active and reactive power, which has to be supplied by the D-STATCOM, is [66-67]:

$$\tilde{p} = p - (\bar{p} + P_{loss}) \quad (5.7)$$

$$q = \bar{q} + \tilde{q} \quad (5.8)$$

Then the instantaneous reference currents in the α - β coordinate can be calculated as:

$$\begin{bmatrix} I_{\alpha} \\ I_{\beta} \end{bmatrix} = \frac{1}{v_{\alpha}^2 + v_{\beta}^2} \begin{bmatrix} V_{\alpha} & V_{\beta} \\ V_{\beta} & -V_{\alpha} \end{bmatrix} \begin{bmatrix} \tilde{p} \\ q \end{bmatrix} \quad (5.9)$$

Finally, these reference currents are transformed to the a-b-c coordinate using the inverse Clark's transformation according to equation 5.8.

$$\begin{bmatrix} I_a^* \\ I_b^* \\ I_c^* \end{bmatrix} = \begin{bmatrix} 1 & 0 \\ -1/2 & \frac{\sqrt{3}}{2} \\ -1/2 & -\frac{\sqrt{3}}{2} \end{bmatrix} \begin{bmatrix} I_{\alpha} \\ I_{\beta} \end{bmatrix} \quad (5.10)$$

These reference currents have to be generated by the D-STATCOM and actually correspond to the oscillating component of the instantaneous active power and both the oscillating and constant components of the instantaneous reactive power. The reference currents are then used by the HCC (Hysteresis Current Control) to generate the firing pulses for the power semiconductor switches.

5.4.2. Hysteresis Current Control

Hysteresis Current Control (HCC) is a stable, fast and accurate method of generating switching pulses for producing the compensating current in shunt CPDs. To generate the compensator current (I_{comp}) a hysteresis band $\pm h$ is used so that,

If $I_{\text{comp}} \geq I_{\text{ref}} + h$, then the compensator current has to be lowered by applying a negative voltage across the output. This is accomplished by turning on the switches on the negative dc line of the inverter.

If $I_{\text{comp}} \leq I_{\text{ref}} - h$, then the compensator current has to be raised by applying a positive voltage across the output. This is accomplished by turning on the switches on the positive dc line of the inverter.

The tracking performance of the hysteresis current control method is inversely proportional to the load inductor and the size of the hysteresis band and directly proportional to the magnitude of dc voltage. As the number of switching increased to get a better tracking, the inverter losses will become higher. The MATLAB/SIMULINK model of the hysteresis current control technique is shown in Figure 5.7 below. A hysteresis band of $[-h, h] = [-0.1, 0.1]$ is used for the simulation in the study.

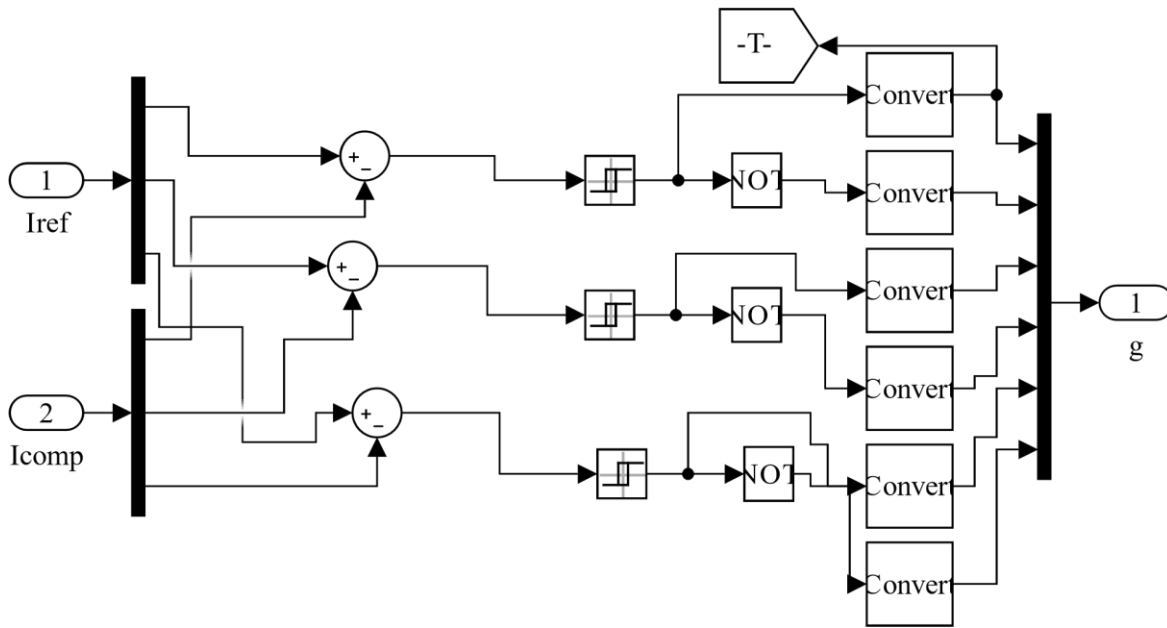


Figure 5. 7: MATLAB/SIMULINK model of Hysteresis Current Control.

5.4.3. Voltage Source Inverter (VSI)

VSI in a D-STATCOM is used to generate the compensating three phase AC currents at any required magnitude, phase and frequency. It consists of power semiconductor switches and DC link capacitor. The power semiconductor device can be a Metal Oxide Field Effect Transistor (MOSFET) or Gate Turn-Off (GTO) thyristor or Insulated Gate Bipolar Transistor (IGBT) or Field Controlled Thyristor (FCT) based on the specific application requirements. Gate turn-off thyristors are recommended for high voltage application with lower switching speeds. On the other hand, MOSFETs have very low switching losses but are not suitable for very high voltage applications. IGBTs and MOSFETs are the preferred devices for distribution system applications as they can carry large current and has fast switching characteristics and low losses. These two-power semiconductor devices are also selected for realizing the VSI of the D-STATCOM proposed for this study. The capacitor at the DC side of the D-STATCOM is responsible for supplying the current harmonics and the fluctuations caused by the compensation of the reactive power. The switching losses and the coupling inductor losses force the DC capacitor to discharge. On the other hand, the average value of the voltage across the capacitor terminals must be kept at a constant value in order to the capacitor perform its duty. The voltage across the capacitor is regulated by absorbing or releasing active power into the electrical network. The Discrete PI (Proportional and

Integral) controller from SIMULINK's Sims cape power system toolbox, with proportional gain $K_p = 0.5$ and integral gain $K_I = 1$, is used to regulate this dc voltage across the capacitor as shown on the D-STATCOM block diagram in Figure 5.4. The DC bus voltage V_{DC} is calculated using the following expression [67].

$$V_{DC} = \frac{\sqrt{2} * V_{LL}}{m_a} \quad (5.11)$$

Where, V_{LL} is the line-to-line output voltage at the D-STATCOM terminal and m_a is the modulation index. By considering a system voltage of 400V, 10% voltage drop at the coupling inductor and maximum variation of 10% in the system voltage, the line voltage required at the VSI becomes 480V and the DC bus voltage becomes 678.8V. However, in the practical case, the attainable voltage at the D-STATCOM output terminal will be less than the estimated one due to the dead-band and the transition times of the switching device. Therefore, taking these factors in to account, a DC link voltage of 850V is selected for the simulation.

5.5. Simulation Results and discussion with and without D-STATCOM

The previous subtopics in this chapter mainly focus on the operating principle and design of the D-STATCOM that is proposed to compensate the current harmonic distortion in Awada industry distribution network. The performance of the D-STATCOM is examined by simulating the industry distribution network with the effect of the non-linear loads and the proposed D-STATCOM included in to the system.

5.5.1. Modeling of Harmonic Current Distortion Caused by Induction Motor

The induction motor starting model is used to simulate harmonic current distortion caused by starting a high-power industry induction motor. The induction motor starting model developed in Simulink is shown in Figure 5.8. The induction motor starting model can be used to simulate harmonic current distortion caused by induction motor starting, The model consists of a 33 kV, 30 MVA, 50 Hz three-phase source feeder block feeding through 33 kV/0.4 kV, 1 MVA delta/bye transformers, a three-phase breaker as motor starting contactor, a three-phase induction motor, and 10 kW resistive load. Similarly, a 0.4-second simulation time is set and ode23tb solver is selected to run the simulation Figure 5.8 shows a three-phase harmonic current instantaneous waveform

caused by a 75 kW (100 hp) induction motor starting upon closing of motor starting contactor at 0.02 second. The speed of the induction motor during starting is set at 1 rad/sec using the constant block. The harmonic current at 0.4 kV bus propagates upstream through the transformer to the 33 kV feeder bus. The harmonic current can only be noticed at 0.4 kV bus waveform. The harmonic current distortion magnitude reduces as it propagates upstream toward the 33kV feeder where the harmonic current distortion becomes insignificant and not noticeable.

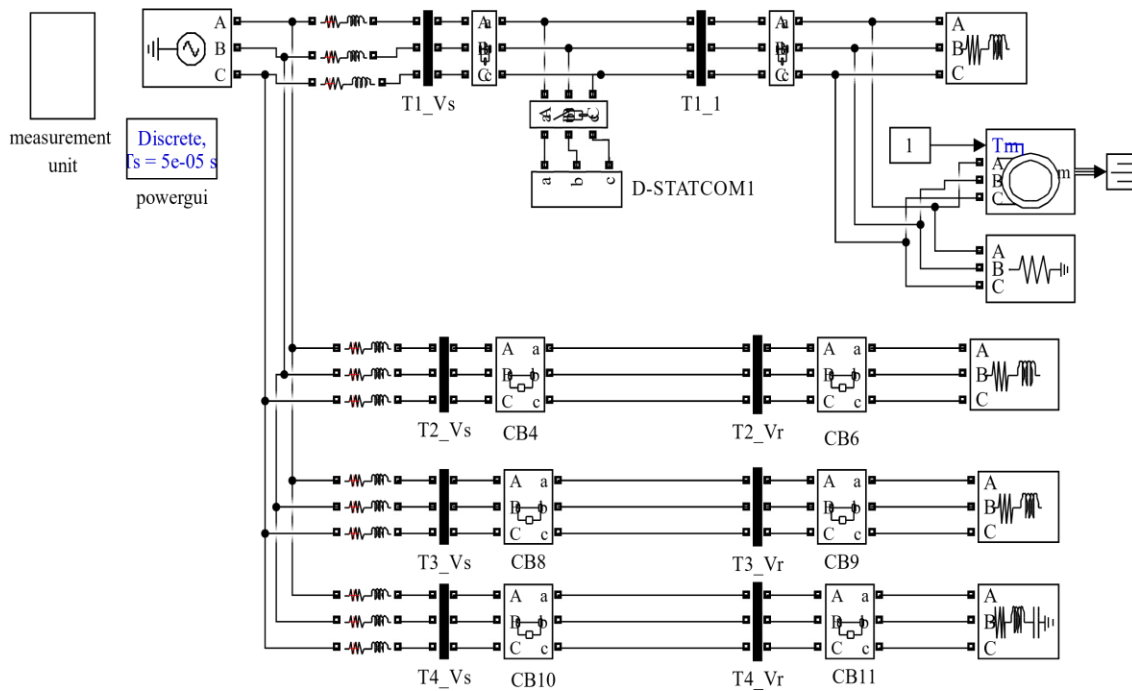


Figure 5. 8: Induction motor starting/load Simulink model.

Figure 5. 9: Induction motor starting/load Simulink model.

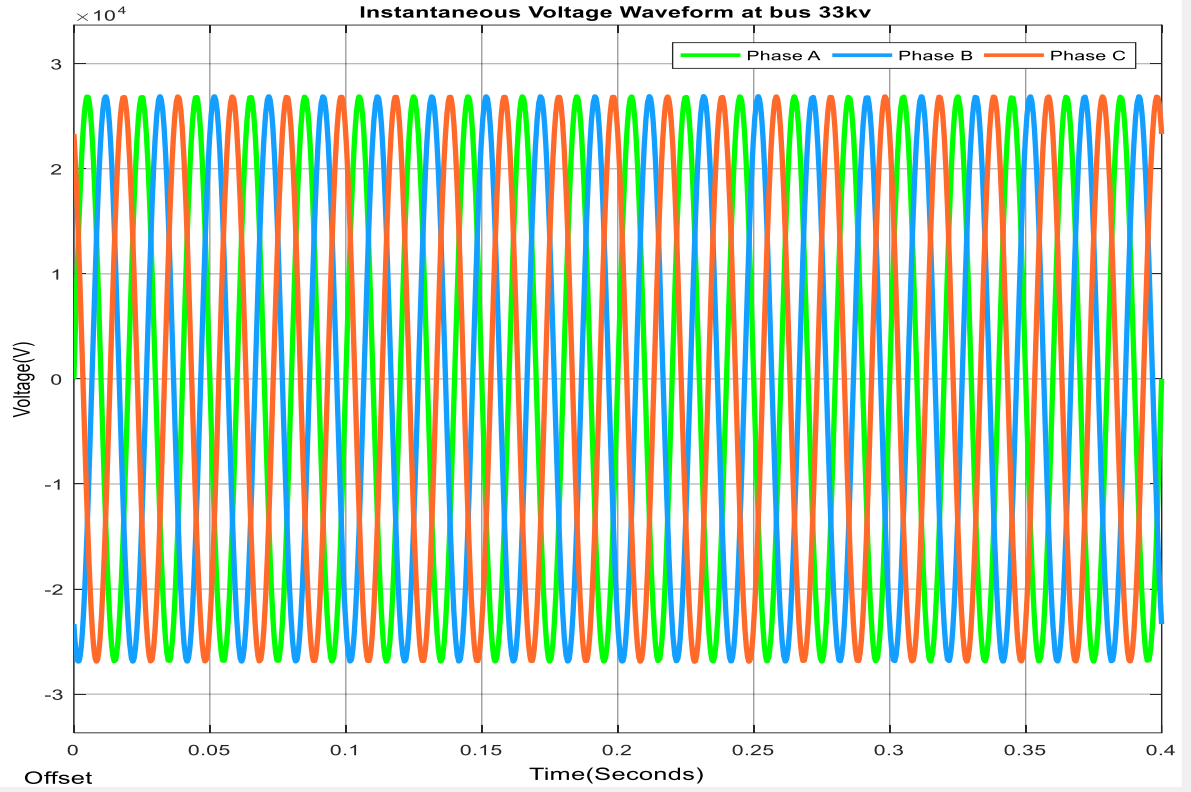


Figure 5. 10: Instantaneous voltage waveform at bus 33kv

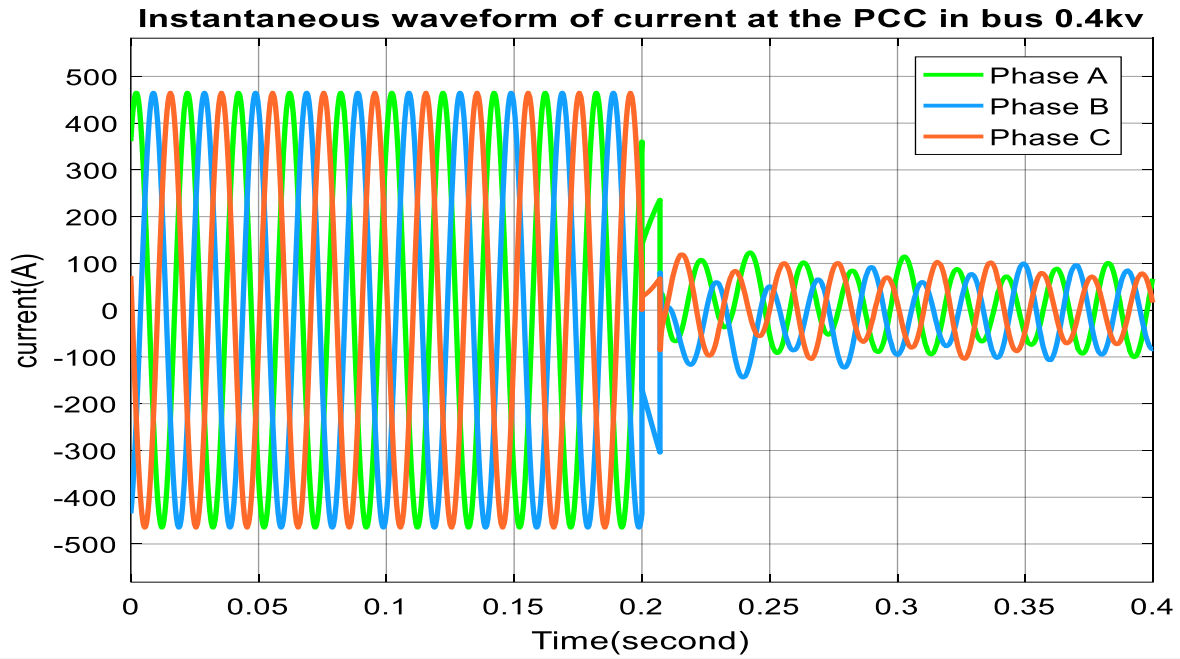


Figure 5. 11: Harmonic current distortion waveform caused by the starting of 75 kW induction motor at 0.4 kV.

Case 1 and 2: Distribution network of T1 with and without D-STATCOM included in the system at 0.02 second.

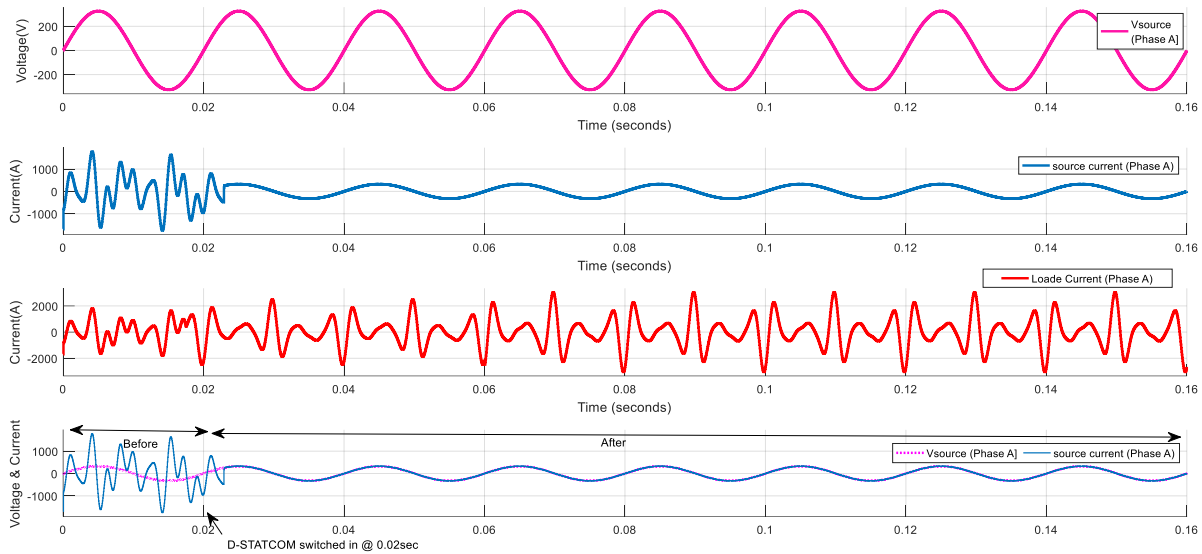


Figure 5. 12: Distribution result of T1 with and without D-STATCOM included in the system at 0.02 sec.

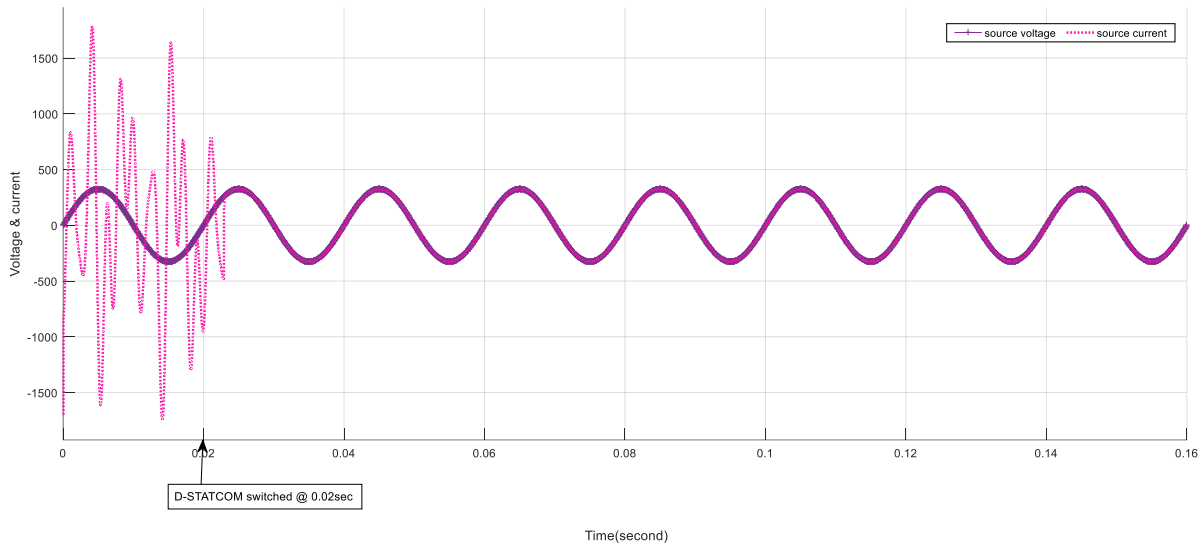


Figure 5. 13: Single-phase Vs, Is, Il and source voltage/current waveforms (from top to bottom).

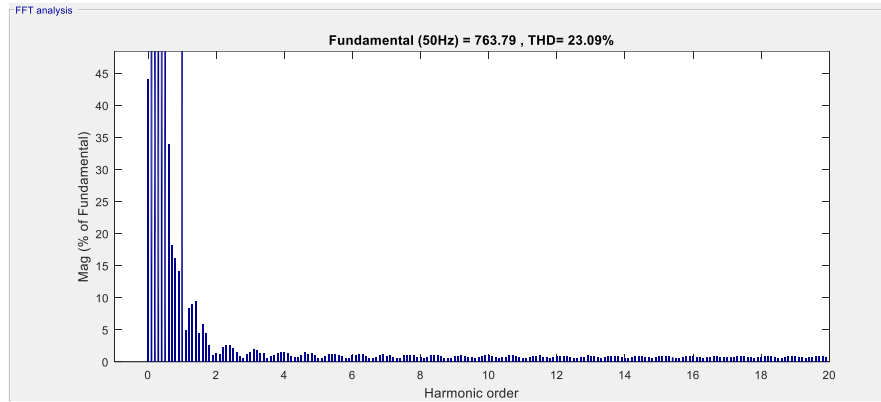


Figure 5. 14: Harmonic Spectrum of the source current on transformer T1 (Case 1)

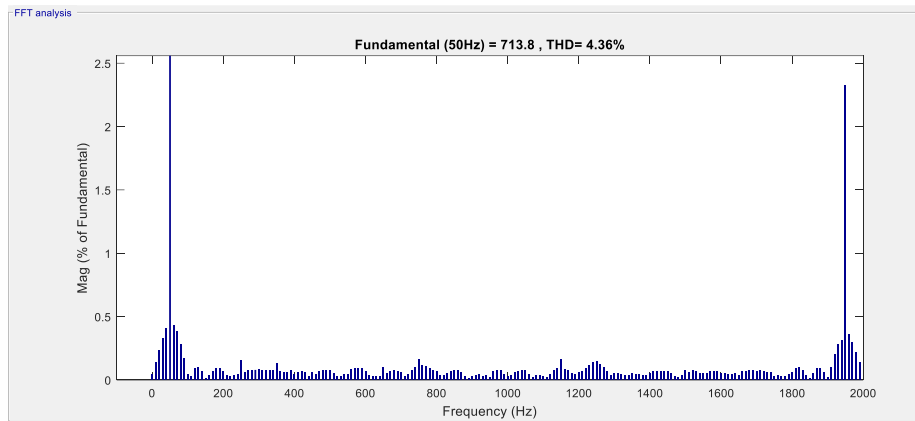


Figure 5. 15: Harmonic Spectrum of the source current on transformer T1 (Case 2)

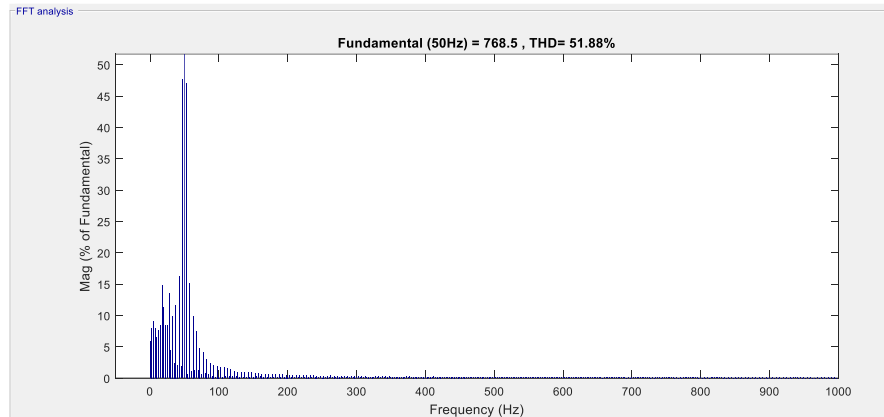


Figure 5. 16: Harmonic Spectrum of the source current on transformer T1.

The simulation results of transformer T1 show that the source current waveform becomes pure sinusoidal and in-phase with the voltage within 0.02 seconds (one cycle) after the D-STATCOM is switched-in to the system. The harmonic spectrum also shows that, when the D-STATCOM is in operation, the THDI level becomes below 4.36 %, which is well below the recommended limits set by IEEE and IEC standards.

5.3.2. Discussion and Summary

The distribution network of Awadda industry zone is simulated with MATLAB SIMULINK environment. The distribution network of the factory is modeled as a linear and non-linear load connected to a balanced 3-phase pure sinusoidal voltage source. The linear loads are characterized by active and reactive power of a series RL load by considering the actual power factor of the loads. The induction motor starting modeled as non-linear loads are a source of harmonic current distortion. The modeled distribution network is simulated for two different cases: the distribution network without and with D-STATCOM. The results of the simulation have been presented on the previous subtopic. The simulation results show that the source current waveform of transformer 1 becomes pure sinusoidal and in-phase with the voltage within 0.02 seconds (one cycle) after the respective D-STATCOM is enabled to the system. The harmonic spectrum also shows that the THDI level becomes below 2% when the D-STATCOM is in operation. Therefore, it can be concluded that the proposed D-STATCOM is able to compensate the current harmonic distortion

in the system at the same time maintain unity power factor at the source, thereby avoiding harmonic distortion related problems like overload and failure of distribution transformers and cables.

5.6. D-STATCOM Capacity, Specifications and Measured Values at the Factory

Referring to the electrical system of Awada industry zone and measured values,

$$V_{PCC} = 0.4KV$$

$$S = 1250KVA, PF = 0.9$$

Maximum three phase harmonic current distortion response (THDI) = 75%

Harmonic duration to protect = 250ms.

$$KVA \text{ Capacity of D-STATCOM} = 1125KVA$$

It is recommended to adopt D-STATCOM technology to compensate the [67] bus voltage with harmonic and restore to 100 % of the rated value. When the harmonic depth is lower than 75 %, therefore, the compensating voltage of D-STATCOM should be 80 % or 0.8 PU. By taking into consideration of peak, load 1250 KVA with power factor of 0.9.

$$\text{The compensation power} = 0.9 * 1250KVA = 1125KVA$$

$$\text{Energy} = \text{power} * \text{time}$$

The duration of harmonic to protect is 250 msec. so,

$$\text{The required energy} = (KVA * PF) * \text{time}$$

$$E = (1250*0.9)*0.25$$

$$E = 281.255KJ$$

For more reliability and availability D-STATCOM with (1150 KVA, 300 kJ) is selected. In addition, it should be installed in the 33-kV side of the system.

5.7. Cost and Payback Period of D-STATCOM

This section describes the cost and benefit analysis of installing D-STATCOM to mitigate harmonic distortion.

Assume cost of D-STATCOM = $C_{D-STATCOM}$

Cost of single harmonic = C_{SH}

Number of issues per year = N_{NH} and Payback period = T (year) then,

$$C_{D-STATCOM} = C_{SH} * N_{NH} * T$$

cost of D – STATCOM = $\$400/\text{KVA} + 5\% (\$400/\text{KVA})$ (Maintenance and running) [7]

$$C_{D-STATCOM} = \$420/\text{KVA}$$

$$C_{D-STATCOM} = \$420/\text{KVA} * 1150\text{KVA}$$

$$C_{D-STATCOM} = \$483,000$$

The cost of harmonic, C_{SH} at Awada industry is (\$2,500/year), and by taking the average number of harmonic occurrence, N_{NH} is 52/year [7]. Then, the payback period will be

$$T = \frac{C_{D-STATCOM}}{C_{NH} * N_{SH}}$$

$$T = \frac{\$483,000}{\$2500 * 52/\text{year}}$$

$$T = 3.715 \text{ years}$$

Hint: this solution is economic because the lifetime of D-STATCOM is about 15 years.

CHAPTER SIX

6. Conclusion, Recommendation and Future Work

6.1. Conclusion

This work presents the identification, classification of power quality issues and mitigation techniques at Awada industry zone. The main advantage offered by the technique is the use of the S-transform to decompose the power line signals into a set of time-frequency components in which simple and powerful feature extraction can be performed. The choice of the S-transform was made due to its characteristics that can uniquely combine a frequency dependent resolution that simultaneously localizes the real and imaginary spectra of the original waveforms. In this thesis, a new identification algorithm and classification technique is proposed for electrical power quality disturbances. Moreover, a validation methodology is conducted based on Stockwell Transform. Compared with existing algorithms, the proposed methodology showed a better performance based on the accuracy achieved. The overall accuracy shows another remarkable change as well, exceeding 97.1%. Nevertheless, another advantage of the proposed algorithm is the reduction of data size without losing the disturbance characteristics. Therefore, a significant reduction in memory space during operations and a decrease of computation cost result. The numerical results obtained with actual power quality data recorded in an industrial power system indicated that the new technique has perfect classification accuracy in the identification of both single and multiple disturbances. The overall accuracy is 98.3% and the misclassification rate of SVM classifier is only 1.7%. Then a D-STATCOM is designed to compensate the current harmonic distortions on one of the transformer among four transforms in Awada industry zone network. Finally, the performance of the designed D-STATCOM is evaluated by simulating an industry distribution network with and without the D-STATCOM in a MATLAB /SIMULINK environment. The simulation results of transformer one (T1) show that the source current waveform of becomes pure sinusoid and in-phase with the source voltage within 0.02 seconds (one cycle) the D-STATCOM is switched-in to the system. The harmonic spectrum also shows that, when the D-STATCOM is in operation, the THDI level becomes reduced from 23.09% to 4.36 %, which is well below the recommended limits set by IEEE 519-2014 and IEC standards.

6.2. Recommendation

In this study, the monitoring has been carried out at the CMDB boards and the system is simulated by connecting the proposed D-STATCOM at these boards. As shown in the simulation in the previous chapter, the harmonic current components from the non-linear loads will propagate in the distribution system up to the CMDB boards. In order to avoid this harmonic distortion propagation in the system, the harmonic current sources have to be identified. Therefore, it is highly recommended to perform similar harmonic distortion assessments by selecting monitoring points close to the loads, in order to identify the harmonic sources and compensate them locally. The identified power quality problems must be given serious attention and the designed appropriate solutions should be implemented and installed by the industry to avoid the loss of money, improve productivity, profitability and early failure of equipment.

6.3. Suggestion for Future Work

Power quality assessment should be done regularly, especially on sensitive loads to keep good performance of the factory and a complete assessment of power quality problems should be done. The time allocated for monitoring should be longer, it should be more than seven days, and this to ensure that, more detailed and complete data could be obtained. More monitoring points to be allocated in the site, so that more data could be gathered on the factory. In future study, this new technique will be used for performing diagnosis on the sources and causes of the power quality disturbances. A broad scope for future research in the PQ monitoring with RE penetration may include:

- Variation of the strength of AC grid with RE penetration is the major source of PQ disturbances and monitoring of these disturbances using the machine, and deep learning based techniques can be a possible future research problem.
- Study to select a generalized methodology for detection and classification of single and multiple PQDs with hybrid RE sources can also be a thrust area for researchers.

REFERENCES

- [1] Dave, "Electrical Substation Components and their Working," 3 april 2018. [Online]. Available: retrieved from http://www.watelectrical.com/electrical-substation-components/#google_vignette.. [Accessed 3 april 2021].
- [2] "Overview of yirgalem substation," 2021.
- [3] V. J. D. a. R. M. B. Prafull A. Desale, "Brief Review.Paper on the Custom Power Devices for Power Quality Improvement," *International Journal of Electronic and Electrical Engineering*, vol. 7, no. ISSN 0974-2174 , pp. pp 723-733, (2014).
- [4] IEEE, "Recommended Practice and Requirements for Harmonic Control in Electric Power Systems, IEEE Std 519-2014 (Revision of IEEE Std 519-1992)," pp. 29. 2014. [Online].
- [5] H. M. E.-E. Fathi, "Power Quality Assessment", PhD thesis submitted to," in *Al-Azhar University*, Cairo, Egypt, 163 pp, (2012).
- [6] K. M. a. S. K. S. Gokulananda Sahu, "Design and performance analysis of D-STATCOM for non-linear load compensation," in *springer international published*, switzerland, (2014).
- [7] K. M. a. S. K. S. Gokulananda Sahu, "Design and Performance Analysis of DSTATCOM for Non-linear Load Composite Compensation," *Jordan Journal of Electrical Engineering*, vol. 2, no. 2, pp. 337-344, (2014).
- [8] D. S. C. M. P. D. Gunjan Varshney, "Modeling, Simulation and Control of Photovoltaic Based DSTATCOM," *Jordan Journal of Electrical Engineering*, vol. 2, no. 2, p. 108-124, (2016).
- [9] A. Y. M. R. a. K. S. Z. Hameed, "Harmonics in Electrical Power Systems and how to remove them by using filters in ETAP," January 2020.

- [10] P. S. S. T. a. P. S. P. P. S. Jain, "Improve Power Quality and Reduce the Harmonics Distortion of Sensitive Load," vol. 2, no. 806–815, p. 6, 2012.
- [11] M. Garg and P. Nijhawan, "Mitigation of Power Quality Problems Using DVR in Distribution Network for Welding Load," *IOSR J. Electr. Electron. Eng*, vol. 10, no. 2278–1676, p. 4, 2015.
- [12] S. Gupta and A. K. Sharma, "Power Quality Identification Using Wavelet Transform : A Review," vol. 2, no. 42–48, p. 3, 2015.
- [13] R. T. a. I. E. D. O. P. Taiwo, "Investigation of voltage unbalance in low voltage electric power distribution network under steady state mode," *IEEE 3rd Int. Conf. Electro-Technology Natl. Dev. NIGERCON 2017*, vol. 5, no. 1, pp. 252-263, 2018.
- [14] M. R. a. M. I. T. H. D. Compensator, "23 rd International Conference on Electricity Distribution single tuned harmonic filter design as total harmonic distortion 23 rd International Conference on Electricity Distribution," 2015.
- [15] Milkias Berhanu, "An Investigation of Power Quality Problems in Distribution Network, Unpublished," MSc thesis submitted to Adama University, (2010).
- [16] T. Thomas and P. A. Michael, "Future power quality issues," *Int. J. Eng. Adv. Technol*, vol. 8, no. 4, pp. 1075–1080., 2019.
- [17] *Power System Instrumentation and Measurements of the IEEE Power & Energy Society*, 2010..
- [18] E. Fuchs et al, "Comparison of wavelet and Fourier analysis in power quality," 2012.
- [19] D. Granados-Lieberman et al, "Techniques and methodologies for power quality analysis and disturbances classification in power systems: a review," *Generation, Transmission & Distribution, IET*, vol. 5, no. (4), pp. 519-529, 2011.

- [20] Y. H. Gu and M. H. Bollen, "Time-frequency and time-scale domain analysis of voltage disturbances," *IEEE Trans. Power Del.*, Vols. vol. 15, (4), pp. 1279-1284., 2012.
- [21] R. Z. a. T. C. H. Qian, "Inter harmonics analysis based on interpolating windowed FFT algorithm," *IEEE Trans. Power Del*, vol. 22, no. (2), pp. 1064-1069, 2007.
- [22] P. S. a. S. K. G. S. Nath, "A wavelet based novel method for the detection of harmonic sources in power systems," *International Journal of Electrical Power & Energy*, vol. 40, no. (1), pp. 54-61, 2012.
- [23] S. Ö. a. T. E. Ö Gencer, "A new approach to voltage sag detection based on wavelet transform," *International Journal of Electrical Power & Energy Systems*, vol. 32, no. (2), pp. 133-140, 2010.
- [24] S. Deokar and L. Waghmare, "Integrated DWT–FFT approach for detection and classification of power quality disturbances," *International Journal of Electrical Power & Energy Systems*, vol. 61, pp. 594-605, 2014.
- [25] S. Alshahrani et al, "Evaluation and classification of power quality disturbances based on discrete wavelet transform and artificial neural networks," in *Power Engineering Conference (UPEC), 2015 50th International Universities*, vol. 3, no. 2, pp. 1-5, 2015.
- [26] W. G. Morsi and M. El-Hawary, "Wavelet packet transform-based power quality indices for balanced and unbalanced three-phase systems under stationary or nonstationary operating conditions," *Power Delivery, IEEE Transactions On*, vol. 24 , no. (4), pp. 2300-2310, 2009.
- [27] T. M. M. G. L. D. E. R. S. F. F. M. V. E. G. Ribeiro, " Real-time system for automatic detection and classification of single and multiple power quality disturbances ,Measurement," vol. 128, no. (4), p. 276–283, Nov. 2018..

- [28] J. Y. a. Y. L. L. Yang, "Disturbance source identification of voltage sags based on hilbert-huang transform," in *2010 Asia-Pacific Power and Energy Engineering Conference*, pp. 1-4, 2010.
- [29] B. S. a. D. T. S. R. Kumar, "Recognition of single-stage and multiple power quality events using Hilbert–Huang transform and probabilistic neural network," *Electr. Power Compon. Syst*, vol. 43, no. 6, p. 607–619, Apr. 2015.
- [30] Y.-C. L. a. J.-Y. Z. P.-Y. Chen, " "Hardware design and implemen tation for empirical mode decomposition," *IEEE Trans. Ind. Electron*, vol. 63, no. 6, p. 3686–3694, Jun. 2016.
- [31] M. S. a. P. K. R. M. Mishra, "An islanding detection algorithm for distributed generation based on Hilbert–Huang transform and extreme learning machine," *Sustain. Energy, Grids Netw*, vol. 9, p. 13–26, Mar. 2017.
- [32] C. Norman et al, "Hybrid wavelet and Hilbert transform with frequency-shifting decomposition for power quality analysis," *IEEE Transactions on Instrumentation and Measurement*, vol. 61, no. (12), pp. 3225-3233, 2012.
- [33] A. H. C. a. C. S. F. Hafiz, ""An approach for classification of power quality disturbances based on Hilbert huang transform and relevance vector machine," , 2012, .
- [34] L. L. W. H. a. J. Q. Huang, "Review of power-quality disturbance recognition using S-transform," in *Proc. IITA Int. Conf. Control, Autom. Syst. Eng. (CASE)*, , vol. 3, no. , p. 438–441, Jul. 2009.
- [35] R. K. R. K. P. V. a. D. K. M. M. J. B. Reddy, "Power quality analysis using discrete orthogonal S-transform (DOST)," *Digit. Signal Process.* , vol. 23, no. 2, p. 616–626, Mar. 2013.

- [36] K. L. a. M. Z. S. He, "A real-time power quality disturbances classification using hybrid method based on S-transform and dynamics," *IEEE Trans. Instrum. Meas.*, vol. 62, no. 9, p. 2465–2475, Sep. 2013.
- [37] G. Q. L. a. L. N. Wu, "Rapid power quality detection based on gen eralized HS-transform," in *Applied Mechanics and Materials*, vol. 568. New York, NY, USA: Trans Tech Publications,, vol. 568, p. 223–226, 2014.
- [38] M. V. R. a. R. Sodhi, "A modified S-transform and random forests based power quality assessment framework," *IEEE Trans. Instrum.Meas.*, vol. 67, no. 1, p. 78–89, Jan. 2018.
- [39] S. Z. G. C. Y. L. B. Y. a. Y. C. T. Zhong, "Power quality disturbance recognition based on multiresolution S-transform and decision tree," *IEEE Access*, vol. 7, p. 88380–88392, 2019.
- [40] M. V. R. a. R. Sodhi, "A rule-based S-transform and AdaBoost based approach for power quality assessment," *Electr. Power Syst. Res*, vol. 134, pp. 66-79, May 2016.
- [41] M. F. a. A. A. Foroud, "Recognition and assessment of different factors which affect flicker in wind turbines," *IET Renew. Power Gener*, vol. 10, no. 2, pp. 250-259, Feb. 2016.
- [42] K. L. a. M. Z. S. He, "A real-time power quality disturbances classification using hybrid method based on S-transform and dynamics," *IEEE Transactions on Instrumentation and Measurement*, vol. 62, no. (9), pp. 2465-2475, 2013.
- [43] R. Yokeeswaran and A. Vetrivel, "Measurement and Comparison of Power Quality Disturbances using Discrete Wavelet Transform (DWT) and Discrete Orthogonal S-Transform (DOST)," vol. 2, no. (3), pp. 808-813, 2012.
- [44] R. S. ., M. P. S. C. Paresh J. Shah, "Artificial intelligence approaches to advances signal processing and simulation methods for efficient power supplies "," *Scientific & Academic Publishing*, 2012..

- [45] W. N. a. A. L. D. Srinivasan, "Neural-network-based signature recognition for harmonic source identification," *Power Delivery, IEEE Transactions On*, vol. 21, no. (6), pp. 398-405, 2016.
- [46] B. S. a. N. B. K. Silva, "Fault detection and classification in transmission lines based on wavelet transform and ANN," *Power Delivery, IEEE Transactions On*, vol. 21 , no. (4), pp. 2058-2063, 2016.
- [47] M. A. a. B. A. S. Alshahrani, "Detection and classification of power quality events based on wavelet transform and artificial neural networks for smart grids," pp. 1-6, 2015.
- [48] V. N. Vapnik, "The Nature of Statistical Learning Theory," 1995. [Online]. [Accessed 27 3 2021].
- [49] G. Lv et al, "PQ disturbances identification based on SVMs classifier," in *Neural Networks and Brain*," 2005.
- [50] C. A. Naik and P. Kundu, "Power quality disturbance classification employing S- transform and three-module artificial neural network," *International Transactions on Electrical Energy Systems*, vol. 24 , no. (9), pp. 1301-1322, 2014.
- [51] A. S. Cerqueira et al, "Power quality events recognition using a SVM-based method," *Electr. Power Syst. Res*, vol. 78, no. (9), pp. 1546-1552, 2008.
- [52] Y. Liao and J. Lee, " "A fuzzy-expert system for classifying power quality disturbances,"," *International Journal of Electrical Power & Energy Systems*,, Vols. vol. 26, (3), , no. pp. 199-205, , pp. vol. 26, (3), pp. 199-205, , 2008..
- [53] S. K. Meher and A. K. Pradhan, "Fuzzy classifiers for power quality events analysis," *Electr. Power Syst. Res*, vol. 80, no. (1), pp. 71-76, 2010.

- [54] M. F. M. S. S. a. H. W. B. Roger C. Dugan, *Electrical Power Systems Quality*”, Second Edition, the McGraw-Hill Companies, (2004), p. 525 pp..
- [55] C. Sankaran, *Power Quality*, CRC press, 2001.
- [56] P. Q. A. Guide, "Voltage Disturbances," *Standard EN*, Vols. 50-160, 2004.
- [57] <http://www.iec.ch> (visited on April 23. [Online].
- [58] https://en.wikipedia.org/wiki/Institute_of_Electrical_and_Electronics_Engineers (visited on April 23. [Online].
- [59] <http://www.ethiostandards.org> (visited on April 23. [Online].
- [60] I. S. 5.-2. (. o. I. S. 5.-1. p. 2. IEEE Recommended Practice and Requirements for Harmonic Control in Electric Power Systems, 2014.
- [61] P. f. r. a. s. l. d. Different Weekly/Monthly reports of Awada industry zone (Maintenance performance report, 2013/14.
- [62] S. Z. G. C. Y. L. B. Y. a. Y. C. T. Zhong, "Power quality disturbance recognition based on multiresolution S-transform and decision tree," *IEEE Access*, vol. 7, p. 88380–88392, 2019..
- [63] M. W. L. Riba, "Continuous inversion formulas for multi-dimensional modified Stockwell transforms," *Integral Transforms Spec. Funct*, 2015..
- [64] L. M. a. R. P. L. R. G. Stockwell, "Localization of the complex spectrum: The s transform," *IEEE Trans. Signal Process*, vol. 44, no. 4, p. 998–1001, Apr. 1996.
- [65] S. P. G. G. N. .. Sahu, "“An improved S-transform for timefrequency analysis’.,” Patiala, India, 2009.

- [66] V. J. D. a. R. M. B. Prafull A. Desale, "Brief Review Paper on the Custom Power Devices for Power Quality Improvement," *International Journal of Electronic and Electrical Engineering*, vol. 7, no. SSN 0974-2174 , p. 723, (2014).
- [67] S. U. a. P. Sharma, "Harmonic Elimination Using D-STATCOM," *Springer India, Proceedings of the Second International Conference on Computer and Communication Technologies, Advances in Intelligent Systems and Computing*, pp. 577-591, (2016).
- [68] D. S. C. M. P. D. Gunjan Varshney, "Modeling, Simulation and Control of Photovoltaic Based DSTATCOM," *Jordan Journal of Electrical Engineering*, vol. 2, no. 2, p. 108-124, (2016).
- [69] R. Naidoo and P. Pillay, "'A new method of voltage sag and swell detection,'" *IEEE Trans. Power Del.*, , Vols. vol. 22, (2), , pp. pp. 1056-1063,, 2007..
- [70] S. M. a. B. S. S. Shukla, "Empirical-Mode Decomposition with Hilbert Transform for Power-Quality Assessment," *IEEE Trans. Power Del*, vol. 24 , no. (4), p. 2159 2165, 2009.
- [71] W. R. A. Ibrahim and M. M. Morcos, "Artificial intelligence and advanced mathematical tools for power quality applications: A survey," 2012.
- [72] I. Monedero et al, "Classification of electrical disturbances in real time using neural networks,"*Power Delivery*," *IEEE Transactions On*, vol. 22, no. (3), pp. 1288-1296, 2007.

APPENDICES

Appendix A: Categories & characteristics of power system electromagnetic phenomena as Presented on IEEE std 1159-2009: IEEE Recommended Practice for Monitoring Electric Power Quality.

Categories	Typical spectral content	Typical duration	Typical voltage magnitude
1.0 Transients			
1.1 Impulsive			
1.1.1 Nanosecond	5 ns rise	< 50 ns	
1.1.2 Microsecond	1 μ s rise	50 ns – 1 ms	
1.1.3 Millisecond	0.1 ms rise	> 1 ms	
1.2 Oscillatory			
1.2.1 Low frequency	< 5 kHz	0.3–50 ms	0–4 pu ^a
1.2.2 Medium frequency	5–500 kHz	20 μ s	0–8 pu
1.2.3 High frequency	0.5–5 MHz	5 μ s	0–4 pu
2.0 Short-duration root-mean-square (rms) variations			
2.1 Instantaneous			
2.1.1 Sag		0.5–30 cycles	0.1–0.9 pu
2.1.2 Swell		0.5–30 cycles	1.1–1.8 pu
2.2 Momentary			
2.2.1 Interruption		0.5 cycles – 3 s	< 0.1 pu
2.2.2 Sag		30 cycles – 3 s	0.1–0.9 pu
2.2.3 Swell		30 cycles – 3 s	1.1–1.4 pu
2.3 Temporary			
2.3.1 Interruption		>3 s – 1 min	< 0.1 pu
2.3.2 Sag		>3 s – 1 min	0.1–0.9 pu
2.3.3 Swell		>3 s – 1 min	1.1–1.2 pu
3.0 Long duration rms variations			
3.1 Interruption, sustained		> 1 min	0.0 pu
3.2 Undervoltages		> 1 min	0.8–0.9 pu
3.3 Overvoltages		> 1 min	1.1–1.2 pu
3.4 Current overload		> 1 min	
4.0 Imbalance			
4.1 Voltage		steady state	0.5–2%
4.2 Current		steady state	1.0–30%
5.0 Waveform distortion			
5.1 DC offset		steady state	0–0.1%
5.2 Harmonics	0–9 kHz	steady state	0–20%
5.3 Interharmonics	0–9 kHz	steady state	0–2%
5.4 Notching		steady state	
5.5 Noise	broadband	steady state	0–1%
6.0 Voltage fluctuations	< 25 Hz	intermittent	0.1–7% 0.2–2 P _{st} ^b
7.0 Power frequency variations		< 10 s	\pm 0.10 Hz

Appendix -B: Measurement data taken from Awada industry zone CMDB-1.

CMDB-1	Time	Cos ϕ	I- Sec.	Vload-n	Harmonic Distortion Current							Harmonic Distortion Voltage						
					TH D-I	1 st	3 rd	5 th	7 th	9 th	11 th	TH D-V	1 st	3 rd	5 th	7 th	9 th	11 th
17/3/2021	1:10PM	0.94	0.93	219	25.8	0.92	0.02	0.2	0.1	0	0.04	20.3	220	0	3	20	1	
17/3/2021	1:40PM	0.92	0.71	225	29.6	0.65	0.01	0.06	0.09	0	0.03	1.9	224	0	2	30	0	
17/3/2021	4:40PM	0.93	0.72	224	28.6	0.7	0.01	0.17	0.09	0	0.03	2	223	0	2	30	0	
17/3/2021	5:00PM	0.94	0.78	224	28.7	0.69	0.01	0.17	0.1	0	0.03	1.8	224	0	2	30	0	
17/3/2021	8:10AM	0.94	0.62	227	29.9	0.6	0.02	0.15	0.08	0	0.03	1.9	227	0	3	20	0	
20/3/2021	8:30AM	0.96	0.49	230	41.8	0.45	0.02	0.16	0.09	0	0.02	1.9	231	0	3	20	0	
20/3/2021	1:05PM	0.96	0.65	226	33.8	0.61	0.02	0.17	0.1	0	0.03	2.4	225	0	4	20	1	
20/3/2021	2:00PM	0.95	0.72	227	33.8	0.69	0.01	0.2	0.1	0	0.04	2.3	226	0	3	30	1	
20/3/2021	4:55PM	0.95	0.77	226	34.1	0.73	0.02	0.22	0.1	0	0.04	2.5	227	0	3	30	1	
20/3/2021	5:05PM	0.96	0.64	228	37.1	0.62	0.02	0.19	0.1	0	0.03	2.3	229	0	4	40	1	
20/3/2021	6:00PM	0.96	0.46	230	38.1	0.49	0.01	0.17	0.09	0	0.02	2	231	0	3	30	1	
22/3/2021	7:00PM	0.93	0.47	230	43.4	0.44	0.02	0.16	0.08	0	0.02	1.7	230	0	2	30	0	
22/3/2021	8:00PM	0.96	0.51	229	38.6	0.47	0.02	0.18	0.09	0	0.03	2.3	231	0	4	30	1	
22/3/2021	9:00PM	0.91	0.75	230	28.5	0.71	0.03	0.17	0.09	0	0.03	2.1	231	0	4	20	1	
22/3/2021	10:50PM	0.92	0.69	229	29.6	0.66	0.03	0.17	0.09	0	0.03	2	229	0	3	20	1	

22/3/2021	3:30AM	0.96	0.47	230	43.8	0.43	0.02	0.16	0.09	0	0.02	1.6	231	0	3	20	0
23/3/2022	6:30AM	0.95	0.48	228	34.7	0.45	0.02	0.12	0.06	0	0.02	2.4	228	0	5	20	0
23/3/2022	8:15AM	0.97	0.15	228	--	0.13	0.01	0.06	0.03	0	0	1.3	228	0	2	00	0
23/3/2022	8:55AM	0.91	0.08	227	--	0.07	0	0.03	0.02	0	0	0.6	232	0	0	10	0
23/3/2022	1:00PM	0.94	0.55	224	26	0.54	0.01	0.11	0.07	0	0.03	1.7	224	0	3	20	0
23/3/2022	1:20PM	0.93	0.63	226	26.9	0.61	0.01	0.16	0.08	0	0.03	1.7	226	0	2	30	0
23/3/2022	5:00PM	0.94	0.54	223	30.9	0.52	0.01	0.14	0.07	0	0.02	1.4	223	0	2	20	0
23/3/2022	6:00PM	0.95	0.58	225	28.2	0.55	0.01	0.13	0.07	0	0.02	1.6	227	0	3	10	0
23/3/2022	8:00PM	0.97	0.47	233	37.2	0.34	0.21	0.11	0.06	0	0.02	1.5	233	0	2	20	0
23/3/2022	9:00PM	0.97	0.2	233	--	0.19	0.01	0.07	0.04	0	0.01	1	233	0	1	10	0

Appendix –C: General rule test each location at PCC for seven days or one week according to IEEE.

Events (21/04/2021 - 27/04/2021)						
			Voltage Levels			Duration
			L1	L2	L3	
21/04/2021	Full day	Normal	Normal	Normal	Normal	Full day
22/04/2021	11:20:25	Harmonic	225	227	224.5	95msec.
23/04/2021	Full day	Normal	Normal	Normal	Normal	Full day

24/04/2021	19:30:20	Harmonic	190.5	195.2	201.2	250msec.
25/04/2021	Full day	Normal	Normal	Normal	Normal	Full day
26/04/2021	Full day	Normal	Normal	Normal	Normal	Full day
27/04/2021	16:30:28	Harmonic	224.5	220	219	150msec.

Appendix –D

% Returns the Stockwell Transform of the time series.

function [st,t,f] = st(timeseries,minfreq,maxfreq,samplingrate,freqsamplingrate)

% This is the S transform wrapper that holds default values for the function.

TRUE = 1;

FALSE = 0;

%%% DEFAULT PARAMETERS [change these for your particular application]

verbose = TRUE;

removeedge= FALSE;

analytic_signal = FALSE;

factor = 1;

if verbose disp(' '),**end**

if nargin == 0

if verbose disp('No parameters inputted.'),**end**

 st_help

 t=0;st=-1;f=0;

return

end

% Change to column vector

if size(timeseries,2) > size(timeseries,1)

 timeseries=timeseries';

end

```

% Make sure it is a 1-dimensional array
if size(timeseries,2) > 1
    error('Please enter a *vector* of data, not matrix')
    return
else if (size(timeseries)==[1 1]) == 1
    error('Please enter a *vector* of data, not a scalar')
    return
end
% use defaults for input variables
if nargin == 1
    minfreq = 0;
    maxfreq = fix(length(timeseries)/2);
    samplingrate = 1;
    freqsamplingrate = 1;
elseif nargin == 2
    maxfreq = fix(length(timeseries)/2);
    samplingrate = 1;
    freqsamplingrate = 1;
    [minfreq,maxfreq,samplingrate,freqsamplingrate] =
check_input(minfreq,maxfreq,samplingrate,freqsamplingrate,verbose,timeseries);
elseif nargin == 3
    samplingrate = 1;
    freqsamplingrate = 1;
    [minfreq,maxfreq,samplingrate,freqsamplingrate]=
check_input(minfreq,maxfreq,samplingrate,freqsamplingrate,verbose,timeseries);
elseif nargin == 4
    freqsamplingrate = 1;
    [minfreq,maxfreq,samplingrate,freqsamplingrate]=
check_input(minfreq,maxfreq,samplingrate,freqsamplingrate,verbose,timeseries);
elseif nargin == 5

```

```

[minfreq,maxfreq,samplingrate,freqsamplingrate]=
check_input(minfreq,maxfreq,samplingrate,freqsamplingrate,verbose,timeseries);
else
    if verbose disp('Error in input arguments: using defaults'),end
    minfreq = 0;
    maxfreq = fix(length(timeseries)/2);
    samplingrate=1;
    freqsamplingrate=1;
end
if verbose
    disp(sprintf('Minfreq = %d',minfreq))
    disp(sprintf('Maxfreq = %d',maxfreq))
    disp(sprintf('Sampling Rate (time domain) = %d',samplingrate))
    disp(sprintf('Sampling Rate (freq. domain) = %d',freqsamplingrate))
    disp(sprintf('The length of the timeseries is %d points',length(timeseries)))
    disp(' ')
end
t = (0:length(timeseries)-1)*samplingrate;
spe_nelements =ceil((maxfreq - minfreq+1)/freqsamplingrate) ;
f = (minfreq + [0:spe_nelements-1]*freqsamplingrate)/(samplingrate*length(timeseries));
if verbose disp(sprintf('The number of frequency voices is %d',spe_nelements)),end
% The actual S Transform function is here:
st=strans(timeseries,minfreq,maxfreq,samplingrate,freqsamplingrate,verbose,removeedge,analyti
c_signal,factor);
if nargin==0
    if verbose disp('Plotting pseudocolor image'),end
    pcolor(t,f,abs(st))
end
return
%-----

```

```

function st=ststrans(timeseries,minfreq,maxfreq,samplingrate,freqsamplingrate,verbose,removeedge,analytic_signal,factor);
n=length(timeseries);
original = timeseries;
if removeedge
    if verbose disp('Removing trend with polynomial fit'),end
        ind = [0:n-1]';
        r = polyfit(ind,timeseries,2);
        fit = polyval(r,ind) ;
        timeseries = timeseries - fit;
    if verbose disp('Removing edges with 5% hanning taper'),end
        sh_len = floor(length(timeseries)/10);
        wn = hanning(sh_len);
        if(sh_len==0)
            sh_len=length(timeseries);
            wn = 1&[1:sh_len];
        end
        % make sure wn is a column vector, because timeseries is
        if size(wn,2) > size(wn,1)
            wn=wn';
        end
        timeseries(1:floor(sh_len/2),1) = timeseries(1:floor(sh_len/2),1).*wn(1:floor(sh_len/2),1);
        timeseries(length(timeseries)-floor(sh_len/2):n,1)=timeseries(length(timeseries)-
        floor(sh_len/2):n,1).*wn(sh_len-floor(sh_len/2):sh_len,1);
    end
    if analytic_signal
        if verbose disp('Calculating analytic signal (using Hilbert transform)'),end
            % this version of the hilbert transform is different than hilbert.m
            % This is correct!
            ts_spe = fft(real(timeseries));
            h = [1; 2*ones(fix((n-1)/2),1); ones(1-rem(n,2),1); zeros(fix((n-1)/2),1)];

```

```

    ts_spe(:) = ts_spe.*h(:);
    timeseries = ifft(ts_spe);
end
% Compute FFT's
tic;vector_fft=fft(timeseries);tim_est=toc;
vector_fft=[vector_fft,vector_fft];
tim_est = tim_est*ceil((maxfreq - minfreq+1)/freqsamplingrate) ;
if verbose disp(sprintf('Estimated time is %f',tim_est)),end
% Preallocate the STOutput matrix
st=zeros(ceil((maxfreq - minfreq+1)/freqsamplingrate),n);
% Compute the mean
% Compute S-transform value for 1 ... ceil (n/2+1)-1 frequency points
if verbose disp('Calculating S transform...'),end
if minfreq == 0
    st(1,:) = mean(timeseries)*(1&[1:1:n]);
else
    st(1,:)=ifft(vector_fft(minfreq+1:minfreq+n).*g_window(n,minfreq,factor));
end
for banana=freqsamplingrate:freqsamplingrate:(maxfreq-minfreq)

st(banana/freqsamplingrate+1,:)=ifft(vector_fft(minfreq+banana+1:minfreq+banana+n).*g_wi
ndow(n,minfreq+banana,factor));
end
if verbose disp('Finished Calculation'),end
%-----
function gauss=g_window(length,freq,factor)
    vector(1,:)= [0:length-1];
    vector(2,:)= [-length:-1];
    vector=vector.^2;
    vector=vector*(-factor*2*pi^2/freq^2);
% Compute the Gaussian window

```

```

gauss=sum(exp(vector));
%-----
function[minfreq,maxfreq,samplingrate,freqsamplingrate]=check_input(minfreq,maxfreq,sampli
ngrade,freqsamplingrate,verbose,timeseries)
s = size(minfreq);
l = max(s);
if l > 1
    if verbose disp('Array of inputs accepted. '),end
    temp=minfreq;
    minfreq = temp(1);;
    if l > 1 maxfreq = temp(2);,end;
    if l > 2 samplingrate = temp(3);,end;
    if l > 3 freqsamplingrate = temp(4);,end;
    if l > 4
        if verbose disp('Ignoring extra input parameters. '),end
    end;
end
if minfreq < 0 | minfreq > fix(length(timeseries)/2);
    minfreq = 0;
    if verbose disp('Minfreq < 0 or > Nyquist. Setting minfreq = 0. '),end
end
if maxfreq > length(timeseries)/2 | maxfreq < 0
    maxfreq = fix(length(timeseries)/2);
    if verbose disp(sprintf('Maxfreq < 0 or > Nyquist. Setting maxfreq = %d',maxfreq)),end
end
if minfreq > maxfreq
    temporary = minfreq;
    minfreq = maxfreq;
    maxfreq = temporary;
    clear temporary;
    if verbose disp('Swapping maxfreq <=> minfreq. '),end

```



```

disp('Default input variables')
disp('MINFREQ- the lowest frequency in the ST result(Default=0)')
disp('MAXFREQ - the highest frequency in the ST result (Default=nyquist)')
disp('SAMPLINGRATE - the time interval between successive data points (Default = 1)')
disp('FREQSAMPLINGRATE - the number of frequencies between samples in the ST results')

```

Appendix – F:

```

function [trainedClassifier, validationAccuracy] = trainClassifier(trainingData)
% To automate training the same classifier with new data, or to learn how
% to programmatically train classifiers, examine the generated code.
% Auto-generated by MATLAB on 09-May-2022 23:43:28
% Extract predictors and response
% This code processes the data into the right shape for training the
% classifier.
inputTable = trainingData;
predictorNames = {'Entropy_original', 'Entropy_apcf', 'Entropy_dtcf', 'Mean_energy',
'Max_percent', 'THD'};
predictors = inputTable(:, predictorNames);
response = inputTable.Event;
isCategoricalPredictor = [false, false, false, false, false, false];
% This code specifies all the classifier options and trains the classifier.
template = templateSVM(...
    'KernelFunction', 'polynomial', ...
    'PolynomialOrder', 3, ...
    'KernelScale', 'auto', ...
    'BoxConstraint', 1, ...
    'Standardize', true);
classificationSVM = fitcecoc(...
    predictors, ...
    response, ...
    'Learners', template, ...
    'Coding', 'onevsone', ...

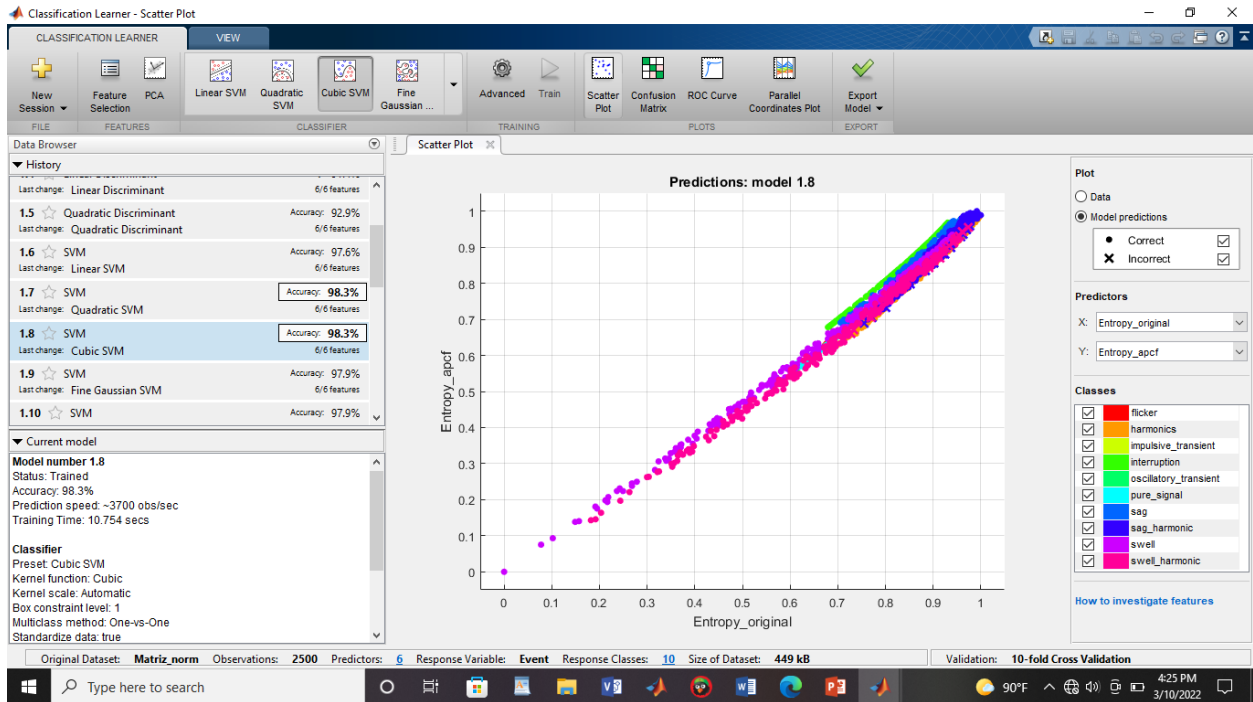
```

```

    'ClassNames', {'flicker'; 'harmonics'; 'impulsive_transient'; 'interruption'; 'oscillatory_transient';
'pure_signal'; 'sag'; 'sag_harmonic'; 'swell'; 'swell_harmonic'}));
predictorExtractionFcn = @(t) t(:, predictorNames);
svmPredictFcn = @(x) predict(classificationSVM, x);
trainedClassifier.predictFcn = @(x) svmPredictFcn(predictorExtractionFcn(x));
trainedClassifier.RequiredVariables = {'Entropy_original', 'Entropy_apcf', 'Entropy_dtcf',
'Mean_energy', 'Max_percent', 'THD'};
trainedClassifier.ClassificationSVM = classificationSVM;
trainedClassifier.About = 'This struct is a trained classifier exported from Classification Learner
R2016a.';
trainedClassifier.HowToPredict = sprintf('To make predictions on a new table, T, use: \n yfit =
c.predictFcn(T) \nreplacing "c" with the name of the variable that is this struct, e.g.
"trainedClassifier". \n \nThe table, T, must contain the variables returned by: \n
c.RequiredVariables \nVariable formats (e.g. matrix/vector, datatype) must match the original
training data. \nAdditional variables are ignored. \n \nFor more information, see <a
href="matlab:helpview(fullfile(docroot, "stats", "stats.map"),
"appclassification_exportmodeltoworkspace")">How to predict using an exported model</a>');
inputTable = trainingData;
predictorNames = {'Entropy_original', 'Entropy_apcf', 'Entropy_dtcf', 'Mean_energy',
'Max_percent', 'THD'};
predictors = inputTable(:, predictorNames);
response = inputTable.Event;
isCategoricalPredictor = [false, false, false, false, false, false];
partitionedModel = crossval(trainedClassifier.ClassificationSVM, 'KFold', 10);
validationAccuracy = 1 - kfoldLoss(partitionedModel, 'LossFun', 'ClassifError');
[validationPredictions, validationScores] = kfoldPredict(partitionedModel);

```

Appendix-E



Appendix – E: Snapshot of the codes in the function blocks of IRP control.

```

%Epaphros Mengistu
%Clark's Transformation of voltage
function [x,y] = VCT(u,v,w)
x = sqrt(2/3)*(u-(0.5*v)-(0.5*w));
y = sqrt(2)*(0+(0.5*v)-(0.5*w));
%Clark's Transformation of voltage
function [x,y] = ICT(u,v,w)
x = sqrt(2/3)*(u-(0.5*v)-(0.5*w));
y = sqrt(2)*(0+(0.5*v)-(0.5*w));
%Instantaneous active and reactive power calculation
function [P,Q,Valpha,Vbeta] =PQ(x1,x2,y1,y2)
P = (x1*y1)+(x2*y2);
Q = (x2*y1)-(x1*y2);
Valpha = x1;
Vbeta = x2;
%Reference current calculation
function [Ic1,Ic2] = ICOM(Posc,q,V1,V2)
Ic1 = (-1/(V1^2+V2^2))*((Posc*V1)+(q*V2));
Ic2 = (-1/(V1^2+V2^2))*((Posc*V2)+(q*V1));
%%Clark's Transformation of current
function [ICa,ICb,ICc] = Ical(Ic1,Ic2)
ICa = sqrt(2/3)*(Ic1);
ICb = sqrt(2/3)*((-0.5*Ic1)+((sqrt(3)/2)*Ic2));
ICc = sqrt(2/3)*((-0.5*Ic1)-((sqrt(3)/2)*Ic2));

```
